ΕΛΛΗΝΙΚΗ ΔΗΜΟΚΡΑΤΙΑ
Εθνικόν και Καποδιστριακόν Πανεπιστήμιον Αθηνών
——— ΙΔΡΥΘΕΝ ΤΟ 1837 ———

ΙΑΤΡΙΚΗ ΣΧΟΛΗ ΑΘΗΝΩΝ

ΕΡΓΑΣΤΗΡΙΟ ΦΥΣΙΟΛΟΓΙΑΣ

Διευθυντής: Καθηγητής Γεώργιος Κόλλιας

Αναζήτηση νέων μορίων αναστολέων για τη θεραπεία χρόνιων φλεγμονωδών νόσων: Ανάπτυξη μιας προτυποποιημένης διαδικασίας ελέγχου

Identifying new small molecule inhibitors for the therapy of chronic inflammatory diseases: Developing of a novel screening pipeline

ΠΑΠΑΔΟΠΟΥΛΟΥ ΔΗΜΗΤΡΑ

ΒΙΟΛΟΓΟΣ

Διδακτορική Διατριβή

Αθήνα 2022

ΙΑΤΡΙΚΗ ΣΧΟΛΗ ΑΘΗΝΩΝ

ΕΡΓΑΣΤΗΡΙΟ ΦΥΣΙΟΛΟΓΙΑΣ

Διευθυντής: Καθηγητής Γεώργιος Κόλλιας

Αναζήτηση νέων μορίων αναστολέων για τη θεραπεία χρόνιων φλεγμονωδών νόσων: Ανάπτυξη μιας προτυποποιημένης διαδικασίας ελέγχου

Identifying new small molecule inhibitors for the therapy of chronic inflammatory diseases: Developing of a novel screening pipeline

ΠΑΠΑΔΟΠΟΥΛΟΥ ΔΗΜΗΤΡΑ

ΒΙΟΛΟΓΟΣ

Διδακτορική Διατριβή

Αθήνα 2022

Στοιχεία ταυτότητας της διδακτορικής διατριβής

α) ημερομηνία αιτήσεως του υποψηφίου: 16/09/2016

β) ημερομηνία ορισμού 3μελούς Συμβουλευτικής Επιτροπής: 29/11/2016

γ) ημερομηνία ορισμού του Θέματος: 08/02/2017

γ) ημερομηνία καταθέσεως της διδακτορικής διατριβής: 21/07/2022

Τριμελής συμβουλευτική επιτροπή

Γ. Κόλλιας, Καθηγητής Ιατρικής Σχολής Αθηνών

Μ. Κουτσιλιέρης, Καθηγητής Ιατρικής Σχολής Αθηνών

Α. Φιλίππου, Αναπληρωτής Καθηγητής Ιατρικής Σχολής Αθηνών

Επταμελής εξεταστική επιτροπή

Γ. Κόλλιας, Καθηγητής Ιατρικής Σχολής Αθηνών

Μ. Κουτσιλιέρης, Καθηγητής Ιατρικής Σχολής Αθηνών

Α. Φιλίππου, Αναπληρωτής Καθηγητής Ιατρικής Σχολής Αθηνών

Π. Σφηκάκης, Καθηγητής Ιατρικής Σχολής Αθηνών

Δ. Βασιλόπουλος, Καθηγητής Ιατρικής Σχολής Αθηνών

Β. Κολιαράκη, Ερευνήτρια Β', ΕΚΕΒΕ Αλ. Φλέμιγκ

Μ. Αρμακά, Ερευνήτρια Β', ΕΚΕΒΕ Αλ. Φλέμιγκ

Επιβλέπων

Γ. Κόλλιας, Καθηγητής Ιατρικής Σχολής Αθηνών

Πρόεδρος Ιατρικής Σχολής

Σιάσος Γεράσιμος, Καθηγητής Ιατρικής Σχολής Αθηνών

ΟΡΚΟΣ ΤΟΥ ΙΠΠΟΚΡΑΤΗ

Ὄμνυμι Ἀπόλλωνα ἰητρὸν, καὶ Ἀσκληπιὸν, καὶ Ὑγείαν, καὶ Πανάκειαν, καὶ θεοὺς πάντας τε καὶ πάσας, ἵστορας ποιεύμενος, ἐπιτελέα ποιήσειν κατὰ δύναμιν καὶ κρίσιν ἐμὴν ὅρκον τόνδε καὶ ξυγγραφὴν τήνδε.

Ἡγήσασθαι μὲν τὸν διδάξαντά με τὴν τέχνην ταύτην ἴσα γενέτῃσιν ἐμοῖσι, καὶ βίου κοινώσασθαι, καὶ χρεῶν χρηίζοντι μετάδοσιν ποιήσασθαι, καὶ γένος τὸ ἐξ ὡύτέου ἀδελφοῖς ἴσον ἐπικρινέειν ἄρρεσι, καὶ διδάξειν τὴν τέχνην ταύτην, ἢν χρηίζωσι μανθάνειν, ἄνευ μισθοῦ καὶ ξυγγραφῆς, παραγγελίης τε καὶ ἀκροήσιος καὶ τῆς λοιπῆς ἁπάσης μαθήσιος μετάδοσιν ποιήσασθαι υἱοῖσί τε ἐμοῖσι, καὶ τοῖσι τοῦ ἐμὲ διδάξαντος, καὶ μαθηταῖσι συγγεγραμμένοισί τε καὶ ὡρκισμένοις νόμῳ ἰητρικῷ, ἄλλῳ δὲ οὐδενί.

Διαιτήμασί τε χρήσομαι ἐπ' ὠφελείῃ καμνόντων κατὰ δύναμιν καὶ κρίσιν ἐμήν, ἐπὶ δηλήσει δὲ καὶ ἀδικίῃ εἴρξειν.

Οὐ δώσω δὲ οὐδὲ φάρμακον οὐδενὶ αἰτηθεὶς θανάσιμον, οὐδὲ ὑφηγήσομαι ξυμβουλίην τοιήνδε. Ὁμοίως δὲ οὐδὲ γυναικὶ πεσσὸν φθόριον δώσω. Ἁγνῶς δὲ καὶ ὁσίως διατηρήσω βίον τὸν ἐμὸν καὶ τέχνην τὴν ἐμήν.

Οὐ τεμέω δὲ οὐδὲ μὴν λιθιῶντας, ἐκχωρήσω δὲ ἐργάτῃσιν ἀνδράσι πρήξιος τῆσδε.

Ἐς οἰκίας δὲ ὁκόσας ἂν ἐσίω, ἐσελεύσομαι ἐπ' ὠφελείῃ καμνόντων, ἐκτὸς ἐὼν πάσης ἀδικίης ἑκουσίης καὶ φθορίης, τῆς τε ἄλλης καὶ ἀφροδισίων ἔργων ἐπί τε γυναικείων σωμάτων καὶ ἀνδρῴων, ἐλευθέρων τε καὶ δούλων.

Ἃ δ' ἂν ἐν θεραπείῃ ἢ ἴδω, ἢ ἀκούσω, ἢ καὶ ἄνευ θεραπηίης κατὰ βίον ἀνθρώπων, ἃ μὴ χρή ποτε ἐκλαλέεσθαι ἔξω, σιγήσομαι, ἄρρητα ἡγεύμενος εἶναι τὰ τοιαῦτα.

Ὅρκον μὲν οὖν μοι τόνδε ἐπιτελέα ποιέοντι, καὶ μὴ ξυγχέοντι, εἴη ἐπαύρασθαι καὶ βίου καὶ τέχνης δοξαζομένῳ παρὰ πᾶσιν ἀνθρώποις ἐς τὸν αἰεὶ χρόνον. παραβαίνοντι δὲ καὶ ἐπιορκοῦντι, τἀναντία τουτέων.

Curriculum Vitae

Papadopoulou Dimitra

Research Experience - Education

11/2016- Today PhD candidate. B.S.R.C. Fleming, National and Kapodistrian University of Athens, Greece. Research Project: "Identifying new small molecule inhibitors for the therapy of Chronic Inflammatory Diseases- Developing of a novel screening pipeline". - Research Team of Prof. G. Kollias, Institute for Bioinnovation.

10/2012- 10/2016 Research Assistant, B.S.R.C. Fleming, Vari, Greece - Research Team of Prof. G. Kollias, Institute for Bioinnovation.

09/2011- 09/2012 Master of Biomedical Research, Medical School, Imperial College London (UK), Grade High Merit. Research projects: a. "Mesenchymal Stem Cells and Chemokines". - Research team of Prof. S.Rankin, National Institute of Heart & Lung. b."Protein crystallization and its role in healing". - Research Team of Prof. N.Chayen, Department of Surgery & Cancer.

07/2011 Graduate of the Department of Biology, Aristotle University of Thessaloniki, Greece. Grade 7.68/ 10.

04/2011- 07/2011 3-month Erasmus funded internship, Aberystwyth University (U.K.). Research project "Genetic development of plants". - Research Team of Prof. J.Doonan, Institute of Biological, Environmental and Agricultural Sciences.

2009-2010 Undergraduate Diploma Thesis, Department of Biology, Aristotle University of Thessaloniki, Greece. Research Project: "DNA barcoding of Labiatae family plants of the Siniatsikon mountain and the National Park of Pindos". - Research team of Assistant Prof. K.Vlachonassios and R. Karousou, Department of Botany.

Publications

- **Papadopoulou D**, Roumelioti F, Tzaferis C, Chouvardas P, Pedersen AK, Charalampous F, Christodoulou-Vafeiadou E, Ntari L, Karagianni N, Denis M, Olsen JV, Matralis AN, Kollias G. Repurposing of Amisulpride, a known antipsychotic drug, to target synovial fibroblasts activation in arthritis. BioRxiv 2022. doi: https://doi.org/10.1101/2022.08.02.500956

- Roumelioti F, Tzaferis C, Konstantopoulos D, **Papadopoulou D**, Prados A, Sakkou M, Liakos A, Chouvardas P, Meletakos T, Pandis Y, Karagianni N, Denis M, Fousteri M, Armaka M, Kollias G. miR-221 / 222 drive synovial fibroblast expansion and

pathogenesis of TNF-mediated arthritis. BioRxiv 2022. doi: https://doi.org/10.1101/2022.07.22.500939

- **Papadopoulou D**, Drakopoulos A, Lagarias P, Melagraki G, Kollias G, Afantitis A. *In silico* Identification and Evaluation of Natural Products as Potential Tumor Necrosis Factor Function Inhibitors Using Advanced Enalos Asclepios KNIME Nodes. Int J Mol Sci. 2021 Sep 23;22(19):10220. doi: 10.3390/ijms221910220

- Ntari L, Nikolaou C, Kranidioti K, **Papadopoulou D**, Christodoulou-Vafeiadou E, Chouvardas P, Meier F, Geka C, Denis MC, Karagianni N, Kollias G. Combination of subtherapeutic anti-TNF dose with dasatinib restores clinical and molecular arthritogenic profiles better than standard anti-TNF treatment. J Transl Med. 2021 Apr 23;19(1):165. doi: 10.1186/s12967-021-02764-y.

- Melagraki G, Ntougkos E, **Papadopoulou D**, Rinotas V, Leonis G, Douni E, Afantitis A, Kollias G. *In silico* Discovery of Plant-Origin Natural Product Inhibitors of Tumor Necrosis Factor (TNF) and Receptor Activator of NF-κB Ligand (RANKL). Front Pharmacol. 2018 Jul 25;9:800. doi: 10.3389/fphar.2018.00800.

- Camargo A, **Papadopoulou D**, Spyropoulou Z, Vlachonasios K, Doonan JH, Gay AP. Objective definition of rosette shape variation using a combined computer vision and data mining approach. PLoS One. 2014 May 7;9(5):e96889. doi: 10.1371/journal.pone.0096889.

Conferences

- Oral Presentation "*Repurposing of a known antipsychotic drug to target arthritogenic synovial fibroblasts*". **D. Papadopoulou**, F. Roumelioti, V. Mavrikaki, C .Tzaferis, F. Charalampous, N. Karagianni, M. Denis, A. Matralis, and G. Kollias. 1st International Conference on Mesenchymal Cells in Health & Disease (Chania, Crete, June 2022)

- Poster "Repurposing of a known antipsychotic drug to target arthritogenic synovial fibroblasts and scaffold-based design of novel small molecule therapeutics". **D. Papadopoulou**, V. Mavrikaki, F. Charalampous, F. Roumelioti, C. Tzaferis, N. Karagianni, M. Denis, A. Matralis, G. Kollias. 41st European Workshop for Rheumatology Research (Vienna, Austria, May 2022)

- Poster "Identification of RA therapeutics using a novel *in silico* screening approach". **D. Papadopoulou**, P. Chouvardas, E. Christodoulou-Vafeiadou, M. C. Denis, V. Koliaraki, N. Karagianni, G. Kollias, WPC Europe conference (Lisbon, Portugal, November 2017).

- Poster "An integrated cheminformatics pipeline for the discovery of small-molecules dual inhibitors of TNF and RANKL". **D. Papadopoulou**, G. Melagraki, E. Ntougkos, V. Rinotas, E. Douni, A. Afantitis and G. Kollias, 37th EWRR (Athens, Greece, March 2017)

- Poster "Niche-specific chemokine receptor expression of mesenchymal stromal cells" M. François, **D. Papadopoulou** and S. Rankin. Gordon Conference: Chemotactic cytokines (Italy, May 2012)

- Poster and Oral Presentation "The use of the chloroplastic matK region as DNA barcode in the plants of the Labiatae family of Mount Siniatsikon". **Papadopoulou D.**, Karousou R. and Vlachonasios K. 32nd Annual Scientific Conference - Hellenic Society of Biological Sciences, (Karpenisi, Greece, May 2010)

Awards

- Oral presentation award, 1st International Conference on Mesenchymal Cells in Health & Disease (Chania, Crete, June 2022)

- Travel grant, 41st European Workshop for Rheumatology Research (Vienna, Austria, May 2022)

- Travel grant, MouseAGE -Training School, Drug Discovery and Development (Novartis, Basel, Switzerland, October 2017)

Workshops

- **1st LAS Core Modules Course**, Animal handling and ethical regulations (Athens, Greece, July 2020)

- **UCSC Genome Browser Workshop** (Athens, Greece, January 2019)

- **ELIXIR-GR Software Carpentry Workshop**, Basic principles of bioinformatics programming (Athens, Greece, January 2019)

- **MouseAGE -Training School, Drug Discovery and Development,** (Novartis, Basel, Switzerland, October 2017)

Other skills

- English: Excellent level, Certificate of Proficiency in English, University of Michigan

- French: Satisfactory level, Diploma d'études en Langue Française- DELF (Unit A1, A2, A3, A4), L 'Institut Francais.

- European Computer Driving License

- Diploma of Professional School of Dance

Acknowledgments

A lot of people deserve many thanks for all the moments spent in research related to this thesis.

First of all, I would like to thank my supervisor, Professor George Kollias for his continuous support and advice. He made me believe in myself and guided me to be a more determined first human and then, scientist.

I would also like to thank the rest members of my advisory committee, Professor Koutsilieris and Dr Filippou, for their time and academic support throughout the years of my work.

Of course, all the rest members of the seven –member committee also invested time and thought, and I really appreciate that.

My big thanks go also to past and current members of Kollias lab and especially to Alex, Ana, Lida, Fani, Filippos, Lydia and Emilios, who except from excellent colleagues, they have been real friends during happy and not moments.

Also, I would like to thank Vaso and Alexis for their support during the project. On the one hand, Dr V. Koliaraki, has been my mentor, learning me selflessly how to think and work in research. Dr A. Matralis, on the other hand, apart from his great input in the final results of this thesis, he has spent time and effort, for me to understand the "chemical" part of the project and to connect it with biology experiments.

Finally, I want to thank my partner in life, Tasos, for our scientific "home" discussions, but mainly for his love, support, and hug that can easily take all anxiousness away.

Last but not least, I want to thank my parents, Akis and Christina, for their unconditional love and discreet presence throughout my life, standing by me in all my crazy and challenging dreams and goals.

Σας ευχαριστώ πολύ!

Δ.

Table of Contents

Abbreviations

Col15a1	Collagen Type XV Alpha 1 Chain
3R	Replacement, reduction and refinement
5-HT	Serotonin receptor
ACPAs	Anti-citrullinated protein antibodies
ADAM17/ TACE	Disintegrin And Metalloproteinase Domain-Containing Protein
ADMET	Absorption, Distribution, Metabolism, Elimination, Toxicity
ADP	Adenosine di-phosphate
AIA	Adjuvant-induced arthritis
AMP	Adenosine monophosphate
AP-1	Activator protein-1
ASCC3	Activating signal cointegrator 1 complex subunit 3
ATP	Adenosine triphosphate
AXIN	Axis inhibition protein
Bach1	BTB Domain And CNC Homolog 1
Bmp4	Bone Morphogenetic Protein 4
CAIA	Collagen antibody-induced arthritis mode
CAM	Calmodulin
CCL	C-C motif chemokine ligand
CD	Crohn's disease
Cdc42	Cell division cycle 42
CETSA	Cellular ThermoStability Assay
c-FLIP	Cellular FLICE-inhibitory protein

CIA	Collagen induced arthritis
cIAP1/2	Cellular Inhibitor of Apoptosis Protein 1
CID	Chronic Inflammatory Diseases
CNS	Central nervous system
Coch	Cochlin
Col15a1	Collagen Type XV Alpha 1 Chain
Comp	Cartilage Oligomeric Matrix Protein
Cox5a	Cytochrome *c* oxidase 5A
CXCL	C-X-C motif chemokine ligand
DIA	Data-independent acquisition
DKK1	Dickkopf WNT Signaling Pathway Inhibitor 1
Dlx3	Distal-Less Homeobox 3
DMARDs	Disease-modifying antirheumatic drugs
DRD	Dopamine receptor
ECM	extracellular matrix
ELISA	enzyme-linked immunosorbent assay (ELISA)
EMA	European Medical Agency
ENT1	Extracellular Nucleoside Transporter 1
Epcam	Epithelial Cell Adhesion Molecule
ER	Endoplasmic reticulum
FACs	Flow cytometry
FADD	FAS-associated death domain protein
Fbln1	Fibulin 1
FDA	US Food and Drug Administration

FLS	human rheumatoid arthritis fibroblasts
G6PI	glucose-6-phosphate isomerase
Glu	Glutamic acid
GMCSF	Granulocyte- Macrophage Colony- Stimulating Factor
GO	Gene ontology
GWAS	Genome wide association studies
Hhip	Hedgehog Interacting Protein
hTNFtg	Human Tumor Necrosis Factor transgenic
Hyou1	Hypoxia upregulated 1
IFNs	Interferons
IL	Interleukin
IL6R	Interleukin 6 Receptor
IREs	Interferon response elements
IκB	Inhibitor of nuclear factor kappa B
JNK	c-Jun N-terminal kinases
K/bxn	Mice with T cell receptor transgene KRN and MHC class II molecule A(g7)
Kct2	Keratinocyte-Associated Transmembrane Protein 2
KEGG	Kyoto Encyclopedia of Genes and Genomes
Kif5c	Kinesin heavy chain isoform 5C
Klf	Kruppel Like Factor
KRN	T cell receptor recognising bovine RNase
Leu	Leukine
LL	Lining layer
LUBAC	Linear ubiquitin chain assembly complex

Ly6α	Ly6a lymphocyte antigen 6 complex
MAPK	Mitogen-activated protein kinases
MHC	Histocompatibility complex
MLKL	Mixed lineage kinase domain like pseudokinase
MMPs	Metalloproteinases
mRNA	Messenger RNA
MW	Molecular weight
NF-κB	Nuclear factor kappa-light-chain-enhancer of activated B cells
NIK	Mitogen-Activated Protein Kinase Kinase Kinase 14
Notch	Notch Receptor 1
Npnt	Nephronectin
NPs	Natural products
p100/ p52	Nuclear Factor Kappa B Subunit 2
p38	Mitogen-Activated Protein Kinase 14
p50	Nuclear Factor Kappa B Subunit 1
p65	destabilizing complex I and leading p50/RelA
p65	Nuclear Factor Of Kappa Light Polypeptide Gene Enhancer In B-Cells
PDGFRa	Platelet Derived Growth Factor Receptor Alpha
PDPN	Podoplanin
Phe	Phenylanine
PI staining	Propidium Iodide staining
Pi16	Peptidase Inhibitor 16
Pmcs	Peritoneal macrophages
PPI	Protein-protein interaction

PS residues	Phosphatidylserine residues
PsA	Psoriatic Arthritis
QSAR	Quantitative structure–activity relationship
RA	Rheumatoid arthritis
Rag1	Recombination Activating 1 gene
Relb	V-Rel Avian Reticuloendotheliosis Viral Oncogene Homolog B
RF	Rheumatoid factor
RIPK	Receptor interacting serine/threonine-protein kinase
Romo1	Reactive oxygen species modulator 1
ROS	Reactive oxygen species
Runx1	Runt-Related Transcription Factor 1
SAR	Structure–activity relationship
Sca1	Stem cells antigen-1
scATAQ	Assay for Transposase Accessible Chromatin
SCID	Severe combined immunodeficiency disease
SEC62	Translocation protein I
SF	Synovial fibroblast
SFRP2	Secreted Frizzled Related Protein 2
SL	Sublining layer
SLE	Systemic lupus erythematosus
Sox	SRY-Box Transcription Factor
SPF	Specific-pathogen-free
STIA	Serum transfer induced arthritis
SYK	Spleen tyrosine kinase

TAB	TGF-Beta Activated Kinase 1 Binding Protein
TAK	Transforming Growth Factor-Beta-Activated Kinase
TCR	T cell receptor
TCZ	Tocilizumab
TH17	T-helper
TLR	Toll-like receptor
TNF	Tumor Necrosis Factor a
TNFR	Tumor Necrosis Factor Receptor
TRADD	Tumor Necrosis Factor Receptor Type 1-Associated Death Domain Protein
TRAF	Tumor Necrosis Factor Receptor Associated Factor
Treg	T regulatory
Tyr	Tyrosine
UMAP	Uniform manifold approximation and projection
WNT	Wingless-related integration site
WT	Wild type
Zap-70	SH2 domain of the ζ-associated protein of 70 kDa gene
ZIA	Zymosan- induced arthritis
IKK	Inhibitor Of Nuclear Factor Kappa B Kinase Regulatory Subunit Gamma
NEMO	NFκB essential modulator

1. Introduction

1.1 Chronic Inflammatory Diseases- Pathophysiology and aetiopathogenesis of Rheumatoid arthritis

Chronic inflammatory disorders, such as rheumatoid arthritis (RA), Crohn's disease (CD), inflammatory bowel disease, and psoriasis, have been associated with deregulated inflammatory responses to multiple cytokines, which induce immune infiltration and fibroblast activation, leading to tissue damage[1].

Rheumatoid arthritis (RA) is a chronic inflammatory disease characterized by swelling and gradual destruction of the joints, that is marked by increased proliferation of resident mesenchymal cells (paw formation) and influx of the inflammatory milieu in the joint area, supported by increased angiogenesis[2].

RA disease can be met in a prevalence of 0.5–1.0% in average in Western world, although geographic variation has been reported[3]. In general, women are more likely to develop disease which could be attributed partially to the effects that oestrogens could have in the immune system regulation. The hormonal influence in RA development remains under controversy, despite that women with early disease onset present usually disease remission during pregnancy and that in most cases symptoms do develop during menopause[4]. The most common cause of RA related death is the cardiovascular disease, which presents high incidence in RA patients as they often suffer from hypertension, diabetes mellitus and hyperlipidaemia. Mutations at specific genetic loci have been also associated with increased risk of cardiovascular disease in RA individuals[5].

Several RA patients' pathotypes exist, characterized by variable clinical manifestations and different pathogenetic mechanisms. A part of RA patients is characterised by blood autoantibodies detection and is known as "seropositive". Dysregulation of immune responses were described as causal for RA even in early '40s by H.M. Rose[6]. In "seropositive" patients autoantibodies against immunoglobulin G, also referred as rheumatoid factor (RF), and against citrullinated proteins, also known as anti-citrullinated protein antibodies (ACPAs), can be detected and can be used as diagnostic biomarkers.
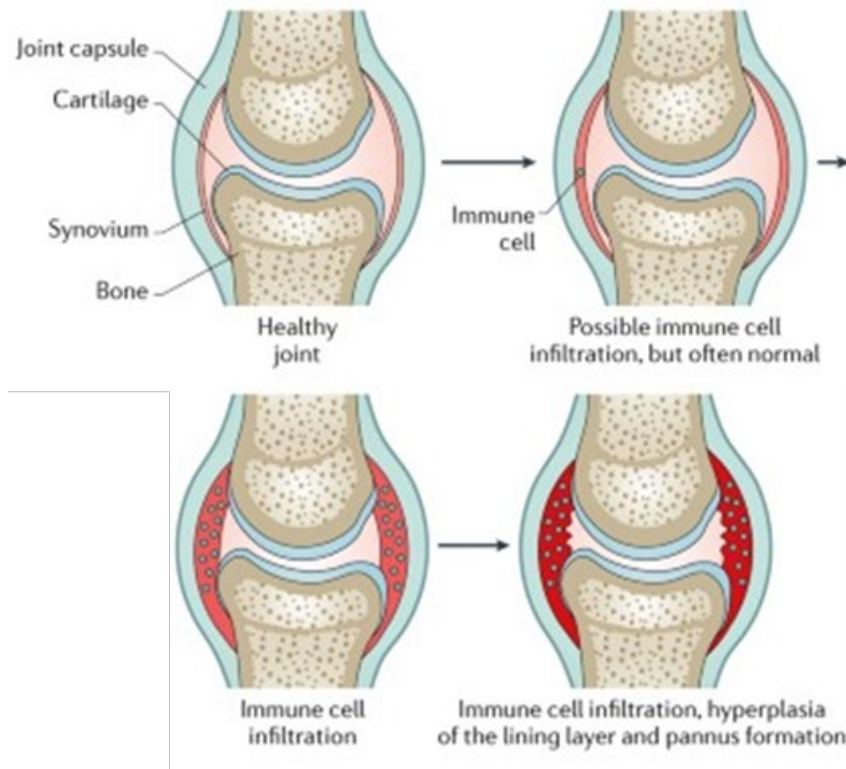
Image 1 Development of RA disease includes immune cell infiltration and synovial hyperplasia that leads to pannus formation, along with cartilage and bone destruction. (Adapted from Smolen *et al.*, 2018)[7]

However, autoantibodies detection is not universal, and other individuals are characterized as "seronegative"[7]. RA pathotypes can be further subdivided in lymphoid, myeloid, low-inflammatory, and fibroid based on the cell type that is mainly abundant in the patients 'synovium. This molecular and cellular heterogeneity in RA patients impacts clinical response to therapies targeting different biological pathways[8].

RA is a multifactorial disease and it can be attributed to a combination of several environmental factors that can trigger disease emergence in individuals with genetic susceptibility. Environmental triggers include but are not limited to smoking, infectious agents, vitamin D deficiency, obesity and microbiota features[9]. Genetic background has also been studied as crucial for RA development, although differences have been found between "seropositive" and "seronegative" patients. Genome-wide association studies (GWAS) have identified candidate gene variants as RA susceptibility loci, revealing new candidate targets for the development of new therapeutics[10]. Understanding disease underlying mechanisms, involving intersection of high-risk genetic loci, together with epigenomic marks, and influence of environmental factors that drive a molecular cascade inducing synovial cells activation, could enable stratification of RA patients, leading to effective prediction of response to

therapeutics[7] (Image 2).
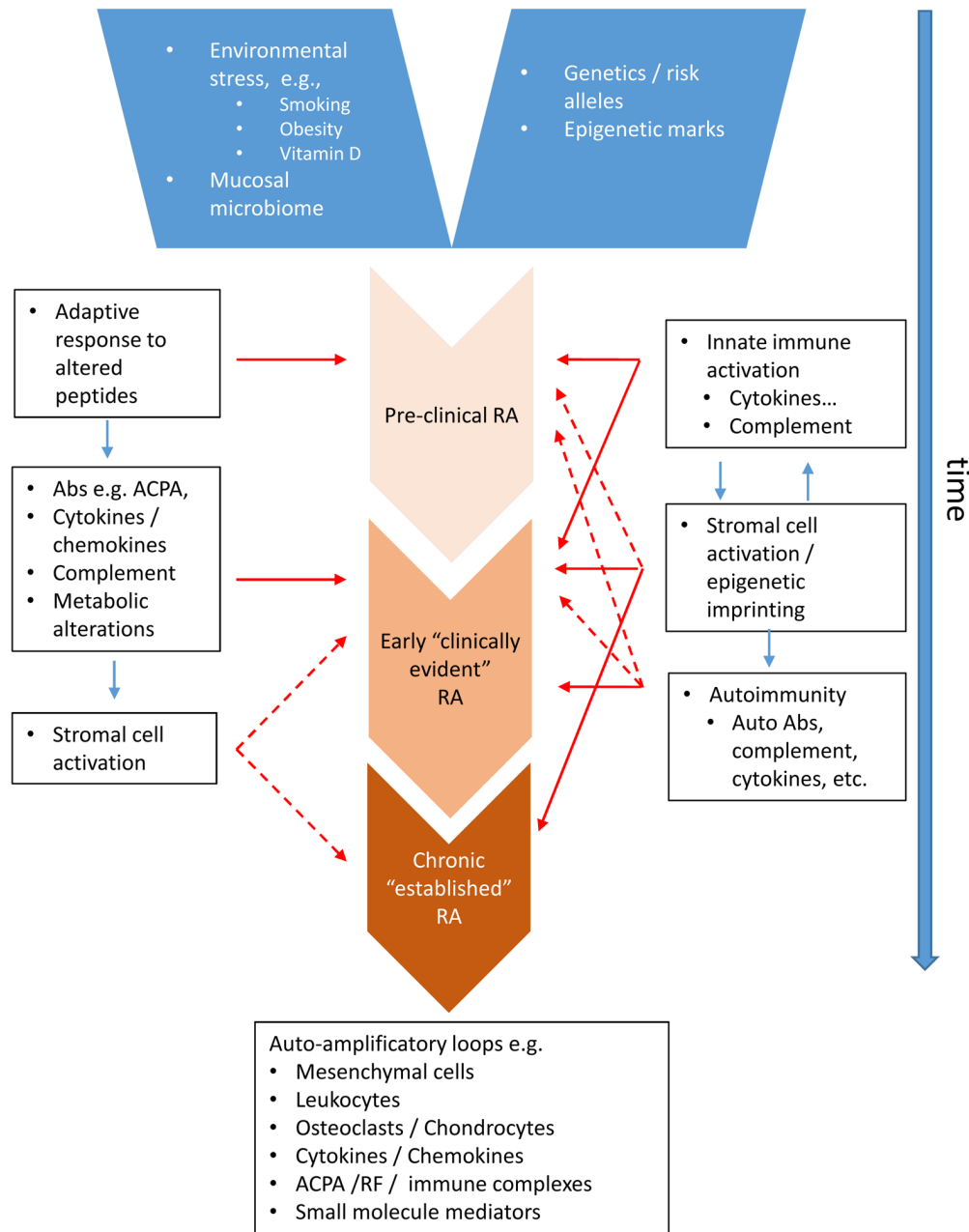
Image 2 Several models have been proposed for the events that lead to RA development. Here, in the model described at the left, an early phase before RA development occurs, including generation of autoantibodies (ACPAs) that bind self-proteins, particularly via citrullination, followed by increase in the cytokines and chemokines levels, and by deregulation of complement elements and metabolism. An environmental stimulus leads subsequently to increased inflammation along with stromal activation. In model described at the right, there is a pre-RA interplay between immune and stromal compartment, driving stromal cell activation. Chronic inflammation can arise after the interaction of the aforementioned events, however it can itself further amplify causal disease events. Both models are not exclusive to each other, as events can intersect, creating several complicated loops. (Adapted from Firestein and MacInnes, 2017)[6]

1.2   Cytokines in Rheumatoid Arthritis

The pathogenesis of RA has been linked to cooperative activation of cells deriving from the myeloid, stromal and lymphoid lineage.

Circulating cytokines control cellular activation and drive deregulation of tissue homeostasis leading from systemic to restrained inflammation[11]. It is believed that cytokines profile drives the disease establishment and can diverse patients' pathotypes, determining the response to therapy and the probability of future disease relapse (Image 3).

A plethora of different cytokines are present in joints of RA patients. These include among others Tumor Necrosis Factor (TNF), several Interleukins (ILs) such as IL6, IL1, IL17, IL23, IL27, IL21, IL8, Interferons (IFNs), Granulocyte- Macrophage Colony- Stimulating Factor (GM-CSF).
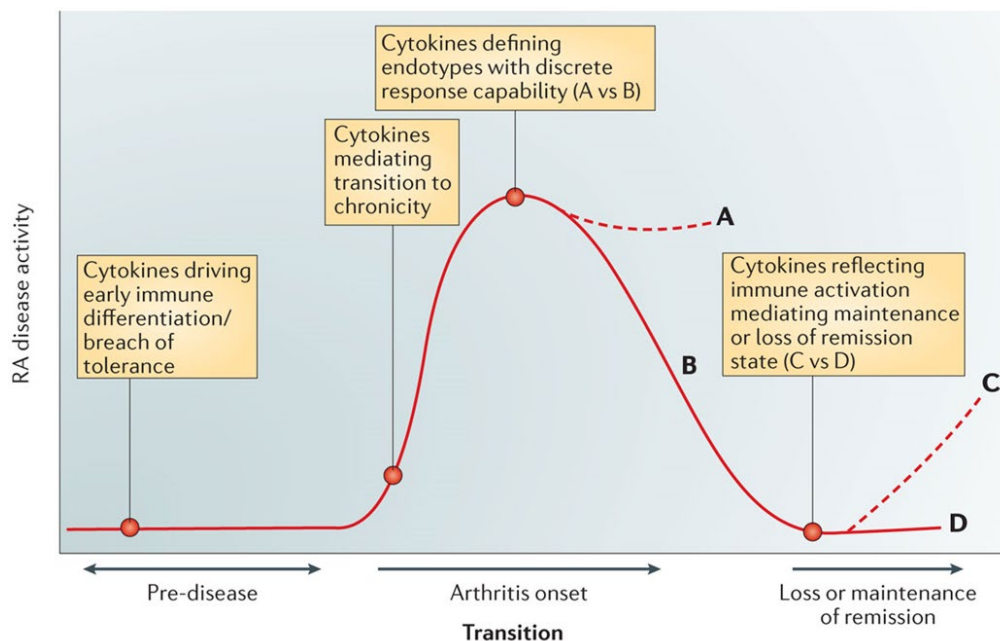
Image 3 Cytokines drive the disease progression and the response to current therapeutics. For instance, diverse cytokine signatures, eg. elevated levels of IL1, IL6, TNF, etc, can classify the patients into A. non- responders and B. responders to current therapeutics. While in remission, RA disease can then relapse, as indicated in C or persist in remission, as described in D. (Adapted from McInnes, I. B. *et al.*, 2015)[11]

IL6 has been reported to participate in both the innate and the adaptive phase of RA progression. Several cell types produce IL6, including monocytes, T-lymphocytes, fibroblasts, and endothelial cells, and its production is strongly enhanced at sites of inflammation. As to innate immunity, IL-6 promotes leukocytes' infiltration as well as neutrophils' and monocytes' migration to the affected joints, while it facilitates endothelial and stromal cell activation.

Regarding the adaptive immunity phase, IL6 regulates the transition of T cells from the naive state into the T-helper (T_H17) or to T regulatory (Treg) state. IL6 has been reported to be able to function through direct or distant interaction with its main receptor (IL6R), which can be found in two forms, transmembrane and circulating. Gp-130 is also a co-receptor of IL6 that facilitates direct or indirect binding to IL6R[12,13]. To date IL-6 function in RA has been successfully inhibited through Tocilizumab (TCZ), which is a humanized anti-IL6 receptor subunit alpha (anti-IL6R) monoclonal antibody. TCZ is blocking effectively both the cis- and the trans-function of IL6, regulating joint inflammation but also comorbidities of RA, such as fatigue, anaemia, bone loss, depression, type 2 diabetes, and cardiovascular diseases[14].

IL-17A levels have also been correlated with RA disease severity and this cytokine has been described to lead the release of additional proinflammatory cytokines, chemokines and matrix metalloproteinases (MMPs) while it promotes osteoclast activation and angiogenesis, helping in apoptosis resistance of RA fibroblasts (FLS)[15]. A loop that underlies IL17 production suggests that IL-6 is necessary for IL17 production, while IL-17 leads to IL-6 production by FLSs. This loop is maybe the basis of the failure of IL17 inhibitors as RA therapeutics.

Concerning IL1, although multiple IL1 family members (IL-1α, IL-1β, IL-1Ra, IL-18, IL-33 and IL-36) can be found in the affected joints of RA patients, IL-1 blockers have not produced promising results as therapeutics[16]. This points out that IL-1 is not placed in the top of the disease molecular cascade, rather than IL-1 is not implicated in the RA development[17].

Discussing further for implicated interleukins in RA disease, IL12 family interleukins (IL12, IL-23, IL27 and IL35) share receptors' components and molecular cascades[18]. IL23 (consisting of IL12p40 and IL23p19 subunit) seem to play a role in regulating T_H17 transition into the pathogenic state, while IL-27 (consisted of subunits EBI3 and p28) can either inhibit T_H17 cell differentiation or promote T_H1 cell development, regarding the T cell maturation state. Additionally, IL-12 (consisted of subunits p40 and p35) and IL-23 (consisted of subunits p40 and p19) are predominantly proinflammatory, and on the other hand IL-35 (consisted of subunits EBI3 and p35) is regulating immune response. Probably, due to the aforementioned balancing intersection of functions, inhibitors of IL12 family cytokines have not presented clinical success.

Interferons are also active in the RA synovium to modulate mainly leukocytes subsets[19]. However, IFNs have been rather used in identifying prognostic biomarkers, as interferon response elements (IREs) can be identified in RA patients' blood, than as successful drug targets.

GM-CSF has also been found elevated in the serum, synovial fluid and bone marrow of patients with RA. It is known to regulate inflammatory activation of macrophages, neutrophils and dendritic cells, driving downstream cytokines' release, that facilitates immune cells' influx and stromal cell activation in the affected tissues[20]. The use of Mavrilimumab, a human monoclonal antibody that inhibits GM-CSF receptor-α, indicated encouraging results in phase II clinical trials for RA disease[21].

1.3 Tumor Necrosis Factor in Chronic Inflammatory Diseases

One of the predominant cytokines that has been linked to RA aitiopathogenesis is Tumor necrosis factor (TNF)[11].

TNF is a soluble cytokine, which belongs to the tumor necrosis family of homotrimeric proteins[22,23]. TNF functions through two receptors: TNFR1/ p55 and TNFR2/ p75. After the protein trimer has been formed, TNF binds to its receptors, leading, respectively, to the initiation of several inflammatory signaling pathways (e.g., NF-κB, JNK, p38-MAPK)[1]. TNF can be found in two forms, soluble and transmembrane. Transmembrane TNF can be enzymatically processed into the soluble form by TNF-α-converting enzyme (TACE), also known as ADAM17. Soluble TNF binds mainly to TNFR1, while transmembrane TNF binds to TNFR2. Pathways implicated in TNF signaling through both receptors are described in brief below (Image 4).

TNFR1 activation leads to the recruitment of "complex I" that includes DD-containing adaptor molecules, such as TRADD and RIPK1, but also TRAF2. The latter is associated further with E3 ubiquitin ligases cIAP1/2, promoting the attachment of ubiquitin to lysine residues of various proteins, including RIPK1 and cellular inhibitor of apoptosis (cIAP)1/2[24]. The ubiquitination of RIPK1 enables recruitment of TAK1 in the TAB2/3 complex and of LUBAC[25]. LUBAC complex can with its turn lead NEMO poly-ubiquitination in the complex I of IKK1/IKK2. TAK1 phosphorylates IKK2, which then phosphorylates IκB, that results in the proteasomal degradation of transcription factor NF-κB, destabilizing complex I and leading p50/RelA (p65) translocation into the nucleus with subsequent activation of various proinflammatory genes that contain NF-κB- specific binding sites. Another TAK1-mediated mechanism through the complex TAK1/TAB2/TAB3 and NEMO-IKK1/2 leads to further proinflammatory gene up-regulation, including phosphorylation of MAPK, such as JNK, p38 and AP-1 complex[26].

Except from the induction of the proinflammatory milieu, TNF-TNFR1 can also lead to two

different programmed cell death cascades, apoptosis and necroptosis. Deubiquitinated RIPK1 and TRADD detach from membrane complex I and form a complex II in the cytoplasm, that consists of FADD and cellular c-FLIP, activating a caspase-8 dependent apoptosis mode. Caspase inhibition leads to RIPK1/RIPK3/ MLKL-dependent necroptosis through breakage of the plasma membrane, leading to the influx of positively charged ions such as Ca2+, Na+, and K+ in the cytoplasm[27].

TNF-TNFR2 interaction, on the other hand, directly recruits TRAF1 or TRAF2 and cIAP1/2 molecules. LUBAC can also be recruited to TNFR2 through binding to cIAP1/2-generated K63-ubiquitin chains. LUBAC then recruits TAK1 and IKK complexes, leading to canonical NFκb signalling, as in the case of TNFR1. Alternatively, a TNFR2 mediated non-canonical NFκb signalling can be activated, through NIK kinase accumulation, which phosphorylates IKK1 complex and it subsequently processes p100[28]. Regulated proteolysis of p100, leads to nuclear translocation of p52/RelB heterodimer, activating nuclear transcription[29]. TNFR2 ligation drives also a TRAF2-MAPK-dependent activation of JNK[30].

The monomeric and dimeric forms of TNF are inactive, and thus, in order to block the TNF relevant signaling, the inhibition of the trimeric form of TNF has been suggested[31].
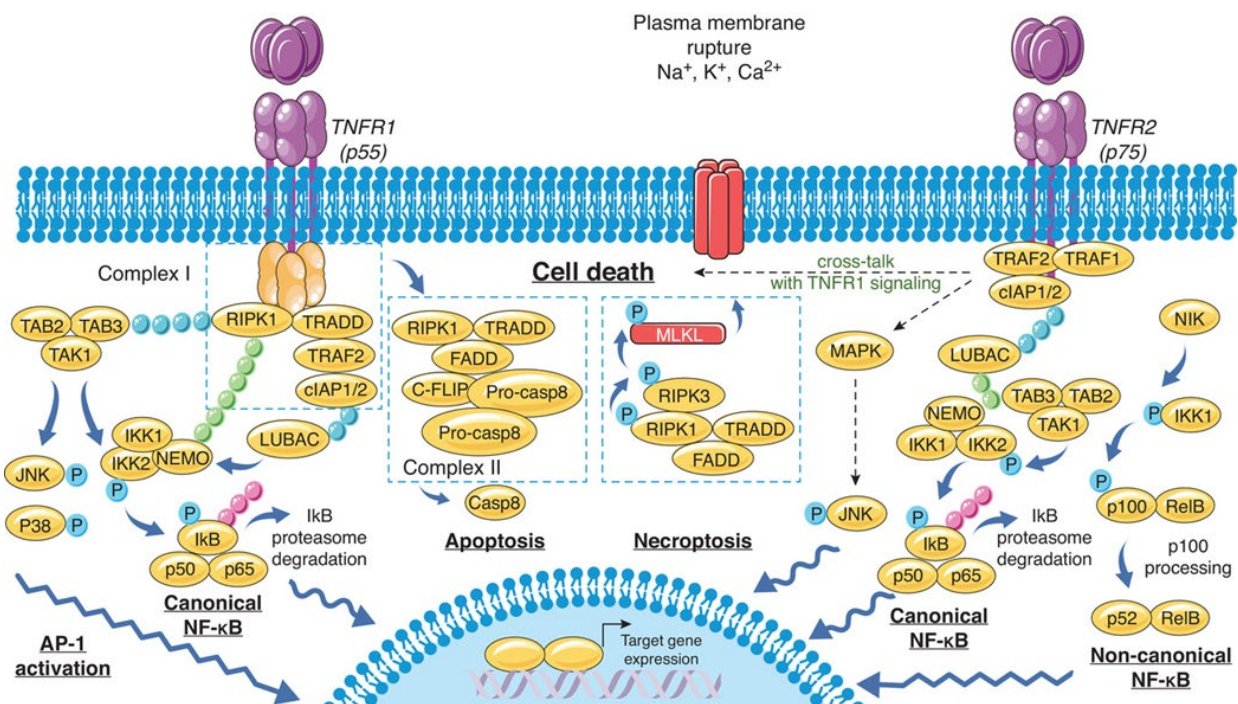

Image 4 TNF binding to its main receptors, TNFR1 and TNFR2, leads to alternative signaling cascades including NFkb pathway activation, apoptosis and caspases independent necroptosis. (Adapted from Atretkhany *et al*., 2020)[32]

Analyzing the TNF crystal structure, the inner part of each TNF monomer consists of hydrophobic residues, while the outer part constitutes the exposed surface of the cytokine. The top of the trimer presents polar interactions, with a possible salt bridge between Glu104 of one subunit and Arg103 of the other subunit. The center consists of hydrophobic contacts involving Tyr119, Leu57 and Leu157. Further hydrophobic interactions are present between Tyr59, Tyr119 and Tyr153 as well as Phe124 of an adjacent subunit. Finally, the bottom of the trimer contains a salt bridge between Lys11 of one subunit and the terminal carboxylate group of Leu156 of another subunit[23].

TNF has been broadly studied and reviewed in the literature[33–39], underlining the importance and the relevance of this growth factor as a valuable drug target.

In brief, TNF has been linked with anti-bacterial host defense, as in case of an infection it can lead to development of septic shock[40–42]. TNF is also regulating the organization of secondary lymphoid organs, as deletion of TNF or TNFR1 leads to impaired development of Peyer's Patches[43,44]. TNF/TNFR2 axis is involved in the maintenance of central nervous system (CNS) included in the protection mechanisms against neuroinflammation[45,46], while TNF/TNFR1 signaling is involved in inhibition of neurogenesis and maintenance of neuroinflammation[47]. Additionally, TNF has been studied in the context of chronic inflammation as mice, described in detail below, with a persistent overexpression of endogenous TNF develop intestinal inflammation and chronic polyarthritis, while overexpression of human TNF (*hTNFtg* mice) lead to chronic polyarthritis phenotype[48]. Interestingly, TNF blockade has been, to date, the most successful therapeutic in clinic against chronic inflammatory conditions[11].

1.4   Animal mouse models of RA disease

Animal models have been widely used to mimic human disease in order to understand the underlining molecular pathways and to find new potential therapeutics. Both the US Food and Drug Administration (FDA) and the European Medical Agency (EMA) require preclinical evaluation of any drugs in disease models in order to ensure their low drug toxicity and their efficacy profile. In RA there is a plethora of animal models, representing the different disease subtypes (depending on abundance of T cells, B cells, myeloid cells, fibroblasts, endothelial cells) and the variable clinical outcome of the disease[49]. The mostly used animal models in RA research are either induced or spontaneous and are described in summary below.

1.4.1 Induced animal models of RA disease

- *Adjuvant-induced arthritis model/ Pristane- induced arthritis*

Adjuvant-induced arthritis (AIA) is an induced rat model that was first developed upon an intradermal injection containing mycobacterial cell walls diluted in mineral oil. This model, however, it has been described as poorly describing RA disease, as it is characterized by acute systemic inflammation, that causes considerable issues for animal welfare[50]. A similar model, but in a closer resemblance with RA disease, induced in rat or mice, has been developed based on pristine, a component of mineral oil (pristane-induced arthritis model), being characterized by joints edema, accompanied by infiltration of inflammatory cells that leads to a chronic relapsing phase. Pristane- induced arthritis model is mainly dependent on the expression of histocompatibility complex (MHC) class II by T cells, thus it can be used for evaluation of therapeutics that affect T cell responses, leading to arthritis amelioration[51].

- *Zymosan-Induced Arthritis*

Another model induced in rats or mice by bacterial cell walls injection is zymosan- induced arthritis (ZIA). ZIA is caused by inoculation with an intra-articular injection of zymosan, an ingredient of the cell walls of Saccharomyces cerevisiae, causing mononuclear cell infiltration and pannus formation, depending on TLR2 activation[52]. The model is fast as the symptoms develop 3 days after the immunization, lasting for seven days, while relapse comes after 25 days.

- *Type II collagen induced arthritis (CIA)*

CIA model is an induced RA model, tested in DBA/1 mice, rats, rabbits and non-human primates. It is caused by an immunization with type II collagen diluted in complete Freund's adjuvant, leading to Th17 responses and to formation of antibodies against the joints collagens, causing joints inflammation and pain[53].

Although fast (onset of the disease at 12 days after immunization, peak of the disease at 30days) and close to human disease, as the animals develop RF and ACPAs, including as well a relapse course, this model is characterized by high variability, depending on the quality of the collagen type II used and on factors such as grouping stress that can even lead to arthropathy phenotype[54].

- *Collagen antibody-induced arthritis model (CAIA)*

Another induced model of arthritis in mice is CAIA, where the immunization is often based on inoculation with a commercial cocktail of monoclonal antibodies against epitopes of Collagen type II[55]. Moreover, the immunization can be performed using serum transfer from another immunized mouse or even by serum transfer from RA patients, that include relevant monoclonal antibodies[56]. The model is even faster that CIA (onset at 48h and the peak of the disease is reached at 7 days after immunization), characterized by full penetrance and by involvement of macrophages and fibroblasts but not of T and B cells. Although CAIA combine innate and adaptive responses, it does not fully recapitulate human disease as it does not at all implicate immune compartment. If a commercial antibody mix is used, different LOT numbers/ batches can also produce variable results.

- *Serum- transfer Induced arthritis (STIA)*

This model develops induced arthritis, but depending on a spontaneous model. The model is actually induced by the serum transfer of K/bxn model itraarticularly, which, as described in more details below, develops spontaneous arthritis by expressing both the T cell receptor (TCR) transgene KRN and the MHC class II molecule A(g7)[57]. Serum-Induced arthritis model reaches peak of the disease at about 14 days after induction and it can be applied in different mouse strains, although there is a variability in disease phenotype, depending on the strain.

- *Human chimeric transfer model*

Similarly to Serum-induced arthritis model, a chimeric model of human and mouse rheumatoid arthritis has been developed[58]. Severe combined immunodeficiency disease (SCID) mice are being implanted with synovial tissue isolated from RA patients, developing disease symptoms, characterized by pannus formation and cartilage destruction. The model is much slower to evolve, as 35 days after induction are required for the first histological bone erosion signs, while pannus invasion starts at day 105.

1.4.2 Spontaneous animal models of RA disease

- *K/BxN model*

Mice expressing both the T cell receptor (TCR) transgene KRN and the MHC class II molecule A(g7) (K/BxN mice) develop severe inflammatory arthritis, as they develop autoantibodies recognizing glucose-6-phosphate isomerase (G6PI)[59]. Although K/BxN mice lack rheumatoid factor (RF), while G6PI antibodies in RA patients remains debatable, this mouse model develops a plethora of similar characteristics to human RA, such as synovitis and fibroblasts proliferation, cartilage and bone destruction, polyclonal B cell activation, and autoantibody production. K/BxN mice spontaneously develop arthritis at 15 days after birth, while the peak of their disease is 3 months after. K/BxN serum is also used to induce arthritis in the Serum induced arthritis model, as described above.

- *IL-1ra-deficient mice*

Total knockout of Interleukin 1 (IL1) receptor in inflammatory- susceptible mouse strains leads to systemic upregulation of IL1, that leads to spontaneous T-cell dependent chronic arthritis development[60]. The mice are characterized by the presence of RF and by systemic upregulation of cytokines such as IL1, but also of IL6, TNF, IL17. Autoantibodies against collagen and double stranded DNA are also present. The onset of the disease is when mice are 5 weeks old and the peak of the symptoms comes at about 16 weeks after birth.

- *SKG mice*

Point mutation of the SH2 domain of the ζ-associated protein of 70 kDa gene (Zap-70), changes thymus T cell selection due to reduced TCR signaling, allowing T cells to travel to the periphery, leading to T-cell driven arthritis onset[61]. Disease of SKG mice is characterized by synovial hyperplasia, synovitis with infiltration of CD4+ T cells, invading pannus in cartilage and bone as well as by autoantibodies and RF serum presence. However, SKG arthritis is vulnerable to environmental factors, as mice in specific-pathogen-free (SPF) conditions do not develop arthritis[62]. The onset of the disease is at 2 months of age while the peak comes 8 months after birth.

- *TNF$^{\Delta ARE/+}$ mice*

TNF$^{\Delta ARE/+}$ mouse model develops chronic polyarthritis, a disease similar to human RA, due to chronic overexpression of endogenous mouse TNF. The mechanism of persistent TNF elevated levels depends on deletion of the AU rich regulatory elements in the 3'area of the TNF messenger RNA (mRNA), that controls its stability and its quantitative translation to the relevant protein[63]. TNF$^{\Delta ARE/+}$ mouse model develops additionally another inflammatory pathology, an enteropathy that mimics human Crohn's disease. The model presents 100% penetrance, however the first disease symptoms appear at 6 weeks of age, reaching the peak at about 16weeks after birth. Arthritis clinical and histological manifestations depend exclusively on TNF overexpression by SFs, while B and T cells are not necessary for disease generation and progression[63,64].

- *hTNFtg mice*

hTNFtg mouse model is a humanized mouse model that carries five copies of the human TNF transgene. Chronic TNF overexpression in this model is achieved by replacement of the 3' untranslated region of the hTNF transgene with the same region of the human β-globin gene (Image 5), that confers continuous stable mRNA expression[48]. The model develops chronic inflammatory polyarthritis, a disease similar to human RA and it was the first *in vivo* proof of the pathogenic role of TNF in RA.

Clinical arthritic phenotype is fully penetrant and first signs of pain and swelling, affecting the back joints, come at 3 weeks of age and develop gradually, reaching dyskinesia even in the front limbs at the age of 10weeks. Histological analysis of the affected joints is characterized by synovial hyperplasia, inflammatory cells' infiltration and cartilage destruction in the joint area, although RF is not detected in any stage of the disease (Image 5). Metalloproteases (MMPs) expression such as MMP-3, -9, -13 is also commonly elevated in both *hTNFtg* joints and in patients' affected areas[65]. Another typical characteristic of *hTNFtg* mice is gradual weight loss that leads to cachexia and death at about 12weeks of age. Neutralization of the arthritic phenotype with specific monoclonal antibodies against human TNF added further evidence that the pathology of the model is due to the deregulated expression of hTNF.

hTNFtg derived SFs show an activated phenotype, with upregulated proliferative, adhesive and migrating properties, expressing also high levels of inflammatory cytokines, characteristics also developed by RA FLS[66,67]. SFs have been found to be the driving force of

the pathology in *hTNFtg* mice, as they are the main producers of hTNF, while they are able to promote the pathogenesis of the disease in an immunodeficient Rag-/- background[68]. TNFR1 receptor expression on SFs seems indispensable for the pathology development, although the lack of TNFR1I signals does not appear to affect the onset of the disease[69,70].

Additional studies in *hTNFtg* mice provided further information on the pathophysiology of RA. Administration of antibodies against IL-1 receptor I, which inhibits the action of both IL- 1a and IL-1b, prevents the development of arthritic pathology, which emphasizes the position of IL-1, immediately after TNF, in phenotype regulation[71], while, although IL6 is elevated in *hTNFtg* serum , development of the disease in the absence of IL-6 does not appear to affect pathology[72].

Recent studies have shown that *hTNFtg* mice suffer also from TNF driven heart pathology with common characteristics to cardiac comorbidities that RA patients usually develop[73].

Despite the existence of all the aforementioned animal models, there is a necessity of new models design, allowing easy genetic manipulation and phenotyping. A database including systematic recording of "positive" and "negative" experimental data of the relevant animal models will allow their easier and more comprehensive evaluation in the scientific community. In this way, "reduction, replacement and refinement" (3Rs) of animal use in experimental protocols could be more easily attained, certifying animals' welfare and reduced cost[49].
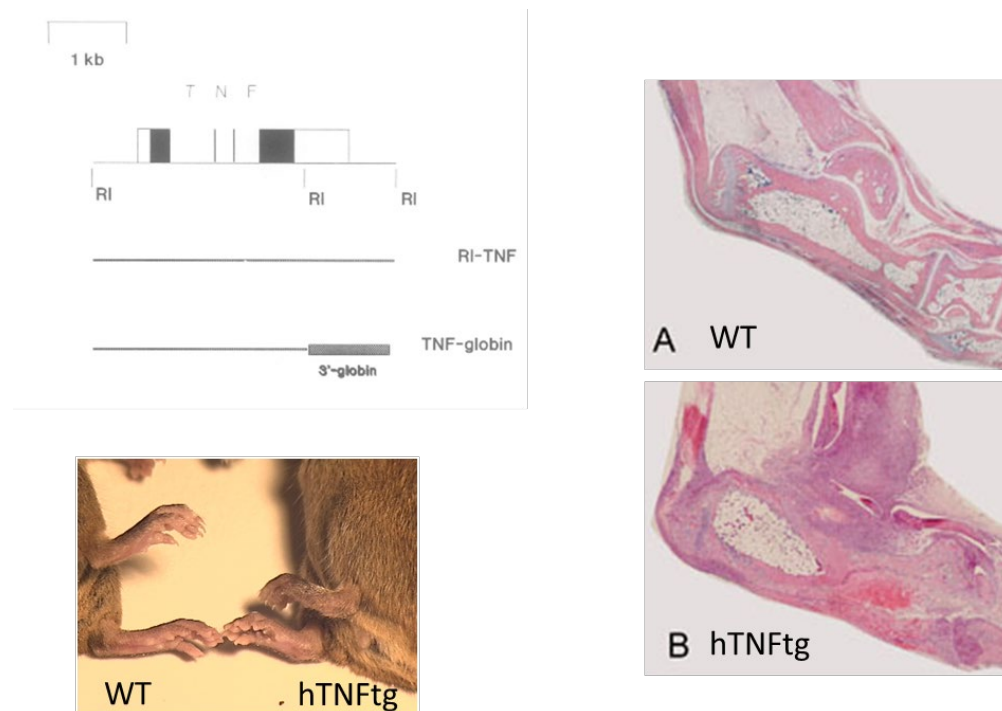
Image 5 *hTNFtg* mouse carries 5 copies of the *hTNFtg* transgene, developing clinical and histological characteristics of chronic polyarthritis, a disease that resembles human RA. (Image adapted and edited from Keffer *et al*., 1991)[48]

1.5   Fibroblasts in health and disease

Fibroblasts are non-hematopoietic, spindle-shaped, tissue resident cells which have been known to produce extracellular matrix proteins, but are also now known to play a multifunctional role in regulation of naïve and disease states (eg cancer, fibrosis, chronic inflammatory diseases)[74]. Fibroblasts can detect mechanistic or pathogen related activation of molecular cascades, that activate proinflammatory signals, while they regulate leukocytes infiltration, by producing several cytokines and chemokines. Initiating signals and tissue environment regulate fibroblasts' responses, shaping their function and thus, their response to several therapeutics[75].

Fibroblasts are mainly characterized by the absence of protein markers such as CD45 (myeloid-hematopoietic marker)/ CD31 (endothelial marker)/ Epcam (epithelial marker), and not by the presence of positive ones, such as Podoplanin (PDPN) or Platelet Derived Growth Factor a (Pdgfra), as these have been found both not uniform nor unique among several fibroblastic populations. Recently, single cell technologies have been used to identify positive markers of fibroblasts' clusters that present distinct roles in healthy and disease conditions[75,76].

Even in healthy tissues, fibroblasts have been found heterogenic and with distinct transcriptional profiles according to tissue location. For example, in the gut WNTa and WNTb are both expressed in the villi fibroblasts, but only WNTb is expressed in the lamina propria ones[77] (Image 6).
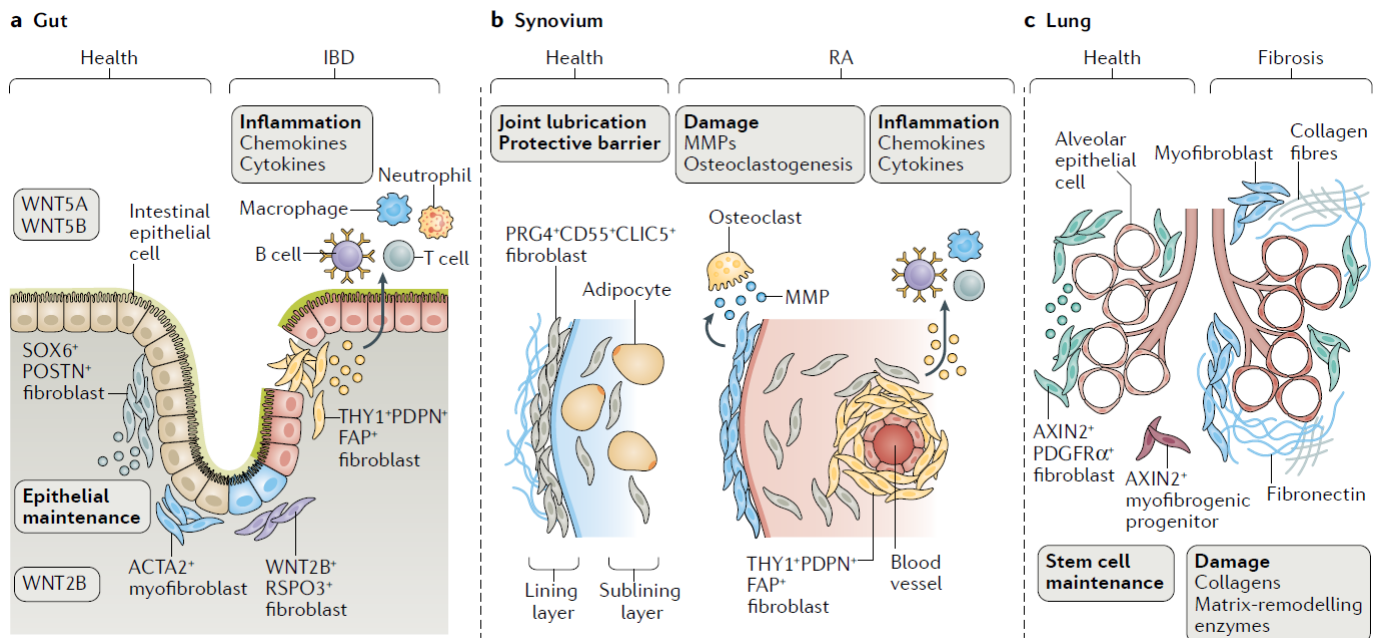

Image 6 Expression of molecular markers of fibroblasts in healthy and disease conditions. Fibroblastic markers of a. healthy and Inflammatory Bowel Disease gut, b. healthy and Rheumatoid Arthritis synovium and c. healthy and fibrotic lung. (Adapted from Davidson *et al.* ,2021)[75]

Similarly, in disease conditions, single cell analysis revealed that different transcriptomic profiles and molecular markers indicate fibroblasts with distinct roles. For instance, AXIN1+/ PDGFRa- fibroblasts lead fibrosis in lung disease, while AXIN1+/ PDGFRa+ fibroblasts support the alveolar epithelium in homeostatic conditions[78] (Image 6).

Interestingly, a fibroblast-specific single-cell atlas, compartmentalized fibroblasts into healthy state clusters and into activated subtypes at disease conditions[76]. Homeostatic clusters were identified by studying 16 healthy tissues (Lymph node, pancreas, muscle, tendon, mesentery, omentum, subcutaneous and visceral adipose tissue, artery, bone, heart, intestine, skin, lung, liver and spleen), generating an integrated Uniform manifold approximation and projection (UMAP). Across tissues 10 clusters of fibroblasts at healthy state were identified (Pi16$^+$, Col15a1$^+$, Ccl19$^+$, Coch$^+$, Comp$^+$, Cxcl12$^+$, Fbln1$^+$, Bmp4$^+$, Npnt$^+$ and Hhip$^+$). Notably, two cell clusters were found universally; a cluster that is Pi16^{high} and one that is Col15a1^{high}. Col15a1$^+$ universal cluster is characterised by an extracellular matrix proteins (ECM) related

transcriptomic profile, supporting its role in the secretion of main membrane proteins in tissue homeostasis. The Pi16^{+} cluster, on the other hand, expresses a variety of stemness related genes (eg Ly6α and Sca1), supporting its function at the basis of fibroblast differentiation[76]. Comparing the homeostatic profile with the diseased one Buechler *et al.*, studied 13 diseased tissues (Lymph node, pancreas, skin, muscle, joint, bone, heart, artery, liver, adipose tissue, intestine, lung). This approach identified ten fibroblastic clusters; Pi16^{+}, Col15a1[+], Ccl19^{+}, Cxcl12^{+}, Comp[+], Npnt[+], Hhip[+], Adamdec1[+], Cxcl5^{+} and Lrrc15^{+}. The Adamdec1[+] and Lrrc15^{+} clusters represented disease activated fibroblasts while the Pi16+, Col15a1[+] subpopulations were again universal across tissues in disease state.

In RA, Synovial fibroblasts (SFs) consist one of the main cell types in the joints, which have been extensively associated with RA progression as they produce inflammatory cytokines/ chemokines and degrading metalloproteinases, leading progressively to increased joint inflammation, stiffness and pain[2]. Importantly, TNF signalling in SFs has been found sufficient and necessary for chronic polyarthritis development in mice[64,69], while pathogenic fibroblasts were capable of initiating disease when transferred to the knees of healthy mice, even in the absence of immune compartment[68,79,80], underlining once more the dominant role of SFs in RA pathology initiation and progression (Image 7).

Recent studies revealed defined fibroblasts clusters in the arthritic joints of both mouse and humans.

Focusing on the STIA mouse model in the peak of inflammation, but also in human RA synovial biopsies, Croft *et al.* described markers of two main mesenchymal compartments in the synovial membrane of the joint, namely lining (LL) and sublining (SL) population, both of which hyperproliferate during RA disease progression[81] (Image 8). The lining population consist of fibroblasts, that have been found PDPN+/ FAPα+/ PRG4+/ CD90-, displaying destructive transcriptional signature, with upregulation of genes such as CCL9 and RANKL (inducers of osteoclastogenesis), Mmp3 and Mmp9 (degradating metalloproteinases). On the other hand, the sublining compartment, which is the most present in the arthritic joint, consist of PDPN+/ FAPα+ / CD90+ fibroblasts, regulating mainly the immune response, by high expression of cytokines and chemokines, such as IL6 and IL33. The aforementioned fibroblast clusters are located in different regions of the joint[82]; lining fibroblasts and lining CXCR3^{+} lining macrophages[83] form an outer layer close to the bones that internally adjusts to the sublining cluster, that except from fibroblasts include macrophages, adipocytes, etc (Image 8).
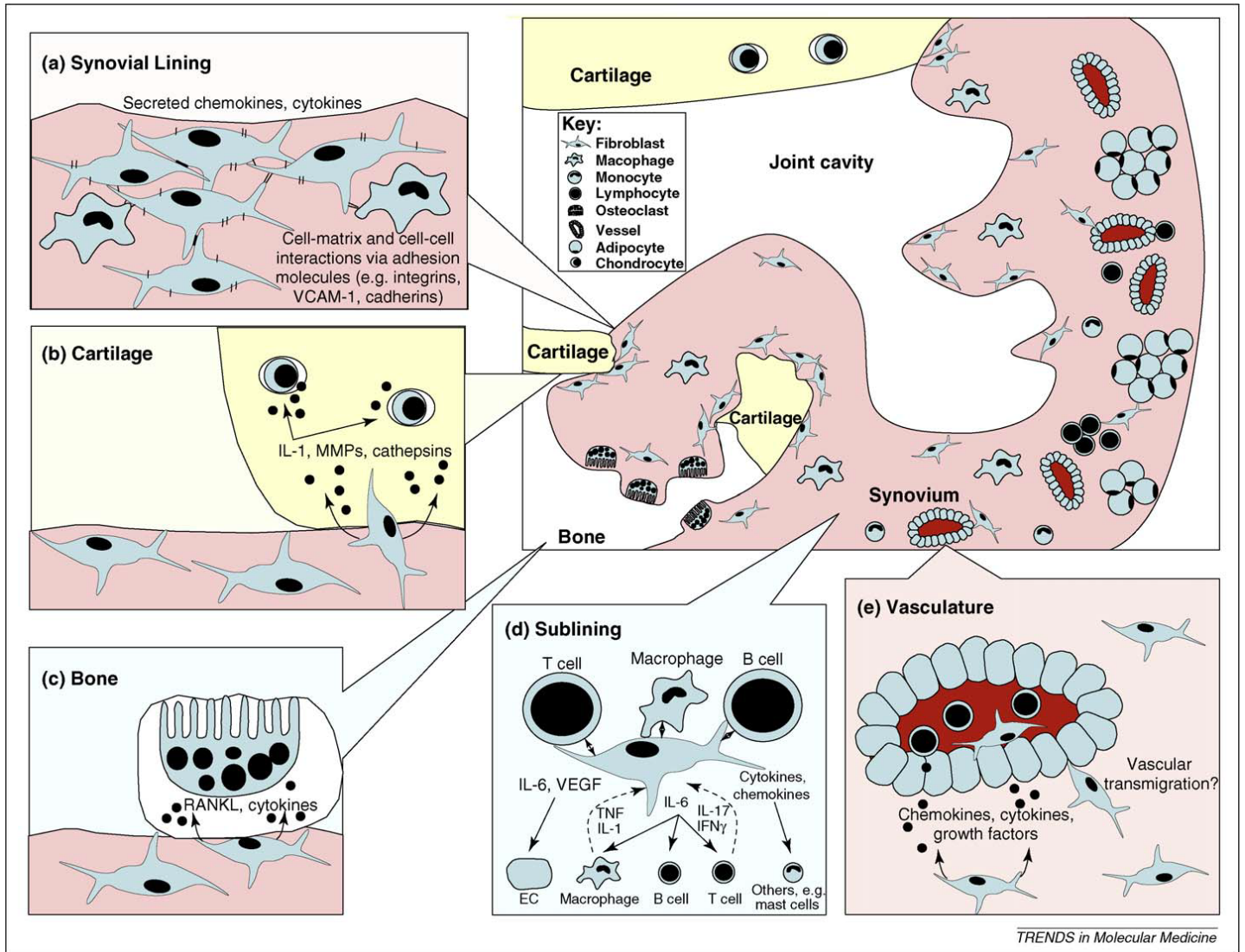
Image 7 Activated RA SFs drive cartilage and bone destruction, but simultaneously lead to inflammatory influx in the affected joints a. Macrophages interplay with RASFs of synovial lining, but RASFs also interact with each other via adhesion molecules and cytokines, growth factors and chemokines secretion. Adhesion molecules also lead the adhesion of the hyperproliferative synovium (pannus) to cartilage. b. The pannus gets into the cartilage and bone, degrading cartilage by metalloproteinases c. RASFs also activate osteoclasts by secreting RANKL d. RASFs communicate with immune cells, macrophages and endothelial cells (ECs), which amplify further the activation of RASFs e. RASFs increase the inflammatory infiltration of the synovium but they also activate ECs, promoting the angiogenesis. (Adapted from Neumann, 2010)[2]

Stromal interactions shape the progression of chronic inflammatory diseases, regulating the proliferation and the function of both destructing and inflammatory fibroblasts. Interestingly, it has been reported that Notch signalling from endothelial cells initiates transcriptional profiles of fibroblasts, leading nearby perivascular mural cells, expressing Notch 3 receptor, to differentiate into CD90^{high} sublining and subsequently to CD90^{low} lining fibroblasts, suggesting the presence of intermediate populations in between the two main SFs clusters[84].
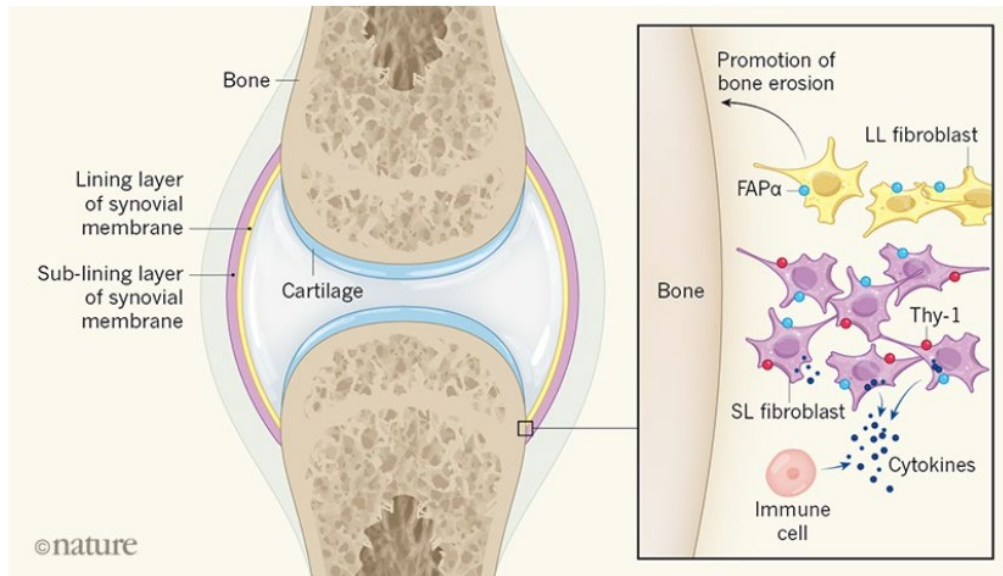
Image 8 Fibroblasts of lining and sublining cluster have distinct location and function in rheumatoid arthritis joints. (Adapted from Wynn, 2019)[82]

Similarly, in the *hTNFtg* animal model of chronic polyarthritis, clusters attributed to sublining, intermediate and lining fibroblasts have been found[85]. In fact, Armaka *et al*. reported that the homeostatic synovium of Wild type (WT) joints consists of a plethora of subpopulations, reflecting the multifactorial character of SFs even in non-diseased conditions. Additionally, single cell transcriptomics during the disease progression (4 and 8 weeks) in *hTNFtg* model were integrated with single cell Assay for Transposase Accessible Chromatin (scATAQ) studies, revealing that transcription factors, such as Runx1, along with Rel, Nfkb2, Dlx3 and Bach1 drive the regulation of the disease specific subpopulations (Image 9). Indicating common clusters of *hTNFtg* SFs with human RA FLS in single cell level, it was once more highlighted that *hTNFtg* model can serve as a valuable tool to dissect interspecies SFs responses and functions.

Recent evidence confirmed the existence of lining, sublining and intermediate clusters in RA FLS, as well as the function of the panfibroblast Pi16+ subpopulation as "progenitor" cluster, highlighting however a HLA-DR+ cytokine-activated lining FLS cluster, capable of presenting antigens to CD4+ T cells[86]. In scATAQ experiments, AP-1 transcription factor seemed to control the HLA-DR+ cluster gene regulation, while factors such as SOX and KLF were enriched in the Pi16+ subpopulation. *Ex vivo* stimulation experiments showed that sublining fibroblasts response to a combination of TNF and IFNγ, while lining fibroblasts are regulated by a triple combination of TNF, IFNγ and IL1β[86].
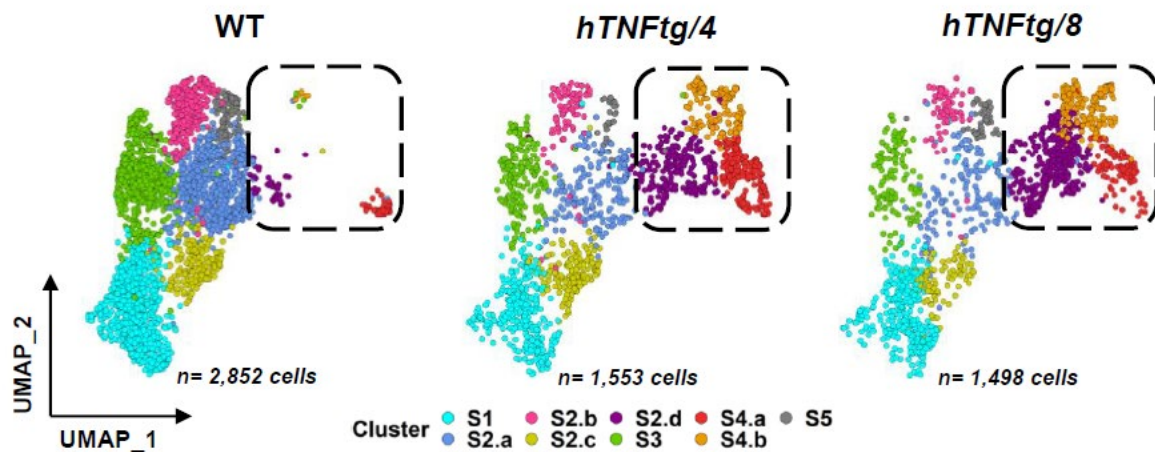
Image 9 Comparison of single cell transcriptomics between WT and *hTNFtg* disease progression (4weeks and 8 weeks old) revealed the existence of a pathogenic branch. SFs-specific clustering showed the existence of nine fibroblastic clusters that were characterized as Lining SFs (S4a, (Prg4+)), Sublining SFs (S1, S2a, b, c, S3, S5 (Thy1+)) and Intermediate SFs (S2d and S4b). (Adapted from Armaka *et al.*, 2021)[85]

1.6   Current therapies

Focusing on RA, according to recent recommendations[87], first-line treatment should include conventional disease-modifying antirheumatic drugs (DMARDs), such as methotrexate and glucocorticoids. For non-responsive patients, targeted synthetic DMARDs, inhibiting several kinases—Janus kinases (JAKs), mitogen-activated protein kinase (MAPK) and spleen tyrosine kinase (SYK)-Bruton's tyrosine kinase (BTK) (SYK-BTK)[88] as well as biologic agents for blocking proinflammatory cytokines, including IL-6 and TNF—are administered.

As mentioned above, TNF antagonists have been widely used and proved effective in clinic[33]. However, these antagonists are mainly biologics, i.e., monoclonal antibodies (infliximab, adalimumab, certolizumab pegol, golimumab)[33,89,90] and fusion proteins (etanercept), which bear certain drawbacks. Such disadvantages include causing hypersensitivity, increased risk of patients to develop serious infections, such as tuberculosis and hepatitis B because of the caused immune system suppression, loss of patients' response during therapy due to arisen immunogenicity, invasive administration and high cost of production and supply[34,36,37,91–96]. Thus, there is a great need for the development of potent therapeutic small molecules, as they can be inexpensively produced and distributed; they can be formulated to accommodate a plethora of administration routes (e.g., per os) while they can also present lower immunosuppressive side effects than biologics[34,36,37,95].

Cytokine	Typical cellular source(s)	Cellular target(s) [and effect(s)]	Proposed role(s) in rheumatoid arthritis	Targeting strategy/ies
TNF	Monocytes/ macrophages.	SFs (pro-inflammatory cytokine production) Osteoclasts (differentiation, activation) Endothelium (neovascularization) - Lymphocytes (Treg inhibition)	Pro-inflammatory Bone erosion Systemic (?fatigue)	Anti-TNF (infliximab[o], adalimumab[o], golimumab[o], cerolizumab[o]), TNFR (etanercept[o]).
IL-6	Monocytes/ macrophages, stroma/SFs	SFs (activation, proliferation) Macrophage (osteoclast differentiation) T cells (proliferation, survival, Th17 differentiation) B cells (survival, antibody production). Hepatocytes (acute phase reactants)	Pro-inflammatory Systemic (atherosclerosis, impaired lipid metabolism, anaemia)	Anti-IL-6R (tocilizumab[o], sarilumab), anti-IL-6 (sirukumab)
IL-1α/β	Monocytes/ macrophages, DCs	Osteoclasts (activation) T cells (Th17 differentiation) Endothelium (vasodilation) Autocrine (pro-inflammatory)	Pro-inflammatory (contributory rather than dominant role)	IL-1RA (anakinra), anti-IL-1β (canakinumab).
IL-17A/F	Th17 cells, neutrophils, ILCs, iNKT cells.	SFs (proliferation, pro-inflammatory cytokine production, including IL-6) - Chondrocytes (metalloproteinase induction) Myeloid cells/neutrophils (chemotaxis) Endothelium (neovascularization)	Pro-inflammatory (?contributory versus dominant role depending on disease subset)	Anti-IL-17A (secukinumab), anti-IL-17RA (brodalumab).
IL-23	Macrophages, DCs	Th17 cells (development, maintenance and expansion; IL-21/IL-22 induction)	Th17 responses	Anti-p40 (common subunit of IL-23/12; ustekinumab), anti-IL-23 (guselkumab)
IL-21	Th17 cells, Th2 cells, NK cells, Tfh cells.	B-cell maturation, plasma cell development/antibody production	?Role in arthritogenic autoantibody glycosylation	Anti-IL-21 in development
IL-12	Macrophages, DCs	Th1 cells (differentiation, autocrine)	?Cell-mediated immune reposes, Th17 plasticity.	Anti-p40 (common subunit of IL-23/12; ustekinumab)
GM-CSF	Monocytes/ macrophages, lymphocytes, stroma/ SFs	Myeloid cells (differentiation/ proliferation) Macrophages (pro-inflammatory phenotype) DCs (activation)	Pro-inflammatory, ?Pain	Anti-GM-CSF-Rα (mavrilimumab)
Th2 cytokines	Th2 cells, mast cells	Various	Awaits clarification	Strategy to be determined.
Type I interferons	Plasmacytoid DCs	CD8^{+} T cells and NK cells (cytotoxicity) Th1 polarization B cells (differentiation; IgG class-switching)	?pathogenesis of seropositive disease	Anti-IFNα (sifalimumab)
IL-8 (CXCL8)	Macrophages, epi/ endothelial cells. Osteoclasts (?response to autoantibodies)	Neutrophils, leukocytes (chemotaxis) Osteoclasts (activation, including autocrine)	Leukocyte chemotaxis ?Bone erosion/pain in 'pre-RA'	CXCR1/2 inhibitor (reparixin)

Table 1 Activated cytokines in RA joints significantly affect the interplay between cell types of the synovium and potent inhibitors of these cytokines have been found to date. Only the indicated inhibitors ([o]) have been approved and are used in clinic. (Adapted from Ridgley *et al.*, 2018[97])

1.7 Anti-TNF small molecules

The first small molecule identified as a TNF inhibitor *in vitro* was suramin, synthesized in 1916[98,99]. Hence, it has been used as a template for identifying other compounds with inhibitory activity, such as Evans blue and Trypan blue, while also setting the basis of structure–activity relationship (SAR) studies for TNF as a biomolecular target[100]. He *et al.*[31]

developed SPD304, which exhibited a micromolar inhibitory activity in TNF-TNFR1 interaction, binding to the TNF dimer as revealed via X-ray crystallography, thus blocking the formation of the active TNF trimer. The structure elucidation of the bound ligand afforded valuable SAR information, which surprisingly does not include any hydrogen bond or electrostatic interactions of the bound ligand with the TNF dimer. All interactions were hydrophobic, while interactions of the ligand with TNF residues Tyr59 and Tyr119 were identified as highly important for TNF inhibition[23]. Albeit the successful inhibition of the formation of the TNF functional trimer, SPD304 has not been efficient *in vivo*, because of its metabolic instability, attributed to the presence of a 3-substituted indole moiety in the compound structure, as well as due to its low kinetic solubility, high toxicity and considerable drawbacks in Absorption, Distribution, Metabolism, Elimination, Toxicity (ADMET) studies[101,102].

Starting from the ligand SPD304 in 2005, several small molecule TNF inhibitors have been developed, including heterocyclic compounds, small organic ligands, natural products (NPs) and metal-complexed compounds[36–38,103–105]. Molsoft software has been used to identify two Food and Drug Administration (FDA) approved drugs that could bind to TNF[106]. Blevitt *et al*. [107] discovered an inhibitor that forms an aggregating conglomerate, which antagonizes a protein subunit of the TNF trimer and alternates the quaternary structure of TNF upon binding. Thus, the binding of the TNF to TNFR1 is disrupted, due to the quaternary structure change induced by the aggregate. O'Connell *et al*.[104] and Dietrich *et al*.[38] developed small molecules with oral bioavailability that bind deeply in the TNF homotrimer, being able to allosterically stabilize an asymmetric complex or the trimer itself, leading to signaling inhibition. Xiao *et al*.[108] also proposed a compound that deforms the TNF trimer upon binding, leading to deregulated signaling upon binding of the TNF trimer to TNFR1.

In silico approaches were recently used to facilitate the identification of new potential anti-TNF therapeutics[95,109,110]. Computational modeling supports drug development, as it reduces both the time and the cost spent; it can predict clinical responses and it supports the 3R concept requests [49,111]. Five novel TNF-α inhibitors were identified, following a structure-based virtual screening in combination with *in vitro* experiments. Saddala and Huang[112] used a chemoinformatic workflow which employed pharmacophore modeling, docking and ADMET properties prediction within the ZINC database to identify potential lead candidates with oral bioavailability for the inhibition of TNF; however, their biological activity has not been addressed. Recently, Melagraki *et al*.[113] developed two dual TNF-RANKL (receptor activator of nuclear factor κ-B ligand) micromolar inhibitors, which impede the active biological form of both cytokines, that play a determinant role in chronic inflammatory diseases. The

compounds have been identified employing the Enalos[114] *in silico* workflow, which combines a structure-based chemical library screening approach together with a ligand-based consensus quantitative structure–activity relationship (QSAR) model, studying molecular dynamics simulations in order to further investigate computationally the compounds' binding mode[109,110,112]. Continuing their work in dual inhibitors, Melagraki *et al.*[35] proposed a NP, named A11 (Ampelopsin H), which efficiently blocks both TNF and RANKL, using a further automated version of the EnalosMD workflow.

1.8   Drug repurposing

The financial and chronological investment for the conversion of a new chemical entity into a traded new drug is usually higher than the actual gain of the drug release into the market. Moreover, drug development is often interrupted due to several drawbacks of the novel compound, increasing further the cost and the risk of de novo drug discovery.

To overcome this bottleneck, Drug Repurposing, a strategy that reclaims approved for other diseases drugs, for new purposes, has been successfully used. Repurposing of drugs may rely on the circumstance that several diseases can be governed by similar pathways or that known drugs can present new off targets, influencing molecular pathways which can be subsequently investigated and end up in further lead compound discovery[115].

Drug repositioning reduces the risk of failure, as the toxicity data of the relevant compound have been already evaluated and most formulation studies have been concluded. Thus, preclinical testing and phase I and II clinical trials are expected to be both faster and more efficient when compared to the relevant phases of a new not tested compound[116].

Several examples confirm that Drug re-tasking can be proven even more successful than the use of the drug for its original indication. Thalidomide, originally used as a drug against nausea, was withdrawn from the market in early 60's, as it was linked with severe skeletal birth defects in children of women who have been administered the drug, during the first 3 months of pregnancy[117]. However, in 1999 the drug was approved for multiple myeloma patients, as it presents antiangiogenic and immunomodulatory properties[118].

Historically, repurposing of drugs has been based on the adverse effects presented in patients who used the drug for its original indication. Such instances include Sildenafil, originally used for angina disease and afterwards used for erectile dysfunction, Minoxidil originally used for hypertension and after marketed for hair loss, etc[117].

Nowadays, the identification of repurposable compounds is less based on serendipity, as multiple systematic approaches, both computational and experimental, are available (Image 10).

Computational approaches reduce the expenses of the drug discovery process and include a. tools that search for drugs that can reverse pathogenic genetic signatures b. drug-drug similarity approaches which compare chemically dissimilar drugs, that however share common expression signatures when added to the cells c. chemical similarities approaches, as chemical homogeneity could suggest shared biological activity and d. approaches that compare the adverse effects of drugs that can lead hypothetically to common mechanism of action.

Another computational method, broadly used to identify new therapeutics, is the computational molecular docking. This is based on a ligand-receptor binding scoring system, requiring that the crystal structure of the receptor is published. The target is usually linked to the activation of a pathogenic molecular pathway; thus chemicals of publicly available databases are tested as to their blocking ability against the receptor and can be tested further in *in vitro* assays. The inverse procedure can also be followed; multiple ligands can be interrogated against a compound of interest in order to investigate its potential multiple targets[115].

Experimental assays can be either proteomics based or *ex vivo* phenotypic screening assays. Examples of mass spectrometry techniques are Cellular ThermoStability Assay (CETSA)[119], where the target identification is based on the exclusion of non-target proteins upon a range of high temperatures or click chemistry based techniques, where a conjugate is attached on the compound of interest in order to pull down, using relevant beads, potential targets[120]. Phenotypic screening relies on evaluation of a compound potential to regulate pathogenic characteristics of diseased cells or animal models, without requesting knowledge of the drug target[115]. Thus, it is the effect and not the mechanism of action of a compound which is mostly being evaluated.

Therapeutics identification against Chronic Inflammatory Diseases (CID), such as RA, CD, Systemic lupus erythematosus (SLE) and Psoriatic Arthritis (PsA) has been a continuous challenge as these diseases are characterized by heterogeneity and versatile aetiology. Deregulation of several cytokines, such as IL6 and TNF, have been linked to the initiation and progression of CID [121]. To date, many standard treatments of CID have been established due to Drug Repurposing approaches, which were mainly based on serendipitous observations and

common underlining mechanisms of these diseases[122]. Examples are methotrexate, which was originally identified as an anticancer agent and is now prescribed for RA[123] and PsA[124] as well as glucocorticoids, which were originally known as anti-inflammatory, but now are also widely applied for most CID[125]. Anti-TNF biologics were also introduced for sepsis but in late 90's were approved for other CID as well, such as CD and RA[126–128]. More recently, small molecule inhibitors have also been widely used in more than one CIDs. Baricitinib, for example, was first approved for RA but now are also tested for SLE[129].
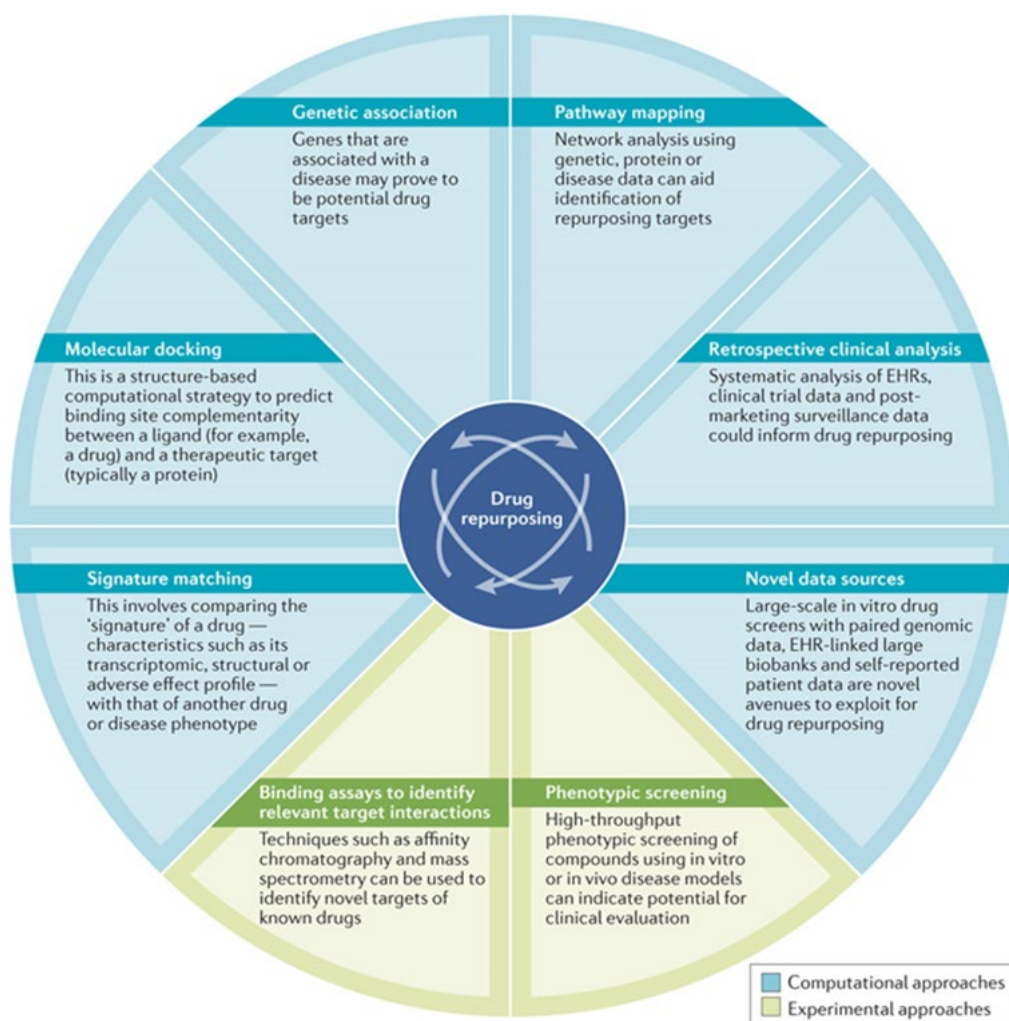
Image 10 Drug repurposing through computational and experimental approaches facilitates faster and more targeted drug discovery. (Adapted from Pushpakom *et al*., 2018[115])

2. Purpose of the study

In this study, we firstly aimed to identify lead compounds that act as protein–protein interaction (PPI) inhibitors, binding to the inactive TNF dimer and inhibiting the formation of the active trimer. Development of small-molecule PPI inhibitors is very challenging[130], as a PPI inhibitor can act on certain "hot spots'' on the protein surfaces[131,132], that are typically large, flat and solvent-exposed, while they are predominantly characterized by non-specific features (hydrophobic and electrostatic interactions)[133,134]. The large size and solvent exposure of the binding site require additionally that PPI inhibitors should achieve high potency and exhibit low molecular weight (MW), optimal lipophilicity and solubility[36,95,134].

To attain these pharmacokinetic properties of a prospective TNF small molecule ligand, we focused on NPs, deeming that, due to their natural origin as plant metabolites, they would bear an improved pharmacokinetic profile in comparison to synthetic compounds. Towards the identification of prospective PPI compounds with TNF inhibitory action, we used an *in silico* pipeline based on Enalos Asclepios workflow to discover new NP lead compounds as potential TNF inhibitors, continuing our previous work in the field[35,113,135–137]. Enalos Asclepios pipeline has been extensively used to identify new lead compounds, based on online available libraries of chemical structures or NPs, that can efficiently bind to the inactive TNF dimer, inhibiting the formation of the TNF active trimer[113,138,139]. The docking was based on the TNF crystal structure[23] and the complex formed when this is bound to SPD304[31], after conducting a homology modelling to fill in missing residues.

Moreover, in the effort of identifying new potential therapeutics for RA treatment, we searched compounds in a repurposing perspective, as this can provide candidates that have been already assessed concerning the toxicity, the diluent and the route of administration[116].

To this end, we applied a similar to the above molecular docking approach in a library containing FDA approved drugs that could be potential PPI TNF inhibitors. Combining computational calculations with drug repositioning can efficiently lead to faster and more efficient identification of new lead compounds that are already characterized by favourable ADMET properties.

In both PPI inhibitors identification, we combined the virtual molecular docking approach, using the improved KNIME nodes[35,139] of the Enalos Asclepios pipeline, with phenotypic screening assays, measuring TNF dependent cell death of L929 cell line or *hTNFtg* mouse joint SFs' secretion of inflammatory chemokines. L929 is a cell line that proceed to necroptosis

upon TNF induction[140] and *hTNFtg* mice have been one of the first in *in vivo* proofs that deregulation of TNF is linked to CID[48].

Additionally, in the attempt to identify new potential small molecules against chronic inflammation, we applied the L1000CDS^2 search engine[141], that has been successfully used before to repurpose small molecules as therapeutics for several diseases[142]. We aimed to identify compounds that could potentially reverse *hTNFtg* SFs' pathogenic gene expression signature or could mimic the *ex vivo* effect of a known anti-TNF biologic, Infliximab, on *hTNFtg* SFs expression profile.

Finally, newly synthesized structures were screened as to their anti-inflammatory and anti-proliferative properties, leading to identification of optimized derivatives. The most promising candidates were evaluated further for their mechanism of action and for their therapeutic potential in animal models of disease.

The originality of this work focuses mainly on three main parameters: (i) the targeting of a cell type (mesenchymal cells), that to date has not been exploited therapeutically, even though it has been shown to play a key role in the pathogenesis of chronic inflammatory disease (ii) the identification of new lead compounds that can lead to the discovery of novel small molecules / TNF inhibitors in high demand from the market as successors of current biological treatments and iii) the study of the mechanism of action that supports the inhibitors' therapeutic potential.

3. Materials and Methods

3.1 Compounds

3.1.1 Natural products

All NPs alphabetically named cis-Diptoindonesin B (CFN93706- Pubchem CID 643710), cis-Miyabenol C (CFN93332, Pubchem CID 5388319), Flexuosol A (CFN 93650, Pubchem CID 71308201), Kobophenol A (CFN92530, Pubchem CID 484758), Miyabenol A (CFN93701, Pubchem CID 16129868), Nepalensinol B (CFN93851, Pubchem CID 46890012), Vitisin B (CFN93805, Pubchem CID 74947464), trans-Diptoindonesin B (CFN93770, Pubchem CID 641676) and trans-Miyabenol C (CFN93716, Pubchem CID 6475924) were purchased from Wuhan ChemFaces Biochemical Co., Ltd., Wuhan, China.

3.1.2 FDA drugs

All compounds namely Acarbose (Prestw-1174), Atorvastatin (Prestw-1232), Bosentan (Prestw-1244), Candesartan (Prestw-1258), Dilazep dihydrochloride (Prestw-236), Diosmin (Prestw-1503), Fosinopril (Prestw-1423), Glibenclamide (Prestw-316), Glimepiride (Prestw-651), Gliquidone (Prestw-991), Irbesartan (Prestw-1736), Irinotecan hydrochloride trihydrate (Prestw-1494), Itraconazole (Prestw-1139), Olmesartan (Prestw-1190), Paclitaxel (Prestw-155), Probucol (Prestw-384), Telmisartan (Prestw-1350), Tribenoside (Prestw-1019) and Zafirlukast (Prestw-1364) were purchased from Prestwick Chemical**.**

3.1.3 Amisulpride

For the conduct of the pharmacological experiments, the commercially available Solian solution (100 mg/mL) was used, while for the chemoproteomic assays, Amisulpride synthesized according to the literature was used.[32]

3.1.4 Novel compounds

The synthesis of novel compounds and click compounds was performed in house by Dr A. Matralis and V. Mavrikaki (https://www.fleming.gr/research/ibi/researchers/matralis-lab).

3.2 SFs isolation

Primary mouse SFs were isolated from ankle joints of either CBA;C57BL/6J, WT or *hTNFtg* mice, at their 8th week of age, as previously described[143]. Briefly, ankle joints were digested

with Collagenase IV (Sigma Aldrich, C5138) and after 5 days in culture, a depletion of CD45+ cells was performed using a Biotin anti-mouse CD45 Antibody (Biolegend, 103104) and Dynabeads™ Biotin Binder (ThermoFisher 11047), according to the manufacturer's protocol.

3.3 Elisa assays

hTNFtg SFs were seeded in a monolayer of a 96well plate. Next day, cells were starved in 1× DMEM, 0.5% FBS, 100 U/mL P/S, overnight (O/N) and treated with different compounds concentrations. Compounds were reconstituted in DMSO to a concentration of 100mM and all further serial dilutions were performed using 1x DMEM (Gibco, 41966-029) supplemented with 0.5% FBS and 50U/ml Penicillin Streptomycin (P/S). CBA/C57 WT SFs do not normally exhibit an activated phenotype, thus after overnight (O/N) starvation in 1× DMEM, 0.5% FBS, 50 U/mL P/S, they were stimulated with hTNF 10 ng/mL (Peprotech, Rocky Hill, USA) or hTNF pre-incubated with different compounds concentrations for 30 min. 48h following the treatment, the cell culture supernatants were collected and were further analysed for the detection of cytokines and chemokines either by ELISA or multiplex analysis. CCL5/ Rantes (DY478, DuoSet, R&D Systems, Minneapolis, MN, USA) and CCL20/ Mip3 (DY760, DuoSet, R&D Systems, Minneapolis, MN, USA) were quantified according to the manufacturer's protocol. hTNF was quantified in cultured SFs' supernatants using the hTNF Quantikine Elisa (R&D Systems, DTA00D). All rest chemokines were analyzed using the Mouse 13plex Legendplex Chemokine (Biolegend, 740007) panel according the the manufacturer's instructions.

3.4 L929 Cell Line and TNF induced cell death assay

The L929 cells (NCTC clone) were obtained from ATCC (Manassas, VA, USA). The L929 TNF–induced cytotoxicity assay was performed as previously described [35,113,139]. In short, L929 murine fibrosarcoma cell line was treated with compounds at different concentrations after being pre-incubated with 0.3 ng/mL recombinant human TNF-α (Peprotech, Rocky Hill, CT, USA) and 2 µg/mL Actinomycin D for 30 min at RT. Control wells were treated with the culturing medium alone, the medium with the respective Actinomycin D and the medium with both TNF and Actinomycin D. After 18–22 h, supernatants were washed out and the plate was stained with Crystal violet. The quantification was performed spectrophotometrically at 570nm, and the results were quantified according to the equation:

(100* [(OD570 of sample) − (OD570 of TNF and ActD)])/((OD570 of ActD) − (OD570 of TNF and ActD))

3.5   Determination of compound cytotoxicity

The toxicity of the test compounds was assessed at several concentrations, using the Crystal Violet assay. Adherent viable cells were Methanol fixed and stained with Crystal Violet. Optical density was quantified at 570nM, as described elsewhere[144].

3.6   *In vivo* experiments

All mice were maintained under specific pathogen-free conditions in conventional, temperature-controlled, air-conditioned animal house facilities of BSRC Al. Fleming with 12 h light/12 h dark cycle, and the mice received food and water ad libitum. All mice were observed for morbidity and euthanized when needed according to animal welfare. All experiments were approved by the Institutional Committee of Protocol Evaluation in conjunction with the Veterinary Service Management of the Hellenic Republic Prefecture of Attika according to all current European and national legislation.

3.6.1   LPS model

In order to evaluate *in vivo* the anti-inflammatory effect of the test compounds, a model of *in vivo* LPS acute systemic inflammation was used where C57BL/6J mice were challenged with an administration of 1μg LPS/ mouse. Tested compounds were administered to C57BL/6J mice per os twice with the indicated doses (t-2, t0). At t0, mice were injected with 1μg LPS intraperitoneally and sera samples were collected 1.5hrs post induction in order to measure the levels of IL6 and mTNF using the Duoset (DY406) and eBioscience (88-7324), respectively, following the manufacturer's protocol.

3.6.2   *hTNFtg* mouse model

In vivo experiments of assessing the effect of compounds in mouse polyarthritis were performed in CBA;C57BL/6J, *hTNFtg* animals[48]. Dosing was performed by oral administration, starting from the 3rd week of age to the 8th week of age. Clinical arthritis score in *hTNFtg* animals was evaluated during disease in ankle joints in a blinded manner, using a semiquantitative arthritis score ranging from 0 to 4: 0: no arthritis (normal appearance and

grip strength); 1: mild arthritis (joint swelling); 2: moderate joint swelling and digit deformation, reduced grip strength; 3: severe joint swelling and digit deformation, impaired movement, no grip strength; 4: severe joint swelling and digit deformation, impaired movement, no grip strength and obvious weight loss cachexia. At the 8th week of age mice were sacrificed. Joints were decalcified and proceeded in further histological evaluation.

3.7   Histology

Formalin-fixed, EDTA-decalcified, paraffin-embedded mouse joint tissue specimens were sectioned and stained with haematoxylin-eosin (H&E), Toluidine Blue or Tartrate-Resistance Acid Phosphatase (TRAP) Kit (Sigma-Aldrich). H&E and TB were semi-quantitatively blindly evaluated for the following parameters: synovial inflammation/hyperplasia (scale of 0–5) and cartilage erosion (scale of 0–5) based on an adjusted, previously described method[145]. TRAP staining of joint sections was performed to measure number of osteoclasts using ImageJ software. Images were acquired with a Nikon microscope, equipped with a QImaging digital camera.

3.8   Immune infiltration FACs analysis

FACS analysis for quantifying populations of immune infiltrating cells were performed by digesting ankle joints of 8week old *hTNFtg* vehicle or Amisulpride treated animals, using 1000U/ml Collagenase IV (Sigma-Aldrich), for 60 minutes at 37°C. After concentrating the cell suspension by centrifugation, the cell pellet was resuspended in FACS buffer (PBS with 0.5% FBS, 0.05% sodium azide and 2mM EDTA). The cells were then blocked by the anti-Fc Receptor (anti-CD16/32) antibody (Biolegend). 1-2 million cells were stained according to the following table.

Analysis was performed using a FACS Canto II Flow cytometer (BD Biosciences) and FlowJo software (FlowJo, LLC). Counting beads were used for quantification of different cell subsets.

Cells subset	Antibodies (Company, Cat. Number)								Live/ Dead Exclusion
Myeloid cells	PE-conjugated anti-CD11b (BD Biosciences, 557397)	A700-conjugated anti-CD45 (Biolegend, 103128)	APC-conjugated anti-MHCII (eBioscience,17-5320-82)	PE/Dazzle594-conjugated anti-CD64 (Biolegend, 139320)	APCFire-conjugated anti-CD24 (Biolegend,101840)	PE/Cy7-conjugated anti-CD11c (Biolegend, 117318)	FITC-conjugated anti-Ly6C (BD Biosciences, 553104)	Biotinylated anti-Ly6G (eBioscience, 13-5931-75) with streptavidin-conjugated PE/Cy5 (Invitrogen)	Dapi (Invitrogen, D1306)
Lymphocytes	PE-conjugated anti-B220 (BD Biosciences, 553089)	ApcCy7-conjugated anti-CD45 (Biolegend, 103116)	PE/Cy7-conjugated anti-CD3 (eBioscience,25-0031-82)	A700-conjugated anti-CD4 (Biolegend, 100536)	APC-conjugated anti-CD8 (Biolegend,100711)				Zombie Green (Sigma, 423112)
Fibroblasts	A488-conjugated anti-CD90.2 (Biolegend, 105316)	A700-conjugated anti-CD45 (Biolegend, 103128)	PE-conjugated anti-CD31 (BD Biosciences, 553373)	PE/Cy7-conjugated anti-PDPN (Biolegend, 127412)					Zombie NIR (Sigma, 77184)

3.9   RNA sequencing

RNA sequencing was performed in three biological replicates of cultured SFs isolated from *hTNFtg* mice and WT littermates at their 8th week of age. Treated *hTNFtg* SFs were incubated with Amisulpride at 500μM for 48h. RNA extraction of cultured SFs was performed using the Qiagen RNA Micro kit (74004), according to the company's guidelines.

RNA extraction of fresh sorted SFs (CD31-, CD45-, PDPN+) of hTNGtg 8w mice treated or not with Amisulpride 20mg/kg was performed using the Single Cell RNA Purification Kit (Norgen, 51800). All samples were quantified by ND1000 Spectrophotometer-PEQLAB, while the quality of the samples was assessed in a Bioanalyzer using the Agilent RNA 6000 Nano Kit reagents and protocol (Agilent Technologies). Only RNA samples with RNA Integrity Number (RIN) >7 proceeded to further analysis. The library preparation was performed according to the 3' mRNA-Seq Library Prep Kit Protocol for Ion Torrent (QuantSeq-LEXOGEN™). The quality of libraries was measured again in a Bioanalyzer, using the DNA High Sensitivity Kit reagents (Agilent Technologies) according to manufacturer's protocol, while after quantification, the libraries were equated at a concentration of 50pM. Templating was performed in the Ion Proton Chef instrument, following the Ion PI™ IC200™ Chef Kit (ThermoFisher Scientific). Sequencing was performed in the Ion Proton™ System according to the Ion PI™ Sequencing 200 V3 Kit on Ion Proton PI™ V2 chips (ThermoFisher Scientific).

3.10 RNA sequencing analysis

The raw bam files were concluded to read counts using the Bioconductor package Genomic Ranges.5. Genes that had zero counts were removed and the gene counts. Gene lists were normalized and subsequently analyzed for differentially expressed genes, using the Bioconductor package DESeq[146]. Differentially regulated genes were concluded using an absolute $\log_2$fold change cutoff value of 1 and a pvalue cutoff of 0.05, through the Bioconductor package metaseqr[147]. R packages[148] were used for generating volcano plots and heatmaps. Venn diagrams were created with the online available tool of InteractiVenn[149]. Functional enrichment analysis was performed using the Enrichr online tool[150] .

3.11 TNF/TNFR1 ELISA assay

TNF-TNFR1 Elisa assay was performed as described elsewhere[113]. In brief, 0.025 µg/mL recombinant human TNF (PeproTech) in PBS was incubated with or without different concentrations of compounds and it was added to a plate pre-coated with 0.1 µg/mL recombinant soluble human TNFR1 (PeproTech). Upon washes, the plate was incubated with a rabbit anti-human-TNF antibody (provided by Prof. W. A. Buurman, University of Maastricht) which was then bound to a secondary anti-rabbit antibody conjugated with HRP (Vector Laboratories). Quantification of the signal was performed in a spectrophotometer at 450nm,

after development with TMB Substrate Kit (ThermoFisher Scientific). Binding was expressed as to TNF with no compound, positive control.

3.12 Click experiments for target identification by Mass spectrometry

In order to identify the possible targets of Amisulpride/ Compound 53 on *hTNFtg* SFs we employed a previously described "click chemistry" protocol[151], by lowering down the amount of total protein used at 4mg.

3.12.1 Mass spectrometry SP3 digestion and clean up

The eluates were processed using the sensitive sp3 protocol (Hughes *et al*, 2014). The cysteine residues were reduced in 100 mM DTT and alkylated in iodoacetamide (I6125, Sigma-Aldrich). 20 ug of beads were added to each sample in 50% ethanol. The beads were washed twice with 80% ethanol and once with 100% acetonitrile. The captured proteins were digested overnight at 37°C under vigorous shaking (Thermomixer) with 0.5 ug Trypsin/LysC (mixture MS grade, Promega) prepared in 25 mM Ammonium bicarbonate. Next day, the supernatants were collected and were further cleaned using the Sp3 protocol. The cleaned peptide mixtures were dried using a vacuum centrifuge, solubilized in a mobile phase A and sonicated. Peptide concentration was determined through absorbance at 280nm measurement.

3.12.2 LC-MS/MS

Nano-liquid chromatography of 500 ng tryptic peptide mixture was carried out using a Ultimate3000 RSLC system configured with a trap column (Acclaim PepMap100, 100μm x 2cm, Thermo Scientific) and then loaded onto a 50cm long C18 column (75 μm ID, particle size 2 μm, 100Å, Acclaim PepMap100 RSLC, Thermo Scientific). Peptides were loaded on the trap column at 10uL/min for 4 min with 0.1% formic acid in water. The separation was achieved using a gradient of 0.1% (vol/vol) formic acid in water (mobile phase A) and 0.1% (vol/vol) formic acid in acetonitrile (ACN) (mobile phase B). In more detail the flow rate was set at 0.3uL/min and the solvent ramped from 5% A to 27.5% over 23 min, 27.5% to 40% A in 4.5min, 40% to 99% in 0.5 min remaining constant for 4min. The column was equilibrated for 18min before the next injection.

The data acquisition was performed in positive mode using a Q Exactive HF-X Orbitrap mass spectrometer (ThermoFisher Scientific). MS data were acquired in a data-dependent strategy selecting up to top 12 precursors based on precursor abundance in the survey scan (m/z 350–

1500). The resolution of the survey scan was 120,000 (at m/z 200) with a target value of $3 \times 10E6$ ions and a maximum injection time of 100 ms. HCD MS/MS spectra were acquired with a target value of 1x10E5 and resolution of 15,000 (at m/z 200) using an NCE of 28. The maximum injection time for MS/MS was 22 ms. Dynamic exclusion was enabled for 20 sec after one MS/MS spectra acquisition. The isolation window for MS/MS fragmentation was set to 1.2 m/z. Data Analysis- Mass spectometry

The acquired raw files were processed using MaxQuant software (1.6.14.0). Default parameters were used for protein identification and quantification. The Mus musculus proteome FASTA database was downloaded 9/3/2020 from Uniprot. Trypsin specificity with two missed cleavages was allowed and minimum peptide length was set to seven amino acids. Cysteine carbamidomethylation was set as fixed, and methionine oxidation, deamidation of asparagine and glutamine and N-terminal acetylation were set as variable modifications. A maximum of five modifications per peptide was set. The false discovery rate both for peptide and protein were set to 1%. For the calculation of the protein abundances, label-free quantification (LFQ) was performed with both 'second peptide' and 'match between run' options enabled. Statistical analysis was performed using Perseus (version 1.6.10.43). Proteins identified as 'contaminants', 'reverse' and 'only identified by site' were filtered out. The three replicates of each condition were grouped (treated versus control condition of vehicle or competition condition). A two-sided Student's t-test of the grouped proteins within each experimental set was performed using p value <0.05 as a significance measurement.

3.13 shRNAS and Lenti-X transfection

In order to achieve a sufficient gene deletion of potential targets of Amisulpride in primary SFs we used the shRNAs Lentivirus transduction system. Each designed shRNA construct contained a unique 19-nt double-stranded target sequence that presented as an inverted complementary repeat, a loop sequence (5'- TTCAAGAGA -3'), the RNA PolII terminator sequence (5'-TTTTTT-3'), and 5' single-stranded overhangs for ligation into HpaI/ XhoI-digested PLB vector.

As a first step, PLB vector was cut using two restriction enzymes, HpaI and XhoI, in order to create two appropriate sticky ends. 0.6% TAE gel was used in order to run and confirm that the PLB DNA plasmid restriction was successful and QIA Quick Gel extraction kit was used for plasmid DNA extraction. In parallel, the shRNA sense and antisense sequences at 2μM were

annealed at 100°C for 5', in annealing buffer containing 10mM TrisHCl (PH=8), 50mM Nacl and 1mM EDTA. Annealed sequences were ligated into PLB vector, that carries a GFP reporter construct as a well as resistance to ampicillin, using Ligase in Quick Ligation buffer at 25°C, for 10'. DH5A competent cells were transformed, by heat shock, at 42°C for 90'' and 4°C for 2'. The colonies of transformed bacteria were chosen after O/N ampicillin selection in LB agar plates and were further cultured O/N in LB with ampicillin, at a 37°C shaking incubator. The DNA of transformed bacterial colonies was then isolated by following an in house boiling mini-preps protocol. The colonies that carried the insertion of the cloned PLB were chosen comparing the fragment sizes upon XbaI/ XhoI digestions. The successfully cloned colonies were cultured O/N at a 37°C shaking incubator and the Qiagen Plasmid Midi protocol (12143) was followed, according to manufacturer's instructions.

The following shRNAs were designed in order to silence its relevant gene

Gene to silence	shRNA sequence
Ascc3	5' T-GGAAGAAGATAGTGAAATT-TTCAAGAGA-AATTTCACTATCTTCTTCC-TTTTTTC 3'
	3' A-CCTTCTTCTATCACTTTAA-AAGTTCTCT-TTAAAGTGATAGAAGAAGG-AAAAAAGAGCT 5'
Kif5c	5' T-GCAAAGACCATCAAGAATA -TTCAAGAGA-TATTCTTGATGGTCTTTGC-TTTTTTC 3'
	3' A-CGTTTCTGGTAGTTCTTAT-AAGTTCTCT- ATAAGAACTACCAGAAACG-AAAAAAGAGCT 5'
Romo1	5' T-GCAAAGACCATCAAGAATA-TTCAAGAGA-TATTCTTGATGGTCTTTGC-TTTTTTC 3'
	3'A-CCCTTTTGGTACTACGTCT-AAGTTCTCT-AGACGTAGTACCAAAAGGG-AAAAAAGAGCT 5'
Sec62	5' T-GGGATTAATTCTTGTGATT-TTCAAGAGA-AATCACAAGAATTAATCCCT-TTTTTC 3'
	3' A-CCCTAATTAAGAACACTAA-AAGTTCTCT- TTAGTGTTCTTAATTAGGG-AAAAAAGAGCT 5'
Cdc42	5' T-GCAAGAGGATTATGACAGA-TTCAAGAGA TCTGTCATAATCCTCTTGC-TTTTTTC 3'
	3' A-CGTTCTCCTAATACTGTCT-AAGTTCTCT- AGACAGTATTAGGAGAACG-AAAAAAGAGCT 5'
Scramble	5' T-GCAGTGCAATATCGGAAAC-TTCAAGAGA-GTTTCCGATATTGCACTGCTTTTTTC 3'
	3' A-CGTCACGTTATAGCCTTTG-AAGTTCTCT-CAAAGGCTATAACGTGACG-AAAAAAGAGC 5'

HEK Lenti-X 293T cell line (Clontech) was plated at a density of 5*10^6 cells/ 100mm cell plate, coated with 50µg/ml collagen at 0.02N acetic acid, O/N. HEK Lenti-X 293T cells were

transfected using the PLB plasmids carrying each shRNA of interest and the Lentivirus second generation packaging system, including pMD2G as the envelope plasmid and psPAX2 as the packaging plasmid. The ratio of plasmids used was 2.8:1.8:1 for transgene: viral packaging (pPAX2): viral envelope (pMD2G), respectively. Specifically, we used 3.75µg of each transgene: 2.43µg viral packaging (pPAX2): 1.32µg viral envelope (pMD2G), which were added in 1ml of Optimem (Gibco, 31985062). Linear Polyethylenimine (PEI) (Sigma, P-3143) at 1mg/ml was used as the tranfection reagent at a ratio of 4:1 of PEI (µg): total DNA (µg). After 20' of incubation of the PEI mix at RT, HEK Lenti-X 293T were transfected at 1xDMEM, free of serum and antibiotics. After 16h, the cells supernatant was removed and the cell culture media was replenished with 1xDMEM supplemented with 10% FBS and 1% P/S. Transfection efficiency was monitored using a fluorescence microscope. 48h and 72h after the initial transfection, the transgene has been introduced in HEK Lenti-X 293T and the virus is produced in the cells supernatant, which was collected and kept at 4°C. After filtrating the virus suspension through a 0.45µm filter, the virus was concentrated following a protocol described elsewhere[152].

The lentiviral transduction of SFs was performed using Hexadimethrine Bromide/ Polybrene (Sigma, H9268) and transduction efficiency was calculated by the FITC positive cells in FACS Canto II Flow cytometer (BD Biosciences) and FlowJo software (FlowJo, LLC). Sorting of the GFP positive cells was performed, when transfection efficiency was less than 70%. SFs tranduced by lentiviruses that carry a vector containing scramble shRNA, were used as a relevant control and were treated accordingly.

The trasduced SFs were first collected for RNA extraction, in order to confirm each target reduction by qPCR, and were then used for chemokines determination in their supernatants. The SFs' RNA was collected following a Trizol (Invitrogen) based protocol.

3.14 Gene expression quantification

To confirm several interesting candidates of RNAseq results, to test if known targets of Amisulrpide are expressed in our cell type (SFs) or to investigate if tranduced SFs underexpress the gene of interest, we performed a qPCR analysis using the Platinum SYBR-Green qPCR SuperMix (Invitrogen), after CDNA synthesis by the MMLV Reverse Transcriptase (Promega). The CFX96 Touch Real-Time PCR Detection System (Biorad) was used and quantification was performed with the DDCt method. Primer sequences (5'-3') are provided below.

3.14.1 Real time Primers' sequences

The table below describe the 5' to 3' sequences of RT primers used. B2m or Gapdh were used as reference genes.

Gene	5'→ 3'sequence
hTNF	5'-CTTCTCGAACCCCGAGTGAC-3'
Mmp3	5'-GTCTCCCTGCAACCGTGAA-3'
Cxcl3	5'-CTGCACCCAGACAGAAGTCATA-3'
Cox2	5'-TCAGTTTTTCAAGACAGATC-3'
DRD2	5'-GTTTCCCAGTGAACAGGCGG-3'
DRD3	5'-TGGCAACGGTCTGGTATGTG -3'
Htr7	5'-TGCAACGTCTTCATCGCCA-3'
Ascc3	5'-GGCCTTACATGGAAGAAGATAGTG-3'
Kif5c	5'-AGCGGGAAGCTGTATTTGGT-3'
Romo1	5'-GAGCACTCTCGCCGCAGAT-3'
Sec62	5'-GCAGTAATAGCAGCCACCCT-3'
Cdc42	5'-GGCGGAGAAGCTGAGGAC-3'
B2m	5'-TTCTGGTGCTTGTCTCACTGA-3'
Gapdh	5'-GTTGTCTCCTGCGACTTCA-3'

3.15 Sample preparation for phosphoproteomics analysis

Samples for proteomics analysis were prepared as cell pellets, by collecting WT SFs activated by hTNF at various time points (5', 15' 15'), with or without pre-incubation for 1h with 500μM of Amisulpride. All samples were prepared in triplicates and processed and analyzed essentially as previously described[153]. Cell pellets were lysed in boiling lysis buffer containing 5% sodium dodecyl sulfate (SDS), 5 mM tris(2-carboxyethyl) phosphine (TCEP), 10 mM chloroacetamide (CAA), 100 mM Tris, pH 8.5 and boiled for 10 minutes followed by sonication

with a micro tip probe. Protein concentrations were estimated using the Pierce BCA Protein Assay Kit (ThermoFisher Scientific). For each sample 500 µg of protein was used for PAC digestion in an automated 96-well format on a KingFisher™ Flex robot (Thermo Fisher Scientific) with 12 hour overnight digestion at 37 °C, using LysC (Wako) and Trypsin (Sigma Aldrich) as described before[153]. Protease activity was quenched by acidification with trifluoroacetic acid (TFA). The peptides mixture was purified and concentrated on reversed-phase C18 Sep-Pak cartridges (Waters) for phosphoproteome analysis.

For phosphoproteome analysis enrichment of phosphopeptides was carried out in 96-well format on a KingFisher™ Flex robot (Thermo Fisher Scientific) based on previously described protocols[153,154]. Peptides were eluted with 75 µl of 80% acetonitrile directly into a KingFisher 96-well plate and subsequently 150 µl of loading buffer (80% ACN, 8% TFA and 1.6 M glycolic acid) was added to each well. Phosphopeptides were enriched using TiIMAC-HP beads (MagResyn, Resyn Biosciences) and eluted in the final plate with 1% ammonia. After the eluted phosphopeptides were acidified with TFA, they were directly loaded onto EvoTips according to the manufacturer's protocol.

3.16 LC-MS/MS phosphoproteome data analysis

All samples were analyzed on the EvoSep One system (using the pre-programmed 60 samples per day gradient) coupled to an Orbitrap Exploris 480 MS (Thermo Fisher Scientific) through a nanoelectrospray source. Peptides were separated on a 15-cm, 150 µM inner diameter analytical column in-house packed with 1.9 µM reversed-phase C18 beads (ReProsil-Pur AQ, Dr Maisch) and column temperature was maintained at 60°C by an integrated column oven (PRSO-V1, Sonation GmbH). Phosphoproteome analysis was performed using data-independent acquisition (DIA) in positive polarity mode with spray voltage at 2 kV, heated capillary temperature at 275°C and RF level at 40. For DIA analysis full scan resolution was set to 120,000 at m/z 200 and the full scan AGC target was 300% with an injection time of 45 ms. Mass range was set to m/z 350-1400. AGC target value for fragment spectra was 1000%. For DIA phosphoproteome analysis 17 windows of 39.5 m/z with an overlap of 1 m/z scanning from m/z 472-1143 was used, and resolution was set to 45,000 with injection time of 86 ms. Normalized collision energy was set at 27%.

All DIA raw files were analyzed using Spectronaut with a library-free approach (directDIA). All files were searched against the mouse UniProt database, supplemented with commonly

observed contaminants. For phosphoproteome analysis phosphorylation of serine, threonine and tyrosine were included as variable modifications and PTM localization cut-off was set to 0.75. Phospho-peptide data was collapsed to site information using the Perseus plugin previously described[155]. DIA raw files for library generation were analyzed using MaxQuant software version 1.6.5.0 with the integrated Andromeda search engine[156,157].

DIA phosphoproteome data were further processed using R (version 3.6.2) with the Prostar data analysis pipeline[158]. Data were log2 transformed and filtered such that a minimum of two valid values in at least one condition were required for a protein/site identification to be included in downstream analysis. Data were normalized by quantile-based normalization and imputation to replace missing values was performed using a two-step approach considering first partially observed values ('Missing completely at random') and next values missing in entire conditions ('Missing not at random')[154]. Data were normalized by row-based median subtraction and heatmaps were generated based on unsupervised hierarchical clustering. Specifically, to assess overall Amisulpride effect, phosphoproteome data were median normalized within groups defining initial treatment (WT, TNF treated) and significantly regulated phosphosites comparing inhibitor treated and untreated samples were identified by t-test using a significance cut-off of 0.05. Volcano plots were generated for visualization of significantly regulated phosphorylations identified by Student's t-test (significance cut-off 0.05). Gene ontology (GO) term enrichment analysis and Kyoto Encyclopedia of Genes and Genomes (KEGG) pathway enrichment analysis were performed using DAVID[159,160] and InnateDb[161], respectively.

3.17 Adhesion assay

SFs at $2*10^4$ cells/ well were allowed to adhere for 30' to a 96well plate covered with Fibronectin at 1μg/ml. Unbound cells were removed with sequential washes with PBS containing Ca++ and Mg++. Adhered cells were then stained with crystal violet, solubilized, and their absorbance was determined at 570 nm.

3.18 Propidium Iodide staining

Propidium Iodide (PI) staining was performed following the online available protocol from Abcam (https://www.abcam.com/protocols/flow-cytometric-analysis-of-cell-cycle-with-propidium-iodide-dna-staining).

3.19 Annexin V staining

For Annexin staining, SFs were seeded at 1,5*10^5 cells in a 6well plate and next day were treated with the indicated compounds' concentration. After 24h treatment, cells were collected by trypsin and centrifugation. After a wash with cold 1XPBS, cells were resuspended in 1X freshly diluted binding buffer, for reaching a concentration of 10^6 cells /ml. Binding buffer 10X was a 0.2 μm sterile filtered 0.1M Hepes (pH 7.4), 1.4M NaCl, and 25 mM CaCl2 solution. Cells were stained with Annexin V FITC antibody (640906, Biolegend) and were run in FACS Canto II Flow cytometer (BD Biosciences) after addition of 400μl of 1xbinding buffer and of 1μg/ λ PI- PE/ Pecy5.

3.20 Wound healing assay

hTNFtg SFs were isolated as described above and seeded in 24well plates at a concentration of 2 x 10^5 cells/well. The next day a straight-line wound was created on the formed cell monolayer using the tip of a 200μl pipette. Images of the wounds were captured by a microscope at a magnification of 4x at two time points. Time point 0 (i.e. the time of the creation of the wound) as well as 24h later (t24). The area of the wound was measured at each time point using the software ImageJ.

The percent closure of the wound was calculated using the following formula:

[(wound area at t0-wound area at t24)/ wound area at t0]*100

3.21 Isolation of peritoneal macrophages

Activated peritoneal macrophages were isolated from the peritoneal lavage of C57BL/6 wild type mice, 5 days after the endoperitoneal administration of 3% Thioglucolate, as previously described[162]. The isolated cells were seeded at a concentration of 5 x 10^5 cells/well in a 48 well plate. 4h after isolation, cells were starved O/N in Optimem (Gibco, 11058, 100U/ml P/S). The cells were further activated with 100 ng/ml Lipopolysaccharide (LPS, Sigma-Aldrich, L2630) along with the test compounds at a dose of 10μM. 48h later the supernatants of the cell cultures were collected and analyzed using the Mouse 13plex Legendplex Chemokine

(Biolegend, 740007) and Cytokine (Bioloegend, 740446) panels according to the manufacturer's instructions.

3.22 Statistical analysis

All experiments were performed at least 3 times. Data are presented as mean $\pm$ SEM. Student's *t*-test (parametric, unpaired, two-sided) or two-way ANOVA were used for evaluation of statistical significance using GraphPad Prism 8 software. Statistical significance is presented as follows: * $p < 0.05$, ** $p < 0.01$, *** $p < 0.001$, **** $p < 0.0001$.

4. Results and discussion

4.1 Identifying new potential inhibitors of TNF based on virtual molecular docking approach

4.1.1 Initial Search and Filtering- Natural products library

Following up on our earlier efforts, an *in silico* optimization of compound A11 (Ampelopsin H)[35] was performed using a modified version of EnalosMD and the Enalos+ suite cheminformatics workflow[35,163]. More specifically, a data mining procedure was performed, using the Enalos PubChem similarity node[114], searching for NPs that would be analogs of Ampelopsin H, which has been proved to be a direct inhibitor of TNF trimerization[35]. Molecular similarity suggests that structurally similar molecules are likely to have similar biological and physicochemical properties. This concept is widely known as the similarity principle, and it is fundamental in cheminformatics, as it is the basis of many property prediction models, as well as compound design models[164]. The model used included a similarity method to search PubChem for molecules, which are similar to the structure of enquiry (Tanimoto similarity 85%)[165]. This search yielded 113 relevant natural compounds, which were selected for molecular docking simulations.

4.1.2 Molecular Docking Simulations Using Enalos Asclepios KNIME rxDock Node- Natural products and FDA approved drugs

The molecular docking studies were performed using rDock[166] and the highest-score values were considered for the complexes' construction. The docking was based on the crystal structure of the complex of TNF dimer and ligand SPD304[31], after conducting a homology modelling approach.

The NPs that were identified by the similarity search were docked into the active site of TNF, and the highest-scored docking poses were selected. The Enalos Asclepios KNIME nodes is a powerful tool, which fully automates the preparation of any ligand–protein complex and performs molecular dynamics simulations, offering optimal performance and versatility, by employing a wide range of functionalities.

This refined docking step resulted in 53 natural compounds, which appeared promising for further study. Out of these 53 identified compounds, we acquired the 9 commercially available (Figure 1) named Vitisin B, Miyabenol A, Kobophenol A, trans-Diptoindonesin B,

trans-Miyabenol C, cis-Diptoindonesin B, cis-Miyabenol C, Nepalensinol B and Flexuosol A, which proceeded in further pharmacological testing.

Natural products use in drug discovery has been challenging, bearing both advantages and disadvantages. On the one hand, NPs are structures characterized by structural variability, offering a variety of scaffolds for drug optimization. They are characterized by a high molecular weight, a higher number of sp3 carbon and oxygen atoms, although bearing fewer nitrogen and halogen atoms, a higher number of hydrogen-bond acceptors and donors, and higher hydrophilicity and molecular flexibility compared with synthetic compound libraries[167–171]. Moreover, NPs use since ancient eras as medical compounds can indicate an adequate efficacy and safety window.
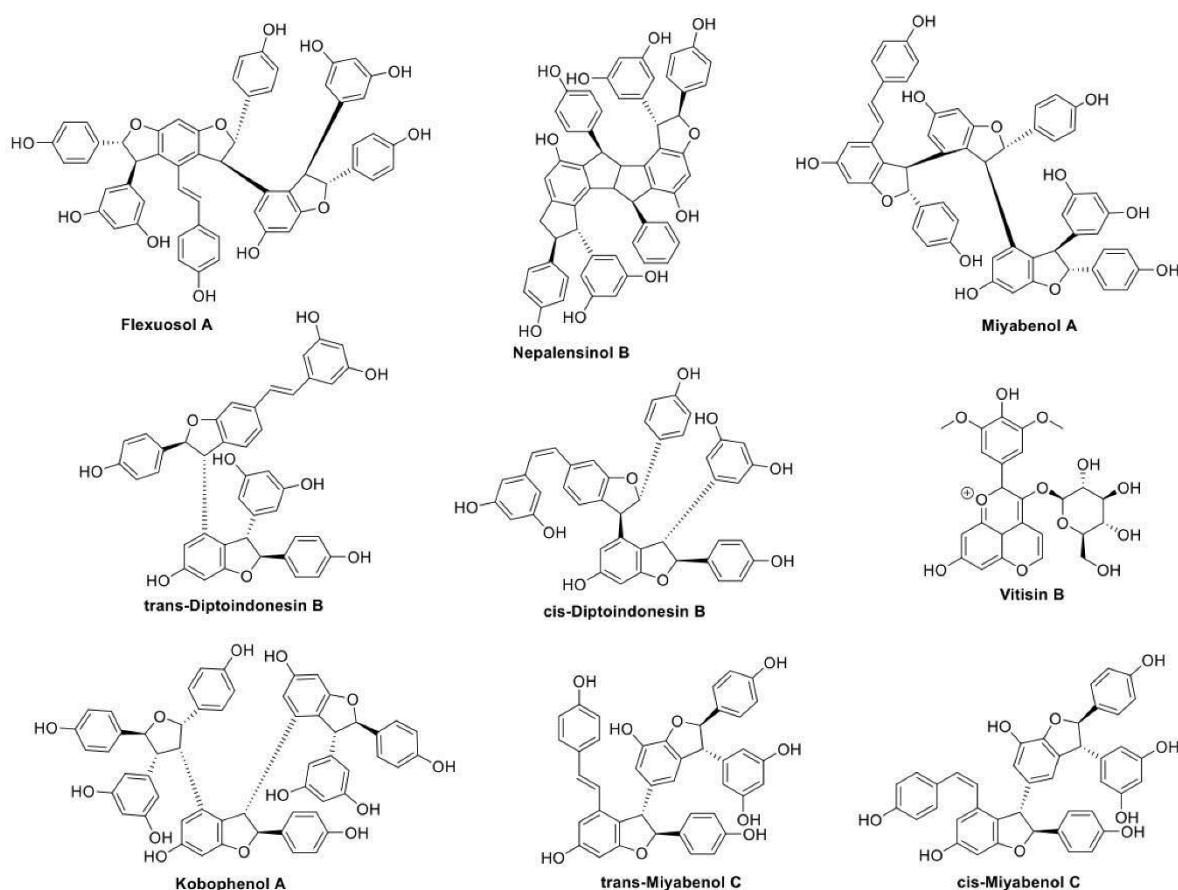

Figure 1 Chemical structures of commercially available natural products identified through molecular docking *in silico* studies as potential anti-TNF inhibitors.

On the other hand, pharmaceutical industry has lately decreased the use of NPs. Target-based assays are often not compatible with NPs extracts, while batch effect is often an issue, as

replication of extracting the bioactive molecules out of natural sources remains challenging[172,173]. Moreover, natural compounds cannot usually be protected by Intellectual properties (IP) rights[174].

Thus, in order to compare synthesized small molecules, with a known safety profile, *in vitro* and *in vivo* in the context of chronic inflammation, with the natural products, identified *in silico* as potential anti-TNF inhibitors, we repeated the molecular docking approach using a library of FDA approved drugs. The refined docking step resulted in 50 compounds which were further filtered, based on literature evaluation of their original use (Table 2).

NAME	Description - Comments
Acarbose	oligosaccharide used as a combination therapy for type 2 Diabetes Mellitus
Alcuronium chloride	neuromuscular blocker used in anesthesia
Argatroban	small molecule trhombin inhibitor - used iv as an anticoagulant in specific cases
Astemizole	histamine receptor1 inhibitor - used as antiallergic drug
Atorvastatin	statin
Avermectin B1	antihelminthic-antiparsitic drug
Azithromycin	antibiotic against mainly gram+ bacteria
Bosentan	endothilin 1 receptor antagonist - used to treat pulmonary arterial hypertension
Candesartan	angiotensin II receptor blocker used to treat hypertension
Ceforanide	antibiotic (2nd generation cephalosporin)
Cefotiam hydrochloride	broad spectrum antibiotic (3rd generation cephalosporin)
Ciclesonide	inhaled glucocorticoid
Cisatracurium besilate	used for muscle relaxation during anesthesia
Clarithromycin	antibiotic (macrolide)
Colistin sulfate	antibiotic
Darunavir	antiretroviral drug
Dilazep dihydrochloride	adenosin uptake inhibitor - vasodilator
Diosmin	small molecule (flavone) used for venous disease
Dirithromycin	antibiotic
Domperidone	dopamin antagonist used to treat hyperemesis
Erythromycin	antibiotic
Fosinopril	ACE inhibitor used to treat hypertension
Fulvestrant	anti-estrogen used in ER positive cancers
Glibenclamide	antidiabetic drug (2nd generation sulphonylurea)
Glimepiride	antidiabetic drug (2nd generation sulphonylurea)
Gliquidone	antidiabetic drug (sulphonylurea)
Indinavir sulfate	antiretroviral drug
Iodixanol	contrast agent for coronary angiography
Irbesartan	angiotensin II receptor blocker used to treat hypertension
Irinotecan hydrochloride trihydrate	antineoplastic agent blocking topoisomerase I
Itraconazole	antifungal / recently found to have anticancer effects in patients
Ivermectin	broad spectrum antiparasite drug
Josamycin	antibiotic
Nadide	dietary supplement used mainly for fatigue syndrome's and Alzheimer's
Olmesartan	angiotensin II receptor blocker used to treat hypertension
Paclitaxel	antineoplastic agent blocking proliferation by interfering with microtubules
Paromomycin sulfate	antibiotic against intestinal infections
Probucol	LDL and HDL lowering agent with antioxidant actions
Raloxifene hydrochloride	anti-estrogen used in ER positive cancers
Reserpine	antihypertensive and antipsychotic drug with serious side effects
Ritonavir	antiretroviral drug
Saquinavir mesylate	antiretroviral drug
Silodosin	a1A-adrenoreceptor antagonist specific for prostate
Telmisartan	angiotensin II receptor blocker used to treat hypertension
Tribenoside	vasoprotective agent that decreases vasulature permeability
Troleandomycin	antibiotic
Tylosin	antibiotic
Verteporfin	photosensitizer used for eye pathologies
Viomycin sulfate	antibiotic
Zafirlucast	leucotriene receptor antagonist used mainly in asthma

Table 2 Description of the current use of the 50 FDA approved drugs identified by the computational docking pipeline.
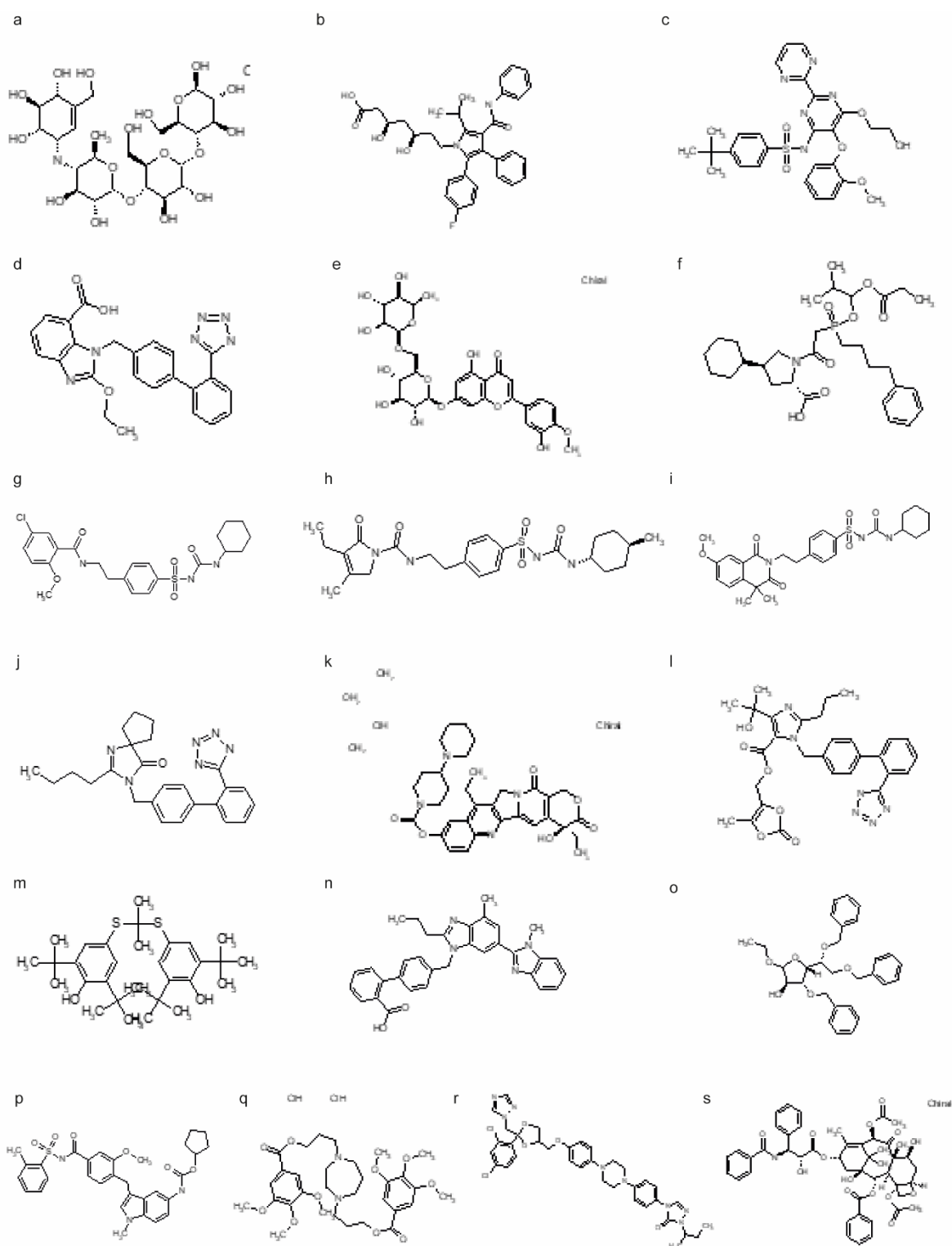
Figure 2 Chemical structures of FDA approved drugs identified *in silico* as potential anti-TNF inhibitors. a. Acarbose, b. Atorvastatin, c. Bosentan, d. Candesartan, e. Diosmin, f. Fosinopril, g. Glibenclamide, h. Glimepiride, i. Gliquidone, j. Irbesartan, k. Irinotecan hydrochloride trihydrate, l. Olmesartan, m. Probucol, n. Telmisartan, o. Tribenoside, p. Zafirlukast, q. Dilazep dihydrochloride, r. Itraconazole and s. Paclitaxel.

For instance, FDA approved drugs, known for their antibiotic or antiviral use, were excluded due to the possible detrimental side effects that they could cause in immune response during a chronic usage. Other drugs such as hormonal and neuromuscular blockers are also expected to have serious side effects upon chronic administration. We ended up in acquiring 18 commercially available compounds (Figure 2). Nadide was not ordered due to no availability in the market.

The 18 FDA approved drugs, that proceeded to a pharmacological screening and to a more detailed *in silico* evaluation were Acarbose, Atorvastatin, Bosentan, Candesartan, Dilazep dihydrochloride, Diosmin, Fosinopril, Glibenclamide, Glimepiride, Gliquidone, Irbesartan, Irinotecan hydrochloride trihydrate, Itraconazole, Olmesartan, Paclitaxel, Probucol, Telmisartan, Tribenoside and Zafirlukast. Fosinopril was finally excluded by the procedure, due to the noticed low dilution potency in aqueous solutions.

Regarding the NPs, the vast majority of the compounds (all except Vitisin B) yielded from the screening procedure are resveratrol oligomers, i.e., they belong to the chemical classes of stilbenes and stilbenoids. These compound classes have been shown to possess a wide range of multifaceted properties of pharmacological interest. Examples include from anticancer, antimicrobial, antioxidant, anti-inflammatory, antiplatelet, antidiabetic, hepato-, cardio-neuro-protective and spasmolytic properties to tyrosin inhibitory and ecdysteroid antagonist effects[175,176].

Examining every compound separately, Flexuosol A is a stilbenoid that belongs to resveratrol tetramers. It is isolated from the plants Vitis flexuosa Vitaceae and Dryobalanops lanceolata Dipterocarpaceae[175,177]. It is known to exhibit moderate antibacterial activity against Staphylococcus strains. Nepalensinol B is also a stilbenoid that belongs to resveratrol dimers and it can be found in the plants Kobresia Nepalensis Cyperaceae, Cenchrus Echinatus L. Poaceae and Sophora Stenophylla Fabaceae. Its total synthesis has been reported, albeit bearing an academic interest rather than providing a commercial perspective since it consists of a 13-step synthetic route. As for its pharmacological properties, Nepalensinol B has shown anticancer activity by inhibiting DNA topoisomerase II, while exhibiting antiproliferative activity against adenocarcinoma cells[178–180]. Both cis-Miyabenol C and trans-Miyabenol C are resveratrol trimers. Cis-Miyabenol C is obtained by various Vitis, Muscadinia and Carex species; its pharmacological interest concerns inhibition of amyloid β fibril formation and ecdysteroid antagonist activity[181,182]. Trans-Miyabenol C is obtained by Caragana sinica of Leguminosae and various Vitis, Muscadinia and Carex species; it has been found to inhibit

protein kinase C while presenting antioxidant activity[181–183]. Cis- and trans-Diptoindonesin B are stilbenoids, resveratrol trimers which were isolated from the plant Dryobalanops oblongifolia Dipterocarpaceae[184]. A recent *in silico* study suggested that they may act as sirtuine1 enzyme inhibitors, therefore demonstrating anticancer activity[185]. Additionally, Kobophenol A is a stilbene, resveratrol tetramer that has been isolated from various plants: Caragana sinica of Leguminosae[183], Carana sinica of Fabaceae[186], and many Carex Cyperaceae species (e.g., Carex kobomugi, Carex buchananii, Carex cuprina, and Carex folliculate)[187,188]. It has exhibited anti-inflammatory activity by downregulating the NF-κB signaling pathway that mediates inflammation[186]. In addition, Kobophenol A has yielded promising results as a potential prophylactic/therapeutic compound for osteoporosis and cardiotoxicity[189–191]. Furthermore, it has shown moderate antibacterial activity against Staphylococcus aureus and also antiproliferative activity[187]. A recent study reported that Kobophenol A could be a candidate lead compound against COVID–19 by inhibiting the interaction between angiotensin-converting enzyme 2 receptor of the host cells and the viral spike protein of SARS-CoV-2[192]. Additionally, Miyabenol A is also a stilbene, resveratrol tetramer and it has been isolated from Vitis ficifolia, Vitaceae and various Carex, Cyperaceae species (e.g., Carex capillacea, Carex fedia var. miyabei, Carex hirta, Carex pendula, and Carex pumila)[187,193]. It has exhibited antimicrobial (Staphylococcus aureus and Bacillus subtilis) [187],anti-inflammatory[194], antioxidative and antiplatelet aggregation activity[195]. Vitisin B, lastly, is a pyranoanthocyanine found in various red wines[196]. Interestingly, it has been successfully synthesized by reacting malvidine-3-monoglucoside with acetaldehyde[197] or vinyloxytrimethylsilane[198], and it has exhibited promising antioxidant activity[199].

Regarding the FDA drugs, most of the selected identified compounds have presented an anti-inflammatory action and/ or a therapeutic potential in animal models of either arthritis or other relevant chronic inflammatory diseases, supporting our identification outcome. Importantly, the use of Acarbose, known as an antidiabetic drug, was associated with a lower RA risk, while in a CIA mouse study, it resulted in attenuation of incidence and severity of the disease, downregulating proinflammatory cytokines in mice paws, including TNF-α, IL-6 and IL-17[200]. Moreover, it was reported that administration of Atorvastatin, a statin normally prescribed for cardiovascular diseases, in patients suffering from RA, as a combinatorial therapy with existing disease-modifying antirheumatic drugs, has added a promising anti-inflammatory effect[201]. The effect of Atorvastatin on RA compared with the first line treatment used, methotrexate, in Complete Freund's Adjuvant rats, also suggested an improved anti-inflammatory potential of the former[202]. Oral treatment with Bosentan, a treatment for

pulmonary artery hypertension, also ameliorated the clinical aspects of CIA (arthritis clinical score, paw swelling and hyperalgesia), reducing joint damage, as well as joints' leukocyte infiltration and proinflammatory cytokine levels (IL-1b, TNFa and IL-17)[203]. Additionally, endothelin receptor antagonists, like Bosentan, could effectively control inflammation, pain and joint destruction during the course of arthritis in Adjuvant Induced model of arthitis. Moreover, Angiotensin II receptor blockers, often used for heart diseases, such as Candesartan, Irbesartan and Olmesartan, have been widely known for their anti-inflammatory effect[204]. Dilazep dihydrochloride, an antiplatelet drug, with vasodilating properties, has presented anti-inflammatory potential as it suppressed the expression of TNF mRNA levels of lipopolysaccharide (LPS) induced Raw 264.7 cells macrophages via adenosine receptors implication[205]. Diosmin, prescribed for the improvement of capillary fragility or venous insufficiency, also, increased the therapeutic efficacy of methotrexate basal treatment in AIA in Rats[206]. Additionally, Glibenclamide, an antidiabetic sulfonylurea, has ameliorated the clinical signs of Experimental autoimmune encephalomyelitis (EAE), reducing the invading lymphocytes and macrophages in mice spinal cord while downregulating the cells expressing proinflammatory cytokines, including TNF[207]. On top, Glibenclamide pretreatment significantly inhibited the serum proinflammatory cytokines upregulation in a mouse sepsis model and suppressed the increase of caspase 1 and cytokines, such as IL1β and TNF, in LPS induced macrophages[208]. LPS induced Raw 264.7 cells, pre-treated with Glimepiride, another second-generation antidiabetic sulfonylurea, also presented significantly reduced TNF, IL-1 and IL-6 secretion and TLR-4 mediated activation[209]. Gliquidone, an NLRP3 inhibitor, used by diabetic patients, has been also proposed for its potential therapeutic effect in chronic inflammation models[210]. The possible role of Itraconazole in inhibiting RA, as it possesses anti-angiogenic properties[211,212], except from the antifungal ones, has also been proposed[213]. Furthermore, Paclitaxel, a chemotherapeutic mitotic inhibitor, has been linked with RA, as it interrupted SFs proliferation in culture, arresting them at G2/M cell cycle phase[214], while it inhibited the progression of CIA in rats, preventing also the joints' destruction[215]. Finally, Telmisartan and Olmesartan, both known to be Angiotensin II receptor blockers, have been reported to be effective in reducing IL-6 and TNF-α levels, based on a meta-analysis of nine randomized controlled trials[216] and suppressive as to the development of severe RA in CIA model, respectively [217]. Lastly, Probucol, a small molecule used to treat cholesterol, has presented an anti-inflammatory activity in an experimental model of chronic inflammation by targeting the NF-κB pathway in peripheral and spinal cord foci[218].

Thus, the compounds that emerged from our initial screening were, according to the literature, interesting candidates for further investigation, as their anti-inflammatory/antioxidant properties could be attributed to the blockade of the TNF trimer formation, as proposed by our computational screening.

4.1.3 Pharmacological Testing

- *Ex vivo and in vitro pharmacological testing*

The cell based pharmacological testing experiments included testing of the compounds in TNF-regulated assays *ex vivo* and *in vitro*. The first *ex vivo* screening of the compounds included quantification of the potential of the compounds to downregulate TNF-induced cytotoxicity in the L929 cell line, as previously reported[138].

Out of the nine NPs tested, five showed an improved potential to block TNF activity (Figure 3A). Four compounds, named trans-Diptoindonesin B, trans-Miyabenol C, cis-Diptoindonesin B, cis-Miyabenol C, were excluded from further validation, as they seemed ineffective to block L929 TNF-induced death (Figure 3B).

L929 cells were also used to assess the compounds' toxicity, measured by a Crystal Violet assay, as described by Melagraki *et al.*, 2017 (Figure 3C)[113,138]. As to their toxicity, compounds Vitisin B, Kobophenol A and Flexuosol A reached a plateau of maximum cytotoxicity at >85% survival at a high concentration range, attaining a satisfactory therapeutic window (Figure 3C).

The half maximal inhibitory concentration (IC50) values of the compounds' efficacy in the L929 TNF-induced assay as well as the half maximal lethal concentration (LC50) values for the influence of the compounds in the L929 cell survival, are described in the table of Figure 3D. Nepalensinol B and Miyabenol A seemed the most effective compounds, as they supported L929 cells survival, upon TNF treatment, with an IC50 of 28.97 µM and 16.03 µM, while they presented LC50 in a higher concentration, at 171 µM and 955 µM, respectively.

Same assays were repeated for the 18 FDA approved drugs, shortlisted out of the results of the molecular docking *in silico* approach, as described above. The initial screening of the drugs in the L929 TNF induced cytotoxicity assay was performed at a concentration of 10µM (Figure 4A) and the ten most effective compounds proceeded in the L929 assay at a concentration range. The dose response curves of the three best compounds of the initial screening (Dilazep Dihydrochloride, Itraconazole, Paclitaxel) describing their ability to inhibit TNF induced death,

are presented in Figure 4B. Seven of the compounds (Atorvastatin, Diosmin, Irbesartan, Irinotecan hydrochloride trihydrate, Telmisartan, Tribenoside and Zafirlukast) presented an IC50 > 100µM, thus they did not proceed in further assays (Figure 4C). Cytotoxicity of Dilazep Dihydrochloride, Itraconazole and Paclitaxel compared with the non-treated control was also measured (Figure 4D), indicating the compounds' efficiency in non-toxic concentrations.
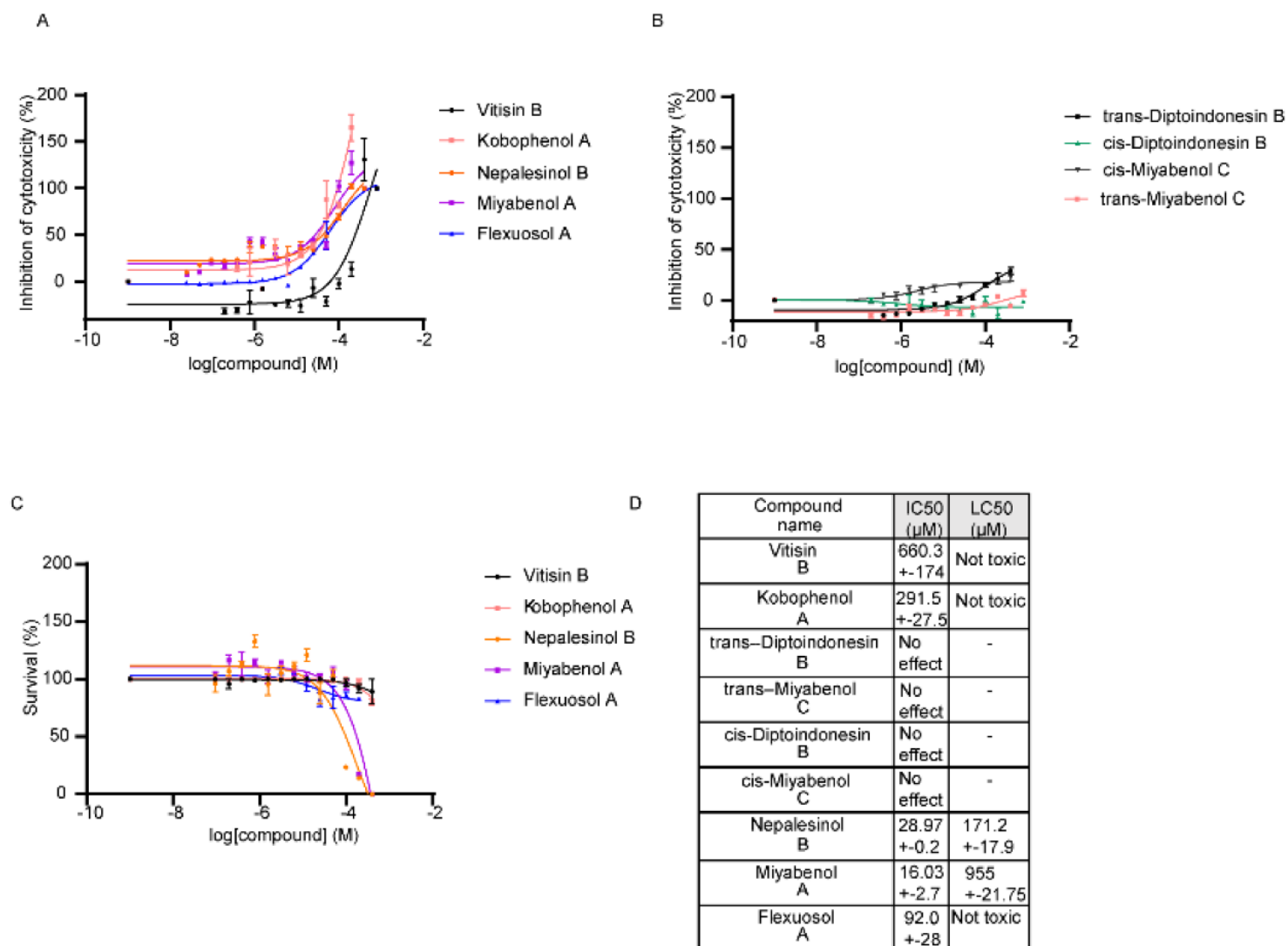

Compound name	IC50 (µM)	LC50 (µM)
Vitisin B	660.3 +-174	Not toxic
Kobophenol A	291.5 +-27.5	Not toxic
trans–Diptoindonesin B	No effect	-
trans–Miyabenol C	No effect	-
cis-Diptoindonesin B	No effect	-
cis-Miyabenol C	No effect	-
Nepalesinol B	28.97 +-0.2	171.2 +-17.9
Miyabenol A	16.03 +-2.7	955 +-21.75
Flexuosol A	92.0 +-28	Not toxic

Figure 3 Pharmacological screening of the natural compounds. A. Compounds that showed potential to downregulate the TNF induced cytotoxicity on L929 cells. B. Compounds that were ineffective in downregulating the TNF induced cytotoxicity on L929 cells were excluded from further analysis. C. Cytotoxicity of the effective compounds described in A on L929 cells. All error bars indicate SEM values. D. Conclusive table of the IC50 values of graph 3A and LC50 values of graph 3C.

In order to validate that the compounds of interest were indeed TNF inhibitors and to confirm further our identification procedure, we tested whether the most efficient compounds of both

the NPs (Nepalensinol B, Miyabenol A and Flexuosol A) and the FDA tested drugs (Dilazep dihydrochloride, Itraconazole and Paclitaxel) were capable of interrupting TNF-TNFR1 binding (Figure 5A and 5B).
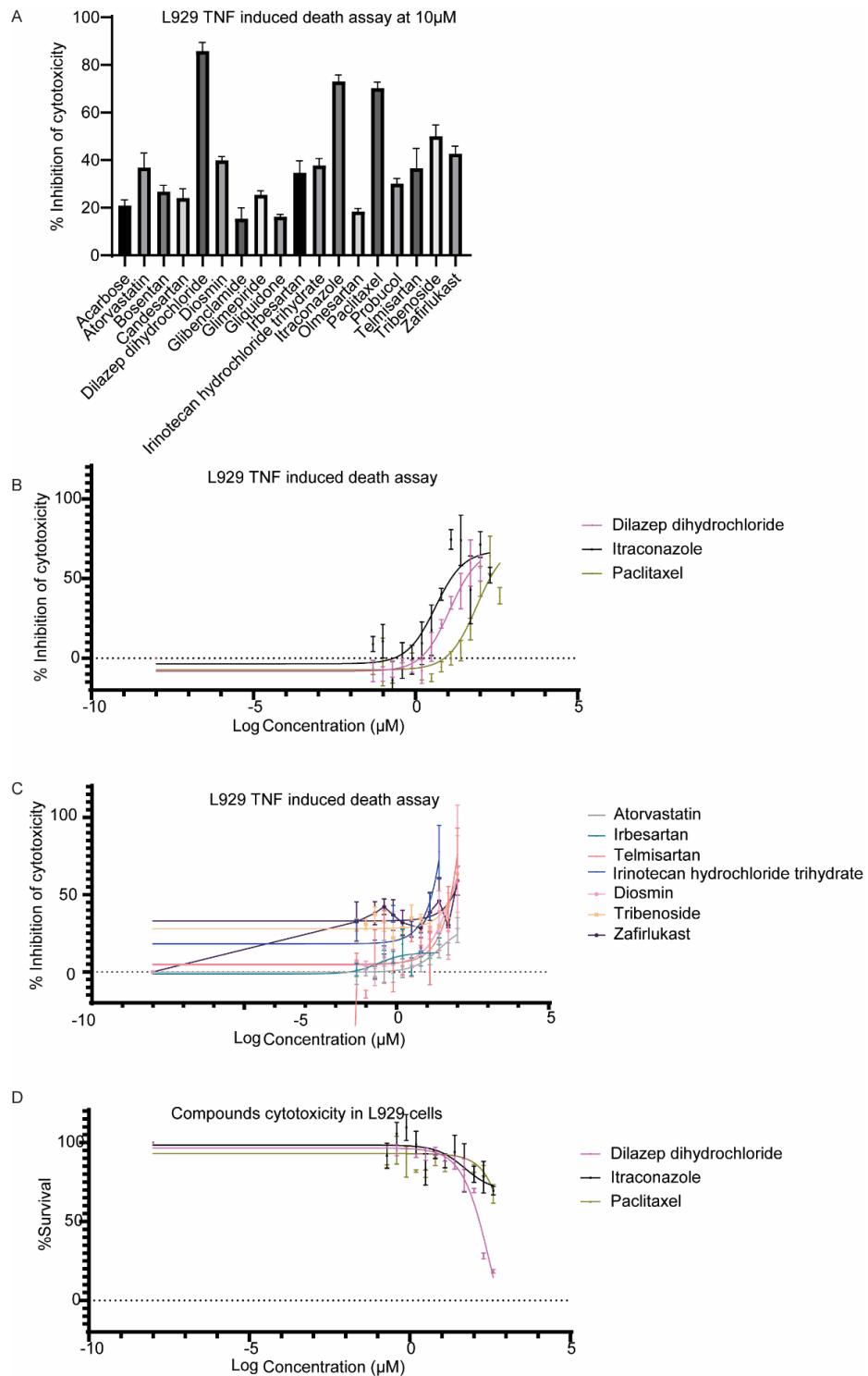

Figure 4 A. Initial Screening of 18 selected compounds at a concentration of 10µM. B. Dose dependent curves of Dilazep Dihydrochloride, Itraconazole, Paclitaxel in the L292 TNF induced death assay. C. Dose dependent curves of less efficient compounds in the L929 TNF induced death assay D. Cytotoxicity curves of the three more effective compounds (Dilazep Dihydrochloride, Itraconazole, Paclitaxel) in L929 cells.

TNF/TNFR1 binding was quantified by an *in vitro* sandwich ELISA (as previously reported)[35,113]. Regarding the NPs, Nepalensinol B showed the highest potential to interrupt TNF-TNFR1 binding, followed by Miyabenol A, with IC50 values of 90.2 ± 19 µM and 132 ± 14 µM, respectively (Figure 5A). However, Miyabenol A did not manage to interrupt the TNF-TNFR1 binding more than 70%, indicating that Nepalensinol B is probably a more promising inhibitor of the TNF-TNFR1 complex formation. Flexuosol A downregulated *in vitro* TNF-TNFR1 binding with an IC50 of 1.8 ± 0.45 µM at about 50%. As far as it concerns Dilazep Dihydrochloride, Itraconazole and Paclitaxel, Figure 5B illustrates that Dilazep Dihydrochloride is the only out of the three compounds that interrupt TNF-TNFR1 binding (IC50=67.88), rendering it as a more promising direct inhibitor of TNF.
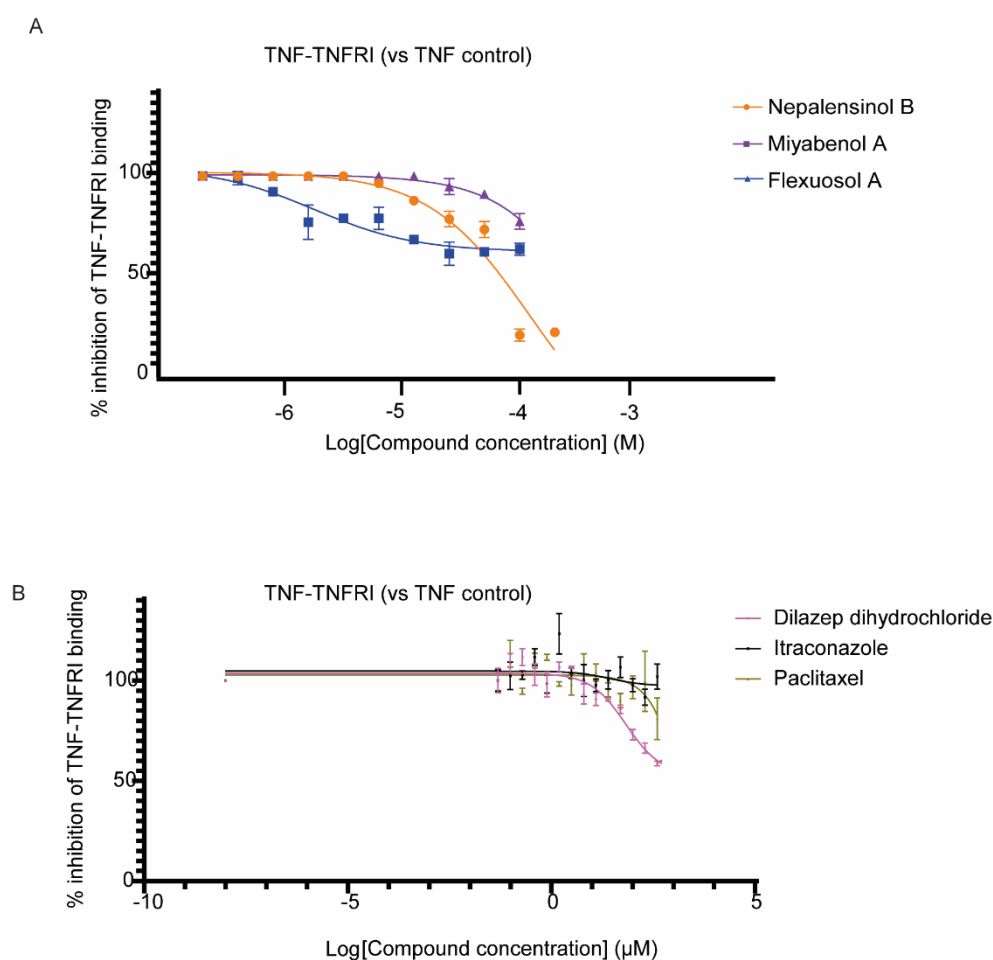
Figure 5 *In vitro* TNF-TNFR1 sandwich ELISA to assess the A. Natural products' and B. FDA drugs' potential to inhibit the interaction of TNF with its main receptor TNFR1. All error bars indicate SEM values.

Table 3 describes in detail the IC50 values of the three most potent selected compounds of the FDA drugs tested, in the pharmacological assays described in Figure 4 and 5.

compound	IC50 (µM)		
	L929 TNF induced death	L929 cytotoxicity	TNF-TNFRI binding inhibition
Dilazep Dihydrochloride	11.42 ± 0.34	332.7 ± 46	67.88 ± 5.88
Itraconazole	3.53 ± 0.7	not toxic	not effective
Paclitaxel	66.38 ± 4.9	not toxic	not effective

Table 3

Additionally, the anti-inflammatory potential of the top selected compounds in between the NPs (Nepalensinol B, Miyabenol A and Flexuosol A) were studied in primary cells, using synovial fibroblasts (SFs), isolated either from the ankle joints of human TNF transgenic (*hTNFtg*) mice, or their wild-type littermates, as previously reported[143]. SFs of the *hTNFtg* model have been highlighted as the key driver cell type in this model of disease, as TNF/TNFR1 signalling in SFs is sufficient and necessary for the disease manifestation[64]. SFs were treated with different concentrations of the experimental compounds with (WT SFs, Figure 6A) or without (*hTNFtg* SFs, Figure 6B) the addition of hTNF. *hTNFtg* SFs secrete spontaneously hTNF, while wild-type (WT) SFs were stimulated with 10 ng/mL hTNF to increase their proinflammatory responses. At 48 h following the treatment of the SFs with different concentrations of the test compounds, their supernatants were analysed by ELISA for the detection of CCL5/RANTES, a pathogenic chemokine in RA. Interestingly, Nepalensinol B and Miyabenol A were effective in downregulating CCL5, presenting, respectively, IC50s values of 7.39 µM and 25.25 µM in WT TNF-induced SFs and 3.7 µM and 2 µM in *hTNFtg* SFs (Figure 6C). Flexuosol A, which presented a higher IC50 in the L929 TNF death–induced assay, was also about 10 times less effective in eliminating CCL5 levels in the tested concentrations (Figure 6C).

Similarly, Dilazep dihydrochloride was also tested in primary joints' SFs. To test if Dilazep dihydrocloride indeed block TNF signalling in both exogenously TNF stimulated or in SFs that carry deregulated TNF expression, we again used either wild type (WT) cells, stimulated with 10ng/ml TNF or arthritic fibroblasts isolated from *hTNFtg* joints. Except from CCL5, CCCL20 was also measured, in order to assess if the drug of interest possess a broader anti-inflammatory profile. Importantly, Dilazep dihydrochloride significantly downregulated the levels of both the pathogenic chemokines tested, CCL5 and CCL20[219] (Figure 7). An anti-TNF biologic used in clinic, Adalimumab, was used as a positive control.
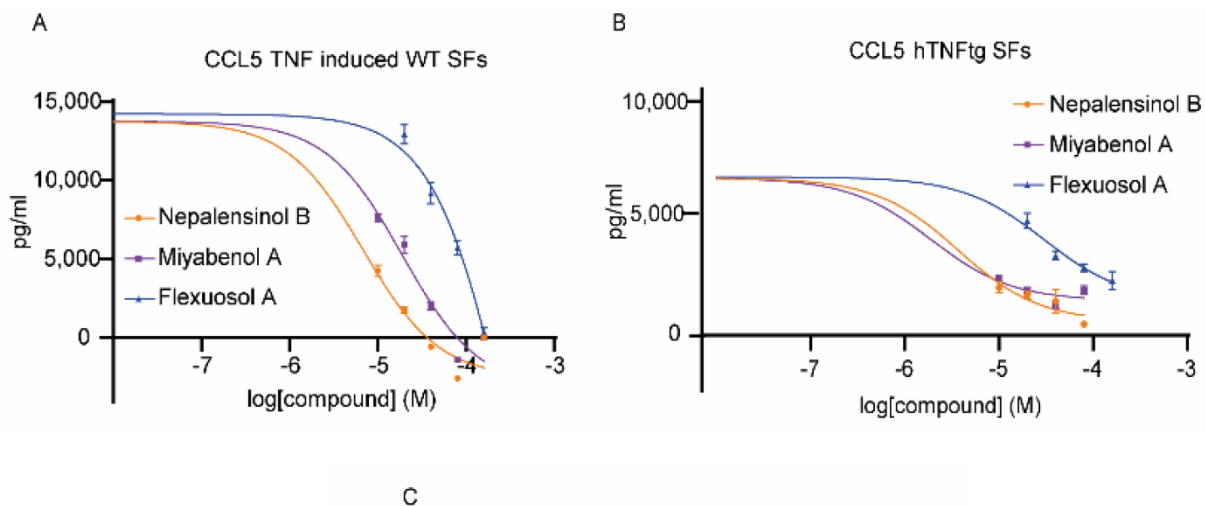
Figure 6 A. Treatment of WT SFs with several concentrations of the NPs compounds to assess the anti-inflammatory potential of the compounds on exogenous induction of TNF. B. Treatment of *hTNFtg* SFs, which overexpress hTNF, with several concentrations of the NPs compounds to assess the anti-inflammatory potential of the compounds. C Table with IC50s values calculated in dose response curved described in A and B.

To conclude among the nine NPs tested *ex vivo* in the L929 TNF induced necroptosis assay[140], we found that, indeed, five compounds were able to support L929 cell survival upon addition to the cells. SPD304, when bound to TNF[31], was found to reduce L929 TNF–induced death (IC50 5 ± 0.2 µM), presenting however high toxicity (LC50 7.5 ± 0.2 µM)[138,220]. Notably, the new two best NPs identified (Nepalension B and Miyabenol A), although ~5-fold less effective than SPD304, presented much less toxicity on the cells (in the range of two orders of magnitude). Additionally, mostly Nepalensinol B, and to a lesser extent, Miyabenol A, were able to downregulate chemokine ligand 5 (CCL5), which was found to be, among others, a pathogenic chemokine, being used for drug testing, both in human RA[221] and mouse chronic polyarthritis[222]. Both Nepalensinol B and Miyabenol A reduced CCL5 in both *hTNFtg* SFs, which spontaneously secrete high levels of chemokines, and wild-type (WT) SFs exogenously stimulated with human TNF in order to increase their proinflammatory potential. Using both cell settings, we show that compounds regulate the SFs responses by interfering with the TNF pathway itself. The combination of low toxicity along with the anti-inflammatory properties

could assign to the most effective compounds, Nepalensinol B and Miyabenol A, a highly promising therapeutic potential, as they can serve as lead compounds addressing drug development for chronic inflammatory diseases. Miyabenol A and Nepalensinol B proceeded also to TNF-TNFR1 binding ELISA studies. Interruption of TNF-TNFR1 interaction contributes to the compounds' desired properties, as disruption of TNF binding to its principal receptor, TNFR1, has been a long-desired goal in the development of novel therapeutics in chronic inflammatory models of disease[223]. Nepalensinol B interrupted TNF-TNFR1 binding at low concentrations devoid of cytotoxicity, indicating that this compound could be employed as a direct TNF inhibitor. Interestingly, Nepalensinol B completely abolished TNF-TNFR1 interaction at tested concentrations over 50 μM (Figure 5A), while Ampelopsin H, used as a scaffold in the molecular similarity search, achieved a downregulation of around 60% of TNF-TNFR1 binding in the same concentration range[138].

Further *in silico* calculations showed that among the NPs tested, Nepalensinol B exhibits an excellent thermodynamic profile, achieving a significantly lower free energy of binding, predominately due to enthalpic parameters and low desolvation penalties. This, in combination with the advantageous Structure-Activity Relationship (SAR) of Nepalensinol B observed in docking and Molecular Dynamics (MD) simulations, leading to a richer H bond network and a highly stable binding, renders Nepalensinol B the most promising lead compound for TNF drug discovery.

Concerning the FDA drugs tested, among the 18 ligands, Dilazep dihydrochloride, an adenosine uptake inhibitor, was the most potent in interrupting not only TNF-TNFR1 binding but also TNF signalling, both in L929 cell line and in primary murine joint's SFs. The result was further supported by further computational studies performed, as Dilazep dihydrochloride formed a strong hydrogen bond network with TNF backbone, while the bound compound conformation drove the piperazine central moiety to be extended to the outside part of the cavity, inhibiting further TNF to bind to its main receptor, TNFR1.
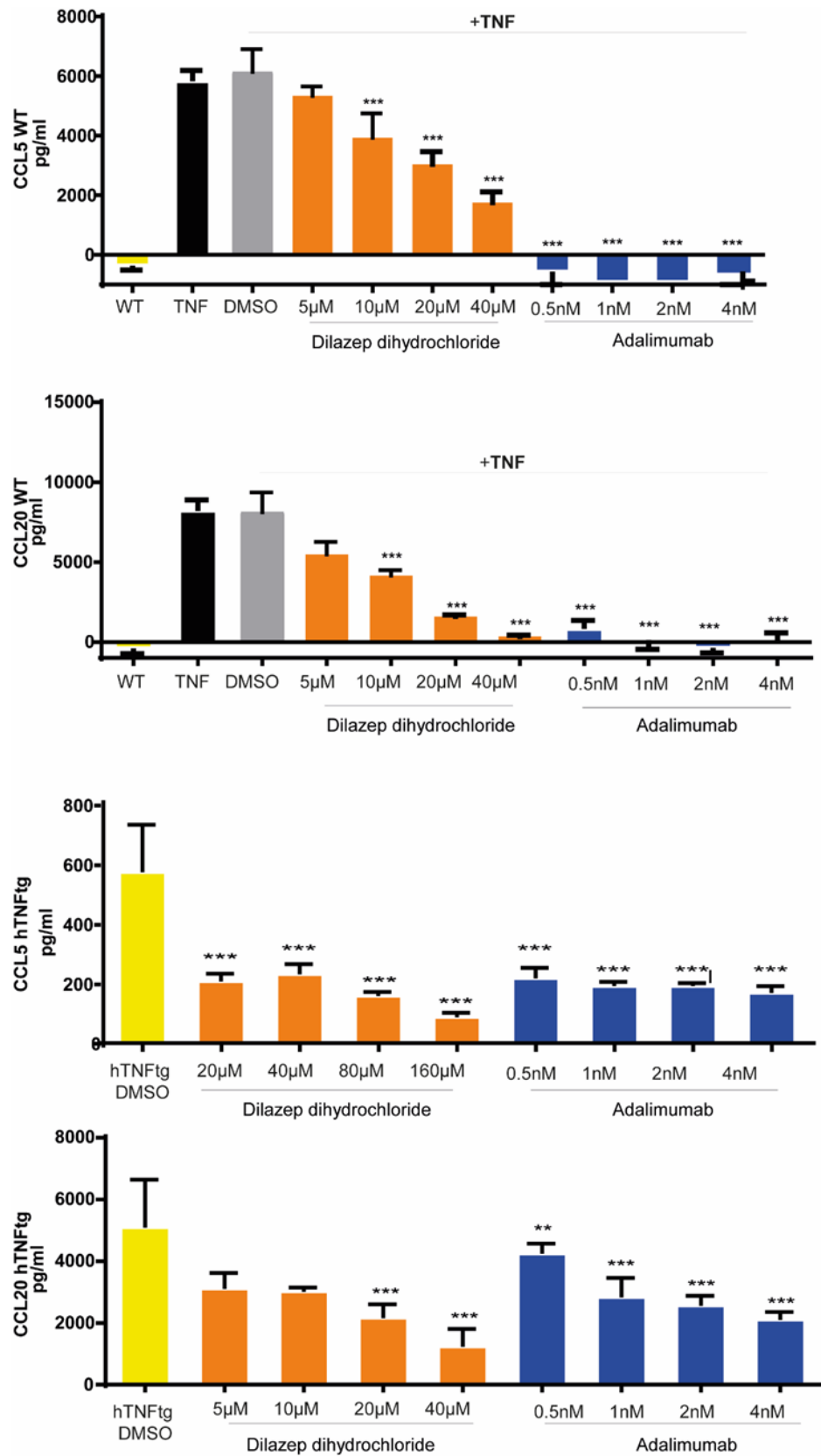
Figure 7 CCL5 and CCL20 levels of WT and *hTNFtg* SFs, when treated with the compound of interest, Dilazep dihydrochloride, or an anti-TNF antibody, Adalimumab in a range of concentrations. Statistical significance is indicated as to WT TNF DMSO treated/ to *hTNFtg* DMSO treated control.

Adenosine has been extensively linked to the regulation of inflammatory processes. The first report for the anti-inflammatory effects of adenosine were presented back in 1983, describing the potential of extracellular adenosine to inhibit stimulated neutrophil superoxide anion production[224]. Since then, adenosine endogenous levels and pharmacological targeting of adenosine through its metabolism regulation or manipulation of its receptors' expression or function have been repeatedly mentioned to play a role in inflammatory processes. Adenosine regulates the activation of human FLS, osteoclasts and chondrocytes, that contribute to the joint destruction in RA. Additionally, synovial fibroblasts' hyperproliferation along with the deregulated vasculature in the inflamed tissues lead to hypoxia, and although acute hypoxic conditions cause accumulation of the protective extracellular adenosine by both the increased transformation of ATP levels to adenosine, along with the additional extracellular production of adenosine through the hydrolysis of adenine nucleotides (ATP, ADP and AMP), chronic hypoxia leads to mitochondrial defects and reduced adenosine levels in the inflamed joints[225]. Several drugs can regulate adenosine levels, even without binding to the known adenosine receptors, including compounds that interfere with the formation, degradation or transport of adenosine. The anti-inflammatory extracellular adenosine accumulation is followed by the uptake of adenosine intracellularly through Extracellular Nucleoside Transporter (ENT1). Methotrexate, the first line treatment for Rheumatoid Arthritis, has been shown to inhibit activation of NF-κB by increasing both adenosine release and activation of adenosine receptor A2a ,limiting immune cells' infiltration in the sites of inflammation[226]. Additionally, several Non-Steroidal Anti-inflammatory Drugs (NSAIDs) or widely used anti-inflammatory drugs can modulate adenosine uptake by binding to ENT1[227,228], which is also inhibited by the drug of interest, Dilazep dihydrochloride[229]. Thus, Dilazep dihydrochloride is an interesting candidate for further preclinical studies in chronic inflammatory diseases as except from its already known beneficial ENT1 inhibition, based on our studies, it could also block TNF mediated pathogenic signaling.

- *In vivo evaluation of the most promising identified TNF inhibitors*

To test whether both Nepalensinol B and/ or Dilazep dihydrochloride could have an *in vivo* effect we employed their administration in the LPS mediated acute sepsis model and in the chronic polyarthritis *hTNFtg* model, respectively. The results were not however promising.

From the one hand, Nepalensinol B, as a natural product, showed quite variable results on downregulating the TNF induced elevated levels of IL6 in the serum of the treated mice, a

result that could be attributed to differences of the active product between the batches, although bought from the same company (Figure 8A).
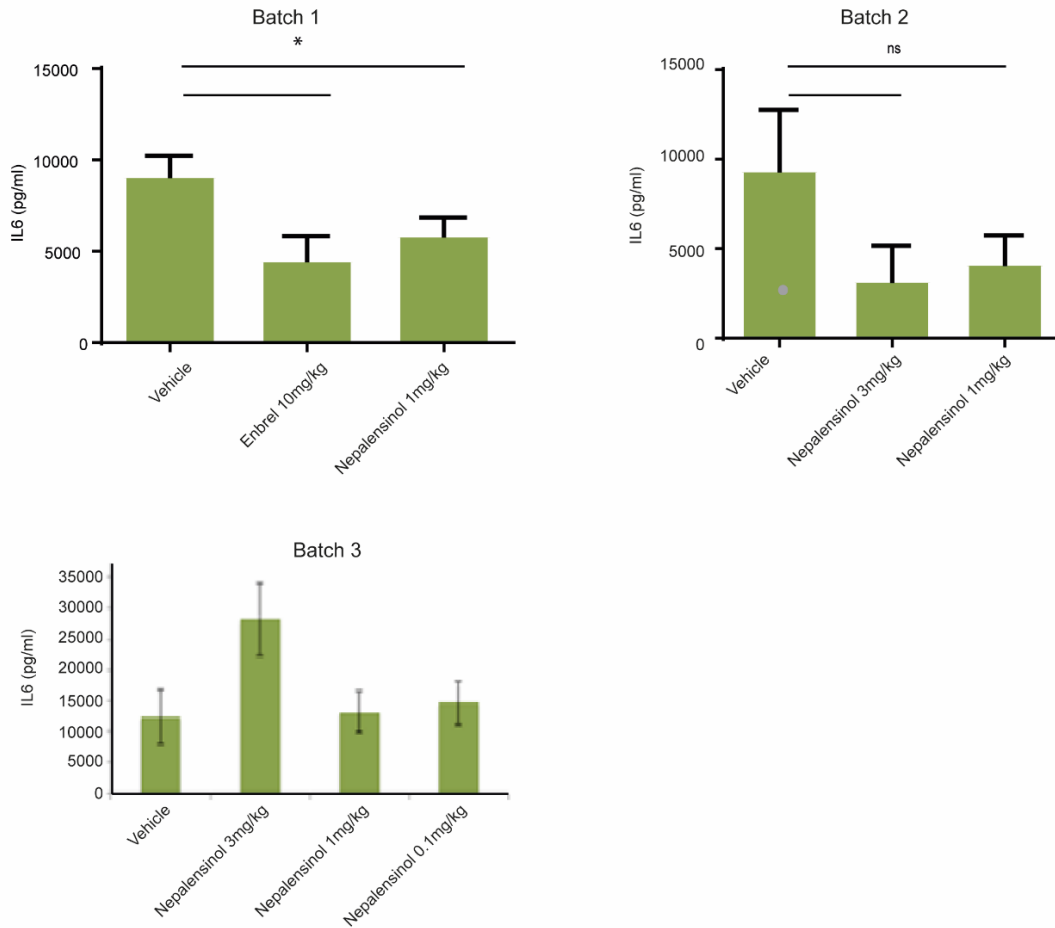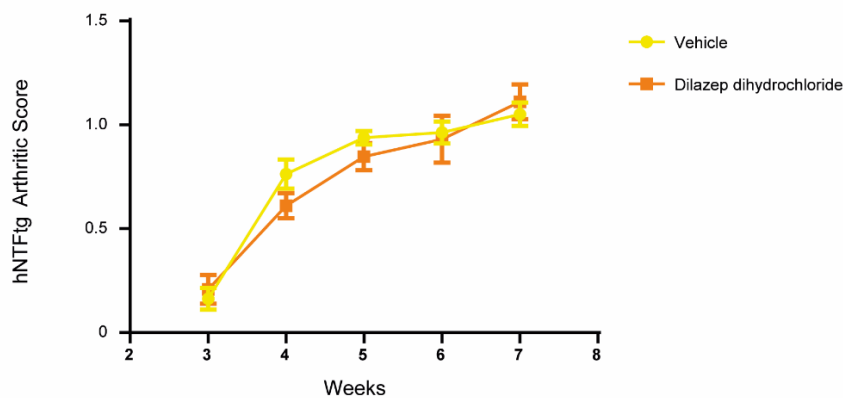

Figure 8 *In vivo* administration of A. Nepalensinol B in the LPS induced acute inflammation model and of B. Dilazep dihydrochloride in the *hTNFtg* chronic polyarthritis model, indicated that both compounds, although they show an adequate profile as TNF inhibitors *in vitro*, they presented a reduced potency to eliminate TNF *in vivo* effects. Etanercept (Enbrel), an anti-TNF biologic was used in A as a positive control.

On the other hand, Dilazep dihydrochloride, as an FDA drug with known safety profile, was directly tested in the *hTNFtg* model of chronic polyarthritis, following a twice daily per os administration of 20mg/kg, starting from week 3 (early phase, before the onset of the disease) till the week 8 (established disease state). However, Dilazep dihydrochloride could not attenuate the *hTNFtg* arthritis score, indicating a reduced potency of the compound to be efficient in eliminating TNF effects *in vivo* (Figure 8B).

4.2 Identification of inhibitors of activation of arthritogenic synovial fibroblasts based on signature matching

4.2.1 Identification of Amisulpride as a modifier of *hTNFtg* SFs activation

In an attempt to identify new drug candidates as potential therapeutics for RA, we employed an approach based on signature matching, exploiting the publicly available database "L1000CDS²". "L1000CDS²" constitutes a signature search engine that searches in a set of ~ 35,000 different signatures produced by ~ 62 human cell lines, treated with ~ 4,000 compounds across a range of concentrations and time points, aiming to find small molecules that either mimic or reverse user's input signature[141]. Interestingly, the cells used, *hTNFtg* SFs, have been found highly correlated with RA human FLS not only as to their gene expression profile[66] but also as to the clusters they form in single cell level, bearing distinct roles in the joint area[81,84,85]. In this basis, 3' mRNA sequencing of SFs isolated from 8-week old *hTNFtg* SFs (established disease) and wild type (WT) controls was initially performed and both groups were subsequently compared to each other. The results of this analysis were then combined with data already published[66], aiming at precisely determining those genes that are commonly deregulated in all stages of the disease (i. at 3 weeks of age, named "early" timepoint, which precedes the onset of the disease, ii. at 8 weeks of age, named "established" timepoint, when the disease is evolving and iii. at 12 weeks of age, named "late" timepoint, when the mice are at the end-disease state) in comparison with WT controls (deregulated genes volcano plotted in Figure 9A). Additionally, the expression profile of *hTNFtg* SFs was further analysed before and after a 48h treatment with 1μg/ml Infliximab, a known widely used anti-TNF drug (deregulated genes volcano plotted in Figure 9B). Subsequently, the "L1000CDS²" database was used, in order to search for small molecules that either reverse the disease profile or mimic our treated signature. After comparing the two aforementioned compounds data lists, it was found that only one drug, namely Amisulpride, looks promising to fulfil our criteria; reversing the disease signature and mimicking the anti-TNF drug effect (Infliximab) on

arthritogenic SFs (Figure 9C). Figure 9D presents the fifty top candidate perturbations that were proposed by "L1000CDS²"[141] search engine to reverse the pathogenic *hTNFtg* signature and mimic the Infliximab treated profile of SFs, respectively.
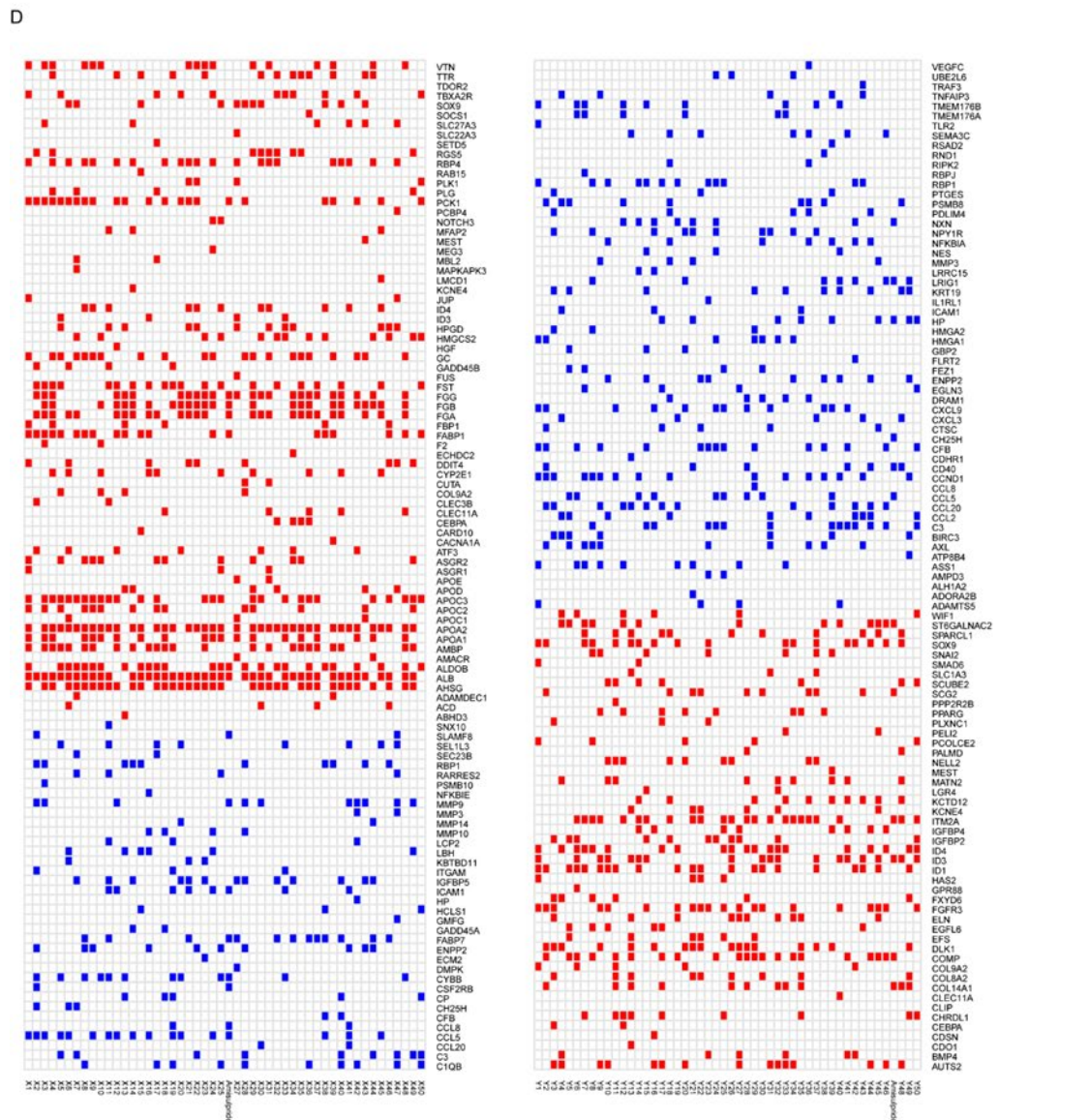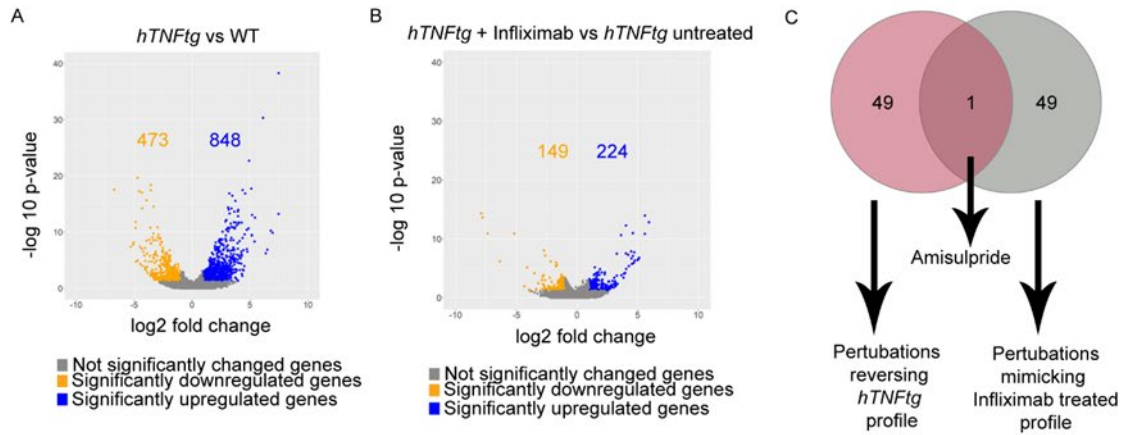
Figure 9 Identification of new candidates for the treatment of RA. A. Volcano plot showing the number of deregulated genes in *hTNFtg* SFs versus WT control. B. Volcano plot showing the number of deregulated genes in *hTNFtg* SFs before and after treatment with Infliximab. C. Venn diagram showing the overlap between perturbations that reverse the *hTNFtg* profile and mimic the Infliximab-treated disease signature. D. Heatmaps presenting the top 50 perturbations proposed by the L1000CDS[2] search engine, that either reverse the *hTNFtg* profile or mimic the Infliximab-treated disease signature, respectively.

Figure 10A presents a graphical summary of the strategy followed to identify and validate Amisulpride function in *hTNFtg* SFs activation.

Amisulpride is an antipsychotic drug acting as a powerful antagonist of D2/D3 dopamine receptors and Htr7 serotonin receptor, which is administered in high doses to treat schizophrenia and in low doses to treat depressive disorders[230,231].

We further validated the effect of Amisulpride in *hTNFtg* SFs by comparing the expression profile of *hTNFtg* SFs treated with Amisulpride for 48h to that of untreated *hTNFtg* SFs. Amisulpride restored a significant number of genes in *hTNFtg* SFs (103 genes in total that are deregulated in *hTNFtg* SFs vs WT controls) including downregulation of 61 genes expressing several inflammatory chemokines and Metalloproteinases (MMPs) (Figure 10B and 10C). Notably, KEGG pathway analysis of these 61 genes, revealed RA pathogenesis and TNF signalling pathway among the top enriched functional terms (Figure 10D). The expression of genes such as *Mmp3*, *Cxcl3* and *Cox2*, that are important in joint inflammation and bone destruction was also validated by quantitative real time PCR (Figure 10E) and it was found to be decreased following Amisulpride treatment of arthritic SFs. Importantly, genes that were restored following treatment with Amisulpride, were also commonly regulated by Infliximab treatment on *hTNFtg* SFs, validating further our identification procedure (Figure 10B and 10C). Additionally, Amisulpride treatment resulted in overexpression of 42 genes that are found to be downregulated in *hTNFtg* vs WT SFs (Figure 10B). Analysis of these genes highlighted Wnt signalling as the top enriched pathway which interestingly, has been also found to be deregulated in human RA and in relevant experimental animal models of the disease[232,233], while it has been suggested to have a protective role in *hTNFtg* mouse model[234].
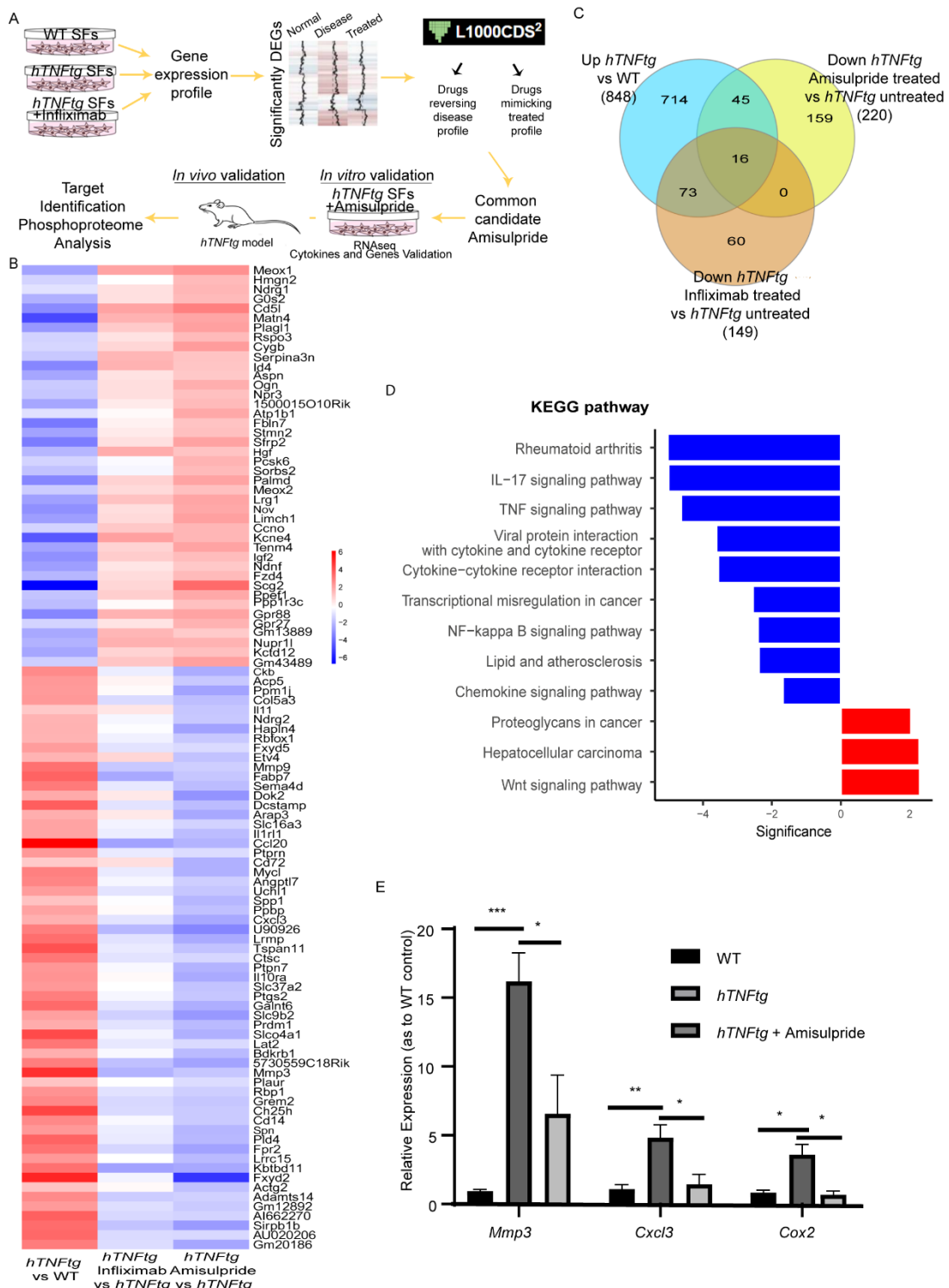
Figure 10 Amisulpride treatment affects the TNF pathway in *hTNFtg* SFs. A. Pipeline used to identify and test Amisulpride as modifier of *hTNFtg* SFs' activation. B. Heatmap of the 103 genes that are deregulated in *hTNFtg* SFs vs WT and are restored upon Amisulpride treatment. C. Venn diagram showing the genes being upregulated in *hTNFtg* SFs vs WT while being downregulated upon Amisulpride/ Infiliximab treatment. D. Kegg pathway analysis of the 103 genes described in B. E. Validation of RNAseq identified genes through quantitative Real Time PCR. (* p-value < 0.05; ** p-value < 0.01; *** p-value ≤ 0.0001, all data are shown as mean ± SEM and all comparisons were made against *hTNFtg* vehicle sample using Student's t test).

The anti-inflammatory profile of Amisulpride was further confirmed in protein level by the dose-dependent reduction observed in the high levels of the proinflammatory chemokines CCL20/Mip3 and CCL5/RANTES in the supernatants of *hTNFtg* SFs treated with the drug for 48h (Figure 11A). A similar effect on CCL5 and CCL20 production was also noticed in WT SFs exogenously stimulated by TNF (Figure 11B), an indication that Amisulpride plays a role in the cell responses downstream of hTNF and that it can produce an effect not only towards chronic hTNF stimulus, but also against induced robust inflammatory signals. Amisulpride also affected both the transcription and the secretion of hTNF by *hTNFtg* SFs, suggesting that the drug targets also the cytokine driver of *hTNFtg* SFs pathogenicity (Figure 11C). Moreover, Amisulpride was able to effectively inhibit the TNF-induced cytotoxicity of L929 cells (Figure 11D) proceeding to necroptosis upon TNF and Actinomycin D addition[235], giving a further evidence about the implication of the drug in the TNF signalling pathway.

Of note, all drug concentrations used were non-toxic according to a crystal violet assay performed (Figure 12A). Moreover, the levels both of the monocyte chemoattractant protein-1, CCL2, and of the angiogenic chemokine CXCL5 were found to be reduced in the supernatants of *hTNFtg* SFs treated with Amisulpride, providing to the drug of interest a wider spectrum of anti-inflammatory properties (Figure 12B).
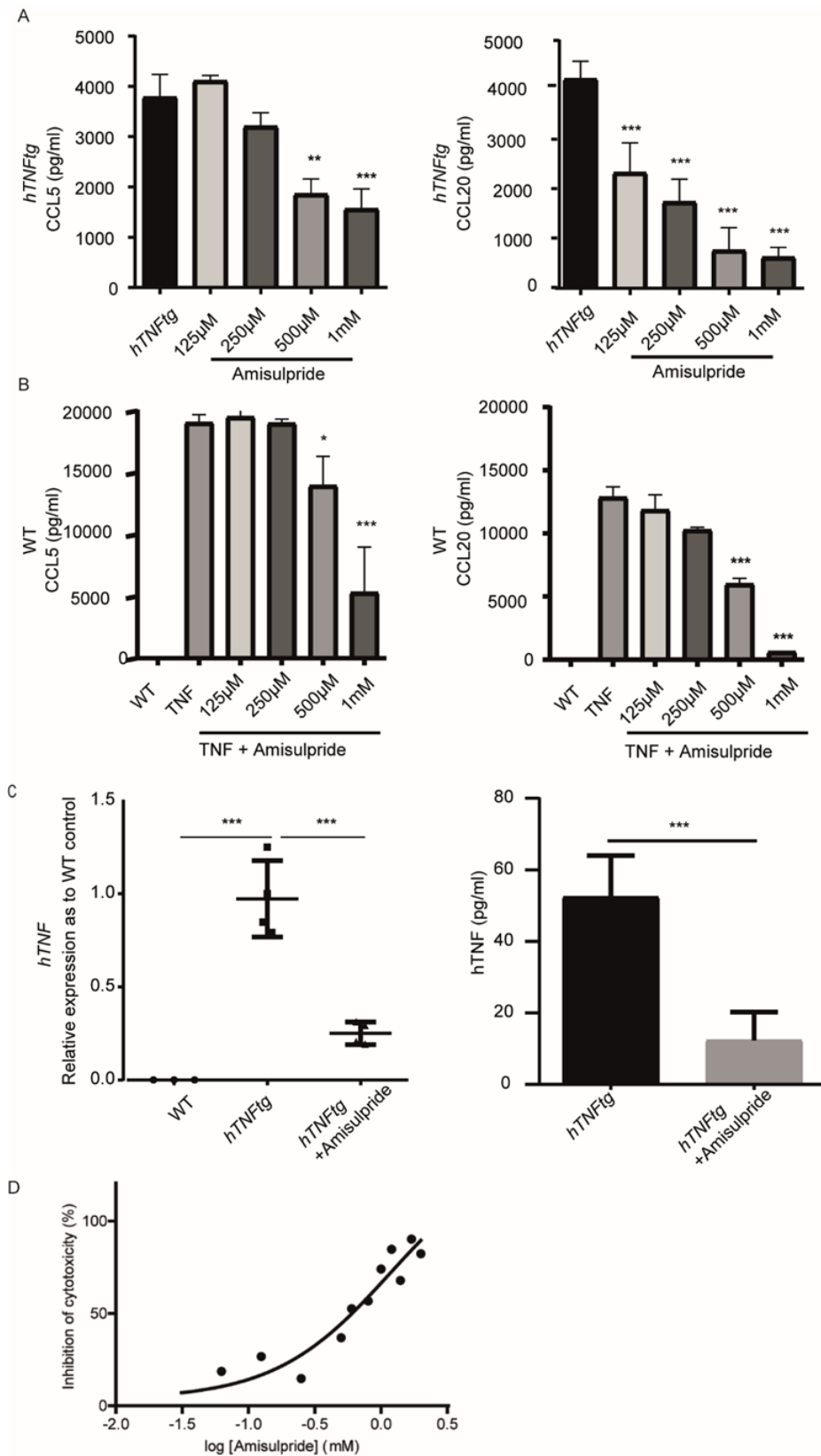
Figure 11 The anti-TNF activity of Amisulpride. Chemokines detection in supernatants of A. *hTNFtg* SFs and B. WT SFs after 48h of treatment with 10ng/ml TNF stimulation and Amisuplride at the indicated concentrations. C. Amisulpride affects both the transcription and the secretion of hTNF in *hTNFtg* treated SFs. D. L929 cells TNF induced necroptosis is inhibited by the addition of Amisulpride in a dose dependent manner. (* p-value < 0.05; ** p-value < 0.01; *** p-value ≤ 0.0001, all data are shown as mean ± SEM and all comparisons were made against *hTNFtg* vehicle/ WT TNF treated sample using Student's t test.)
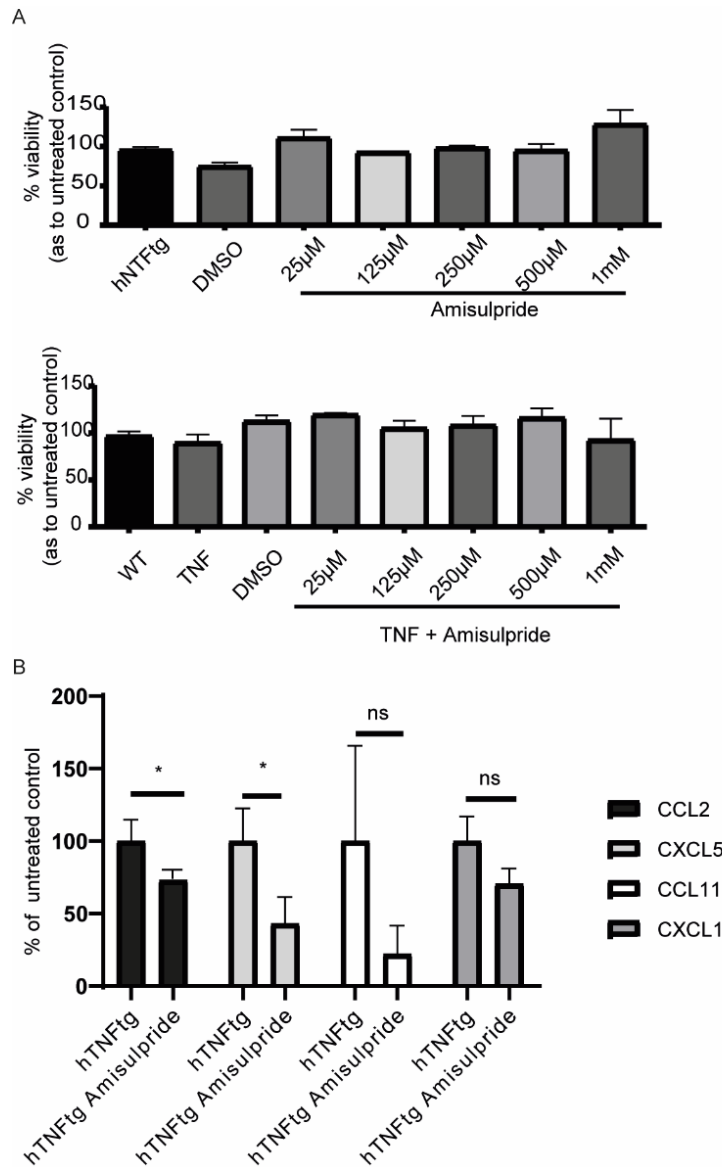
Figure 12 A. Crystal violet viability assay, indicating the non-toxicity of Amisulpride, even in high doses. B. Amisulpride at 500μM downregulates CCL2 (MCP1) and CXCL5 (LIX), measured by Legendplex panel on *hTNFtg* SFs. CCL11 and CXCL1 were not downregulated significantly. TARC (CCL17), MIP-1β (CCL4), BLC (CXCL13) and MDC (CCL22) were not detected in the supernatants. (* p-value < 0.05; ** p-value < 0.01; *** p-value ≤ 0.0001, all data are shown as mean ± SEM and all comparisons were made against *hTNFtg* vehicle sample using Student's t test.)

4.2.2 Amisulpride alleviates acute and chronic inflammation *in vivo*

The activity of Amisulpride was further substantiated *in vivo*, in the LPS experimental animal model, where we showed that administration of Amisulpride downregulated significantly the increased serum levels of mTNF and IL6 dose dependently, 1.5h post infection (Figure 13A). Although dopamine and serotonin, the major targets of Amisulpride, are best known as
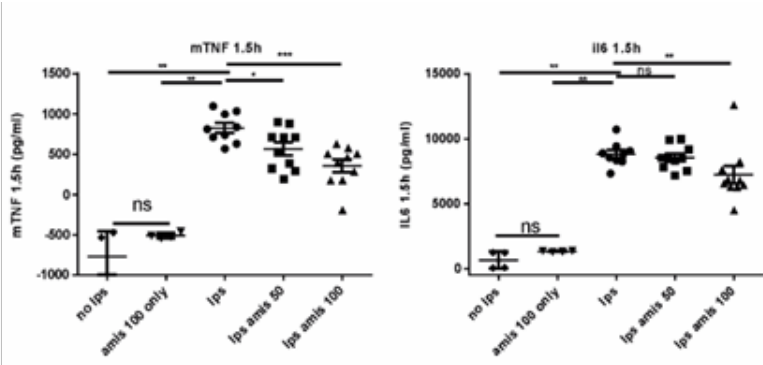
neurotransmitters, several studies have pointed out their additional involvement in the functionality of the immune system. Since the early '90s, Sulpiride, a precursor of Amisulpride, exhibiting potent D_2 dopamine antagonist properties, has been shown not only to significantly decrease the LPS-induced TNF plasma levels in a dose-dependent manner but also to inhibit the LPS-induced NO production by peritoneal macrophages[236]. Furthermore, mice challenged with a lethal dose of LPS were found to be protected by another antidepressant drug, namely bupropion, an effect attributed to the reduction of the high mTNF, IL-1β and IFNγ plasma levels by the treatment[237].

Given the inhibitory activity of Amisulpride on the TNF signalling pathway, both in SFs and in the LPS-induced acute inflammation animal model, the therapeutic potential of Amisulpride was evaluated in *hTNFtg* mice, which have been successfully used for the testing of various drugs[238] since as described in the introduction, they develop an erosive polyarthritis with characteristics similar to those observed in RA patients[48].
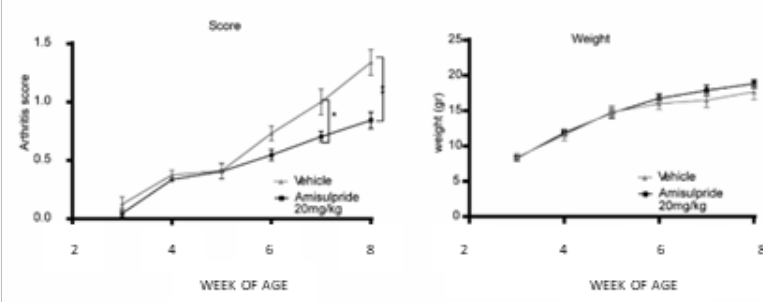
Amisulpride was administered orally (20 mg/Kg) twice per day in arthritic *hTNFtg* mice at a prophylactic mode (before the onset of the disease until the established disease state). The selected dose of Amisulpride was based on the already known toxicity data of the drug and the relevant human dose prescribed for its original use in the field of depressive disorders[239]. As it can be seen in Figure 13B, Amisulpride downregulated the phenotypic polyarthritis score of *hTNFtg* mice, decreasing significantly the synovitis score in H/E histological sections (Figure 13C). Weekly body weight assessment and gross behavioural effect observation confirmed the safety profile of the drug (Figure 13B). Intriguingly, the significant antiarthritic activity of Amisulpride was not associated with a significant effect in both the bone erosion and the cartilage destruction of the treated animals (Figure 13D and 13E), indicating the potential involvement of the drug in attenuating mainly the influx of inflammatory cells in the joints of arthritic mice.

FACs based quantification of infiltrated CD45+ cells, macrophages, monocytes, neutrophils, eosinophils, dendritic cells, CD4+ T cells and CD8+ T cells in the ankle joints of 8 week-old mice treated with Amisulpride showed that the drug attenuates mainly the numbers of monocytes when compared with vehicle treated controls (Figure 14A and 14B).
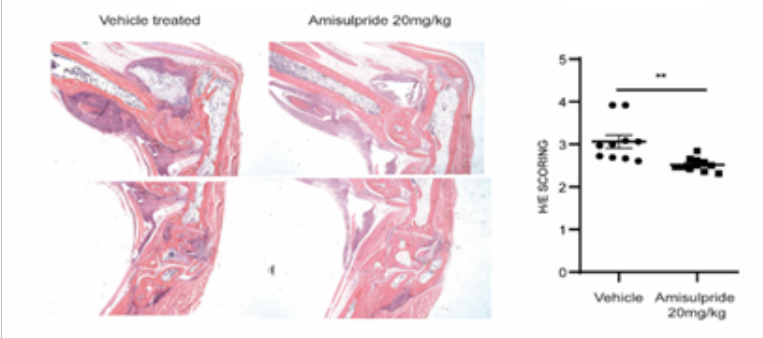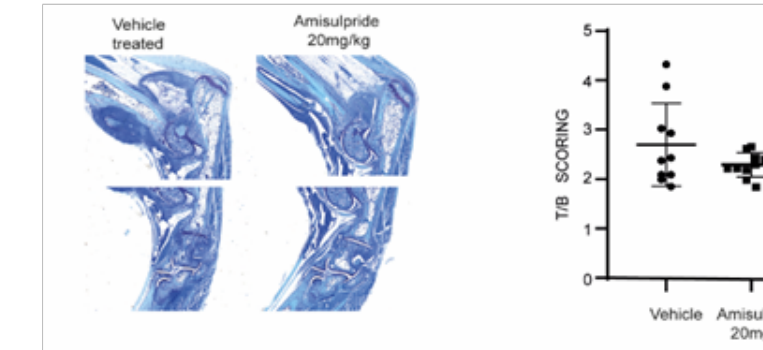
A

mTNF 1.5h

il6 1.5h

B

Score

Weight

C

Vehicle treated   Amisulpride 20mg/kg

D

Vehicle treated   Amisulpride 20mg/kg

E

Vehicle treated   Amisulpride 20mg/kg
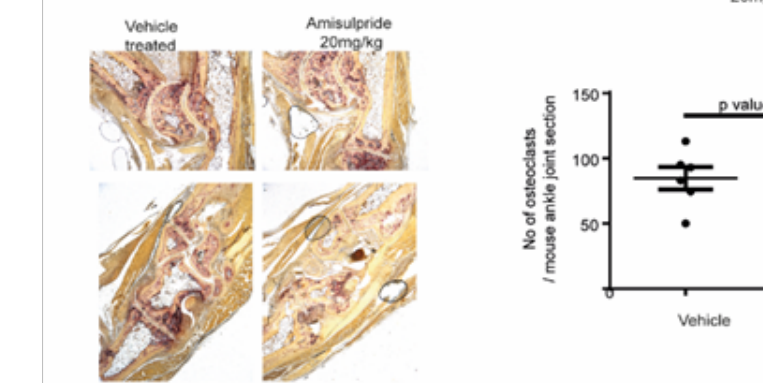

p value= 0.09

Figure 13 *In vivo* effect of Amisulpride. A. Amisulpride treatment in LPS treated acute sepsis model significantly downregulates mTNF and IL6 in the serum of treated mice, compared with the vehicle treated controls. B Arthritis clinical score of *hTNFtg* mouse model is significantly downregulated upon 5weeks of Amisulpride treatment. C H/E stained representative photos and scoring of joints' paraffin sections of *hTNFtg* mouse model upon 5weeks of Amisulpride treatment. D. T/B stained representative photos and scoring of joints' paraffin sections of *hTNFtg* mouse model upon 5weeks of Amisulpride treatment. E. TRAP stained representative photos and scoring of joints' paraffin sections of *hTNFtg* mouse model upon 5weeks of Amisulpride treatment (* p-value < 0.05; ** p-value < 0.01; *** p-value ≤ 0.0001, all data are shown as mean ± SEM and all comparisons were made against vehicle sample using Student's t test.)

To elucidate further the mechanism through which the *in vivo* effect of the drug is exerted, fresh Synovial fibroblasts (CD31-/CD45-/PDPN+) were isolated from *hTNFtg* mice after 5weeks of daily treatment with Amisulpride at 20 mg/kg. Synovial fibroblasts have been found to be the driving force of the pathology in *hTNFtg* mice, as they are the main producers of hTNF, while they are able to promote the pathogenesis of the disease in an immunodeficient Rag-/-background[64,69]. RNA-sequencing analysis of the isolated fresh fibroblasts, comparing the treated animals with the vehicle-treated controls, confirmed the downregulation of inflammatory responses of SFs, which in turn attract less immune cells, therefore helping in the resolution of inflammation (Figure 14C). Likewise, the superoxide anion generation pathway was downregulated in the isolated fresh SFs, pointing out the potential intervention of Amisulpride in ROS homeostasis, which has been found to be deregulated in RA patients and is believed to be a major contributor to RA pathogenesis[240] (Figure 14C).
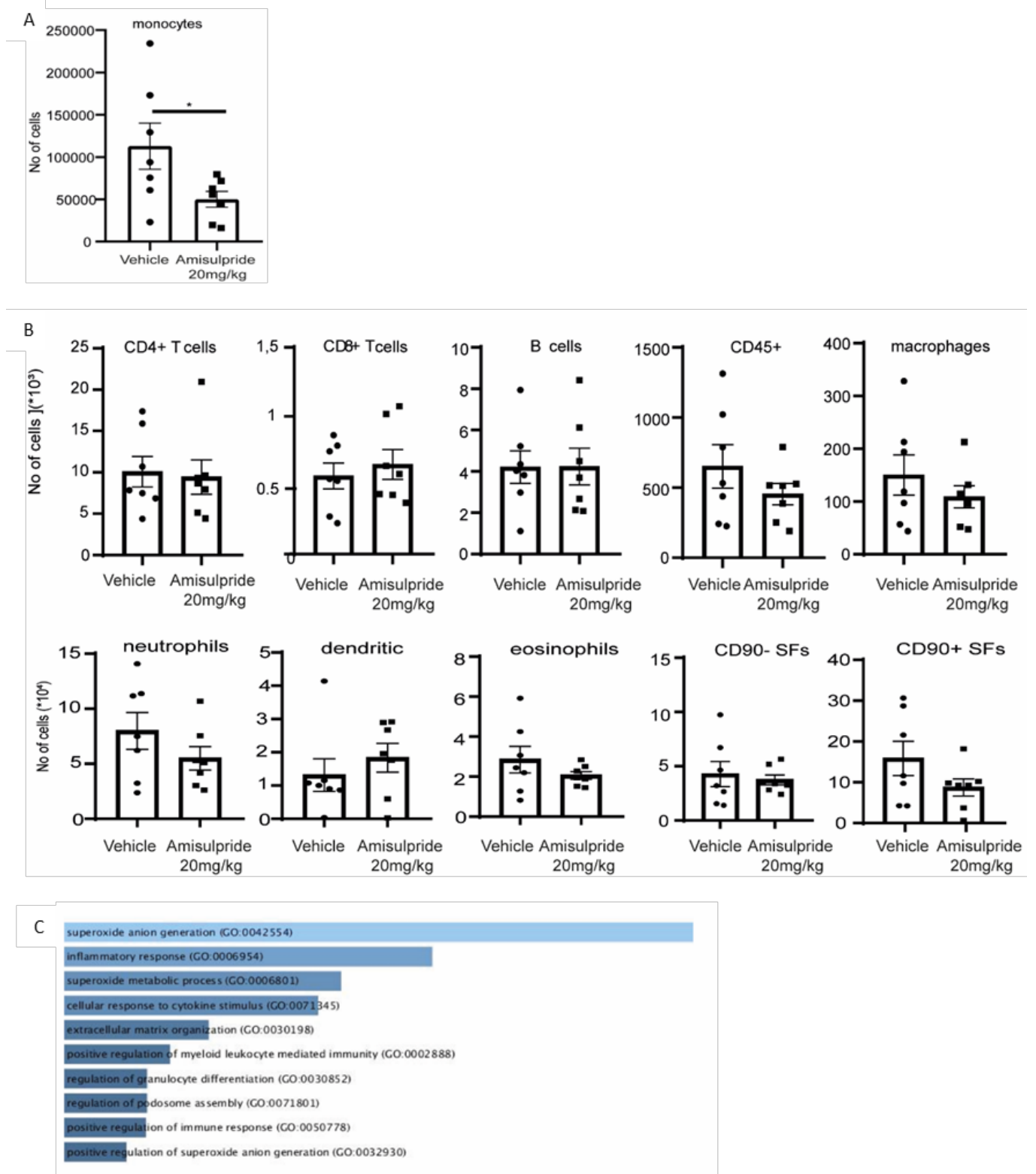
Figure 14 A. Immune infiltration analysis of *hTNFtg* joints reveals that monocytes numbers are significantly downregulated in Amisulpride treated mice. B. Immune infiltration FACs analysis of joints of *hTNFtg* mice treated with Amisulpride for 5weeks, compared with the vehicle treated control. C. Kegg pathway analysis of SFs isolated from the joints of *hTNFtg* mice treated for 5weeks with Amisulpride 20mg/kg (* p-value < 0.05; ** p-value < 0.01; *** p-value ≤ 0.0001, all data are shown as mean ± SEM and all comparisons were made against *hTNFtg* vehicle sample using Student's t test.)

4.2.3 Amisulpride effect on joint fibroblasts is not mediated through its known targets DRD2, DRD3 and HTR7, nor through TNF-TNFR1 binding inhibition.

After demonstrating Amisulpride anti-TNF activity both in cell-based assays and *in vivo*, the next step of our research focused on investigating the molecular mechanism through which the effect exhibited could be attributed to. Towards this end, we aimed to clarify whether Amisulpride effect is mediated through its known targets DRD2/DRD3/HTR7. Although B- and T-lymphocytes, cells of macrophage lineage and dendritic cells have been shown to express dopamine receptors[241], whether RA human fibroblasts show expression or not is controversial[242,243]. The expression of dopamine receptors seems also to be influenced by the age of the patients, implicating mainly the migration and not the inflammatory profile of human FLS[244]. Importantly, our cultured *hTNFtg* synovial fibroblasts gene expression profile showed absence of any expression of dopamine/serotonin receptors, whereas fresh isolated fibroblasts (CD31-/ CD45-/ PDPN+) from *hTNFtg* mice, belonging in lining or sublining subset[81], do not express *Drd2/Drd3/Htr7* receptors either (Figure 15A). As a result, it seems that it is the targeting of other than Amisulpride main proteins that bestows the drug *in vivo* activity in our experimental animal model. Then, and since Amisulpride was proven to be endowed with anti-TNF properties, the ability of the drug to bind directly to TNF was estimated through an *in vitro* elisa assay, measuring the interaction of TNF with its main receptor, TNFR1. Nevertheless, as Figure 15B depicts, it was found that Amisulpride does not suppress the binding of TNF to its main receptor TNFR1, thereby concluding that the anti-TNF effect of the drug is neither mediated through the TNF-TNFR1 binding inhibition.
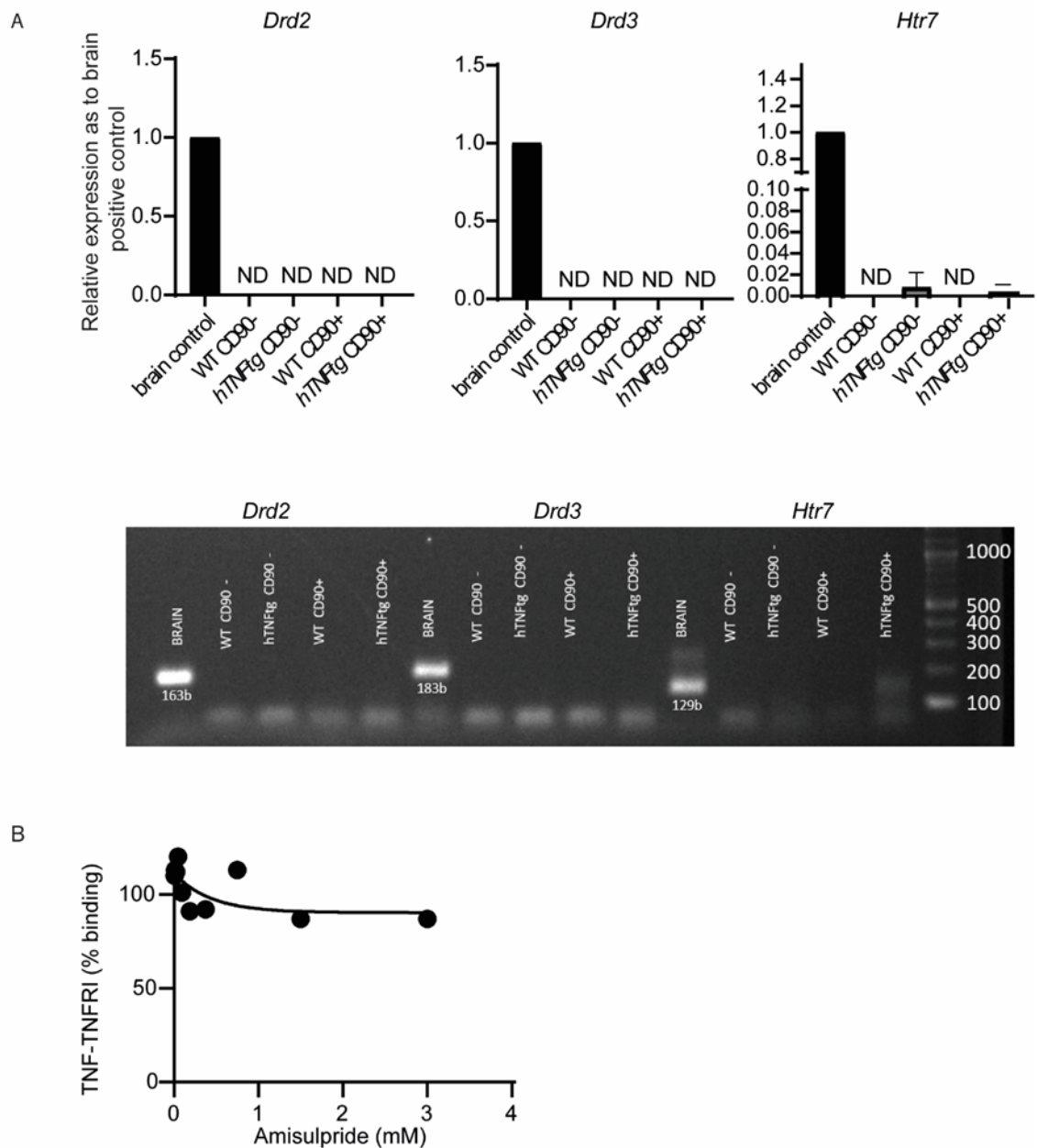
Figure 15 A. Amisulpride effect on SFs is not mediated through the known receptors of the drug *DRD2/ DRD3/ Htr7*, as there is no expression of these receptors in Lining (CD31-/ CD45- /PDPN+/ CD90-) or Sublining (CD31-/ CD45- /PDPN+/ CD90+) *hTNFtg* fresh isolated SFs. ND: Not Detected. Brain sample was used as a positive control. B. Amisulpride effect on SFs is not mediated through the interruption of interaction of TNF with its main receptor, TNFR1.

4.2.4   Chemoproteomic identification of potential molecular targets of Amisulpride

Consequently, our efforts were directed towards setting up a target identification protocol using the pathogenic *hTNFtg* SFs as a cellular context. This task was based first on the design and synthesis of bioactive chemical probes bearing "click" handles that would serve as

functional tools for biorthogonal tag ligation followed by selective pull-down of target proteins[245,246]. Subsequently, the proteins enriched could be digested for LC-MS/MS analysis. Accordingly, the development of our protocol begun with the synthesis of two chemical probes (Figure 16A) which structurally resemble to Amisulpride while containing a click handle (triple bond). The design of two different click probes aimed to exclude as much artefacts (false positive proteins) as possible, and therefore to end up with a reasonable number of potential protein targets for validation. In the first click probe (click 1, Figure 16A), the alkyne was incorporated into Amisulpride as substituent of the pyrrolidine group, while in the second one as substituent of the sulfone group (click 2, Figure 16A).

Validation of individual probe bioactivity was conducted using the same cell-based assays for testing Amisulpride activity (reduction of the pathogenic proinflammatory chemokines CCL5 and CCL20 in *hTNFtg* SFs), and we pleasantly noticed that both click analogues exhibited a similar to or even better effect (Figure 16B) than Amisulpride. Hence, the *hTNFtg* SFs were treated with each click derivative (25 µM), while two groups served as negative controls; the first control group included *hTNFtg* SFs treated with vehicle (dmso, no probe) and the other control was *hTNFtg* SFs treated with each click derivative (25 µM) plus with an excess concentration (10x) of original Amisulpride compound, in order for the target binding sites to be occupied by the drug, blocking binding of the labelled probe.

After cell lysis, the lysate was subjected to the copper(I)-catalysed alkyne-azide cycloaddition click chemistry approach, for conjugating target proteins with a biotin tag. The biotin-tagged proteins were then pulled down on streptavidin beads, and the target proteins were selectively eluted through cleaving an azo-linker in the tag with sodium dithionite. Finally, the proteins enriched in the eluent were identified by mass spectrometry analysis.

The data received were further analysed by creating volcano plots for a) the enriched proteins identified by each probe (click 1 and click 2) compared to vehicle (dmso) control and b) the enriched proteins by click 1 and click 2 in the presence or the absence of the competitor compound (Amisulpride) (Figure 16C). Combining differences (Student's T test difference>1) in proteins identified in both active probe samples but not in the two negative controls (vehicle and click plus Amisulpride) delivered a shortlist of potential targets (Figure 16D, Venn diagram). The six common candidates identified were ASCC3, SEC62, ROMO1, KIF5C, CDC42 and KCT2 (Figure 16D). After checking the expression of these genes in fibroblasts, KCT2 was excluded as it is a protein expressed mainly in keratinocytes, pointing out that it is probably a false positive candidate.
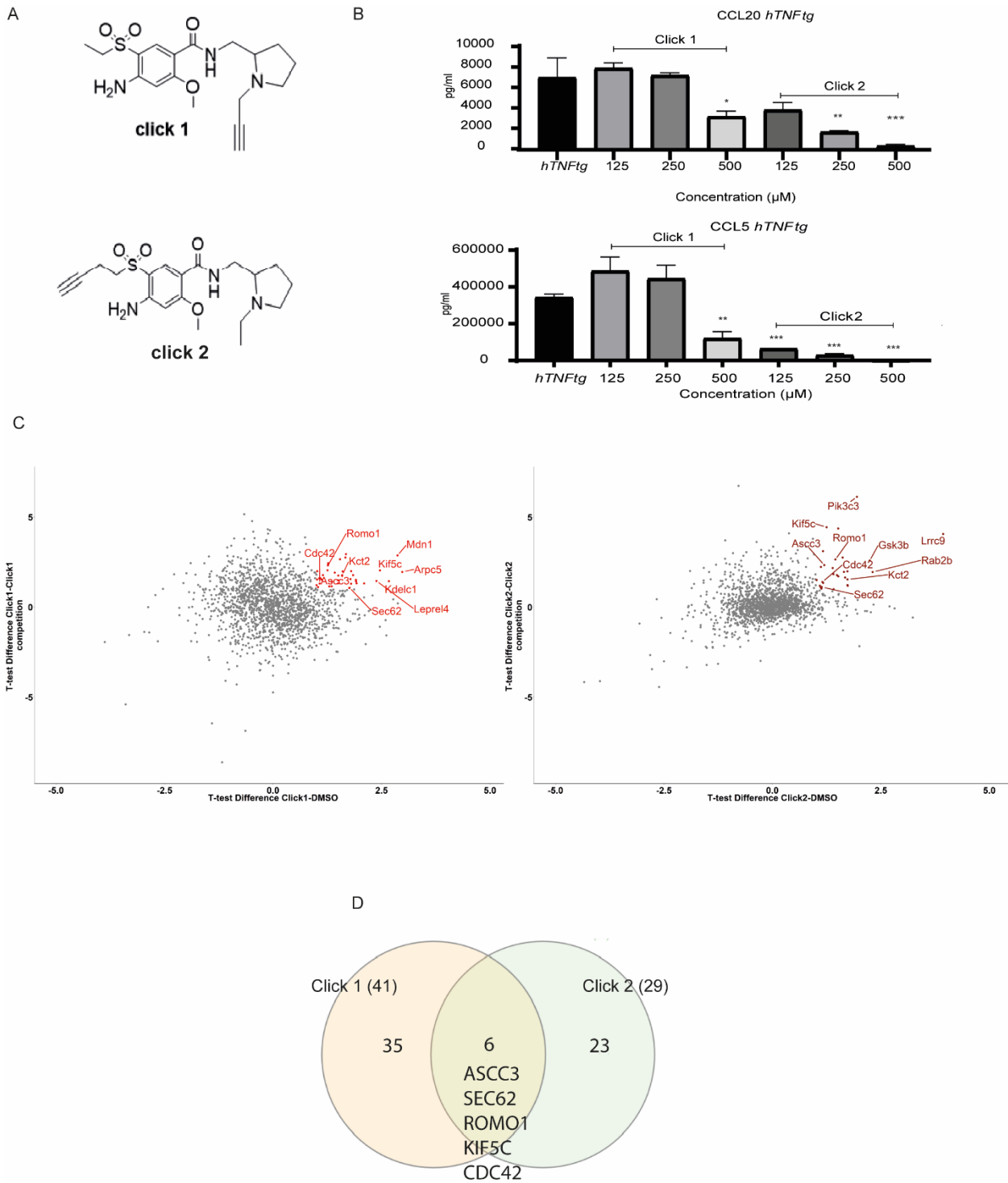
Figure 16 A. Structure of the two synthesized click compounds B. Click compounds maintain their efficacy in downregulating CCL5 and CCL20 at *hTNFtg* arthritic SFs. C. Volcano plots with highlighted candidates, combining differences (Student's T test difference>1) in proteins identified in each active probe sample but not in the DMSO or the competition control. D. Interactivenn of the proteins presented in B, delivered a shortlist of 5 potential targets. (* p-value < 0.05; ** p-value < 0.01; *** p-value ≤ 0.0001, all data are shown as mean ± SEM and all comparisons were made against *hTNFtg* sample using Student's t test.)

Activating signal cointegrator 1 complex subunit 3 (ASCC3) encodes a 3'-5' DNA helicase, whose activity is crucial for the generation of single-stranded DNA, while in cell lines loss of *Ascc3* leads to reduced cell proliferation[247]. Kinesin heavy chain isoform 5C (KIF5C) is located in microtubules, where among other proteins, it has been found necessary for the transport of N-cadherin between the Golgi and the plasma membrane, facilitating cell to cell adhesion in fibroblasts[248]. Cell division cycle 42 (CDC42) has been also associated with adherence of fibroblasts as it belongs to a subfamily of Rho GTPases, that participate in reorganization of actin cytoskeleton[249], while it has been previously linked to antidepressive compounds, that act through targeting of the HTR7 receptor[250]. ROS modulator 1 (ROMO1) is localized in the mitochondria, being responsible for TNF*a*-induced ROS production[251]. Lastly, SEC62 is located in the endoplasmic reticulum (ER) and is responsible, as a member of SEC61/62/63 complex, for proteins translocation in the ER and for cell calcium regulation[252].

To verify further the role of the 5 proteins (ASCC3, CDC42, KIF5C, ROMO1, SEC62) in the *hTNFtg* arthritic SFs activated profile, we designed shRNAs to delete each one of their relevant genes using the Lenti-X Lentiviral expression system. After confirming the downregulation of each mRNA (Figure 17A), we checked which of the genes (*Ascc3, Sec62, Romo1, Kif5c, Cdc42*) could successfully downregulate both CCL5 and CCL20, resulting in an anti-inflammatory effect similar to Amisulpride (Figure 17C). Of note, deletion of *Sec62* and *Ascc3* significantly reduced pathogenic chemokines levels although the viability of the cells was not significantly changed (Figure 17B). This result indicates that the molecular mechanism of the amelioration of *hTNFtg* SFs inflammatory activation offered by Amisulpride is supported by targeting of both ASCC3 and SEC62.

The anti-inflammatory role of ASCC3 and SEC62 as drug targets can also be connected with the effect of Amisulpride on both cultured (Figure 10D) and fresh fibroblasts (Figure 14C). Gene expression profile of treated *hTNFtg* cultured SFs revealed cytokines/ chemokines and NF-κB signalling as main cascades regulated by the drug, while inflammatory response and cellular response to cytokines are highlighted in the regulated pathways of the fibroblasts isolated from Amisulpride treated *hTNFtg* mice, confirming that molecular targets of the drug regulate response to inflammatory signals.
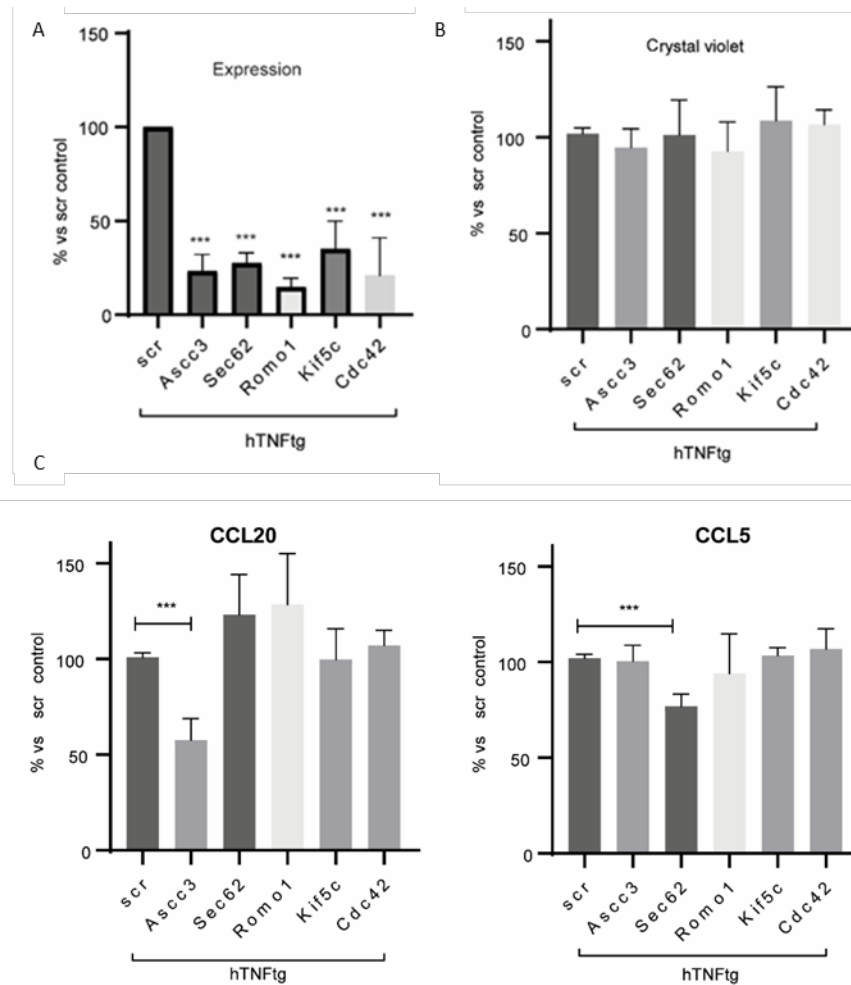
Figure 17 Drug targets' validation A. Efficient downregulation of Amisulpride potential targets, upon Lentiviral transfection of *hTNFtg* SFs with relevant shRNAs. B. Crystal violet assay confirms that the shRNAs transfection is not toxic. C. ShRNAs mediated deletion of *Ascc3*, *Sec62*, *Romo2*, *Kif5c* and *Cdc42*, identified that combined targeting of ASCC3 and SEC62 support the anti-inflammatory profile of the drug (* p-value < 0.05; ** p-value < 0.01; *** p-value ≤ 0.0001, all data are shown as mean ± SEM and all comparisons were made against *hTNFtg* scramble sample using Student's t test.)

4.2.5 Amisulpride influences known pathways that are implicated in arthritogenic activation of SFs

In order to have a deeper insight into the cellular signaling, DIA-based phosphoproteomic profiling in synovial fibroblasts was deployed[253]. For the phosphoproteomics assay, hTNF-induced WT SFs rather than *hTNFtg* SFs were preferred in order for the cells to be more synchronized in the context of TNF stimulation and signaling. Three different time points (5', 15, 30') of hTNF induction were used and compared to cells pretreated with Amisulpride for 1h before being stimulated at similar time points with hTNF (5', 15', 30').

Initially, all treated samples were compared versus the untreated ones. In this way, the effect of the drug can be identified without considering the hTNF effect. Figure 18A displays a volcano plot that integrates the deregulated phosphosites in treated samples when compared with the relevant untreated controls. Notably, as seen in the heatmap of Figure 19A, the phospho-regulations were clustered hierarchically according to the inhibitor treatment and there were clearly distinguishable row-clusters depending on the inhibitor effect. Secondly, the phosphosites affected after treatment of WT fibroblasts with 10 ng/mL hTNF*a* were identified in the three different time points. These phospho-regulations were subsequently compared with the respective ones after pre-treatment of the cells with Amisulpride (500 μM) 1h before each relevant stimulation (volcano plots at Figure 18B and 18C).

Both the Kegg pathways and the Gene ontology terms implicated in all comparisons were analysed (Figure 19B and 19C). Figures 19B and 19C show the significantly enriched pathways, studying the de-regulated phosphrorylations upon Amisulpride treatment. Most of the phosphosites were upregulated upon inhibitor treatment, highlighting cell adherence, focal adhesion and MAPK signalling as implicated processes, pathways that are known to play a determinant role in pathogenic fibroblasts' activation (Figure 19B). Focusing on the downregulated phospho-changes, similar processes were found to be involved, containing cell to cell adhesion, focal adhesion and adherence junction as well as regulation of transcription (Figure 19C).

Notably, adhesion ability is known to be enhanced in pathogenic *hTNFtg* fibroblasts when compared to WT controls[67] and Amisulpride was found to significantly reduce cell adherence, therefore confirming the pathways proposed to be regulated by the drug in the phosphoproteome analysis (Figure 19D).

Interestingly, we noticed that some of the identified protein targets of the drug (Figure 16D) are highly connected with the pathways regulated upon Amisulpride treatment on SFs. In specific, the phosphorylation of SEC62 (at Ser341), validated as one of Amisulpride targets on SFs, seems to be upregulated upon treatment, confirming that the endoplasmic reticulum translocation pathway is affected by the drug treatment (Figure 19B). CDC42 is a Rho GTPase, known to regulate filopodia formation and adherence of fibroblasts[249,254], while Rho protein signal transduction, cell to cell adhesion and actin cytoskeleton organisation were found to be upregulated by Amisulrpide, as seen in Figure 19B. Moreover, CDC42EP1 (MSE55), a CDC42 binding protein, that regulates cytoskeleton dynamics, is dephosphorylated (at S371 and S207) upon Amisulpride treatment, highlighting further cell to cell adhesion alteration (Figure

19C). Finally, ASCC3, as an RNA helicase, is implicated in transcription regulation, one of the top pathways appeared in the phospho-proteome analysis (Figure 19C).
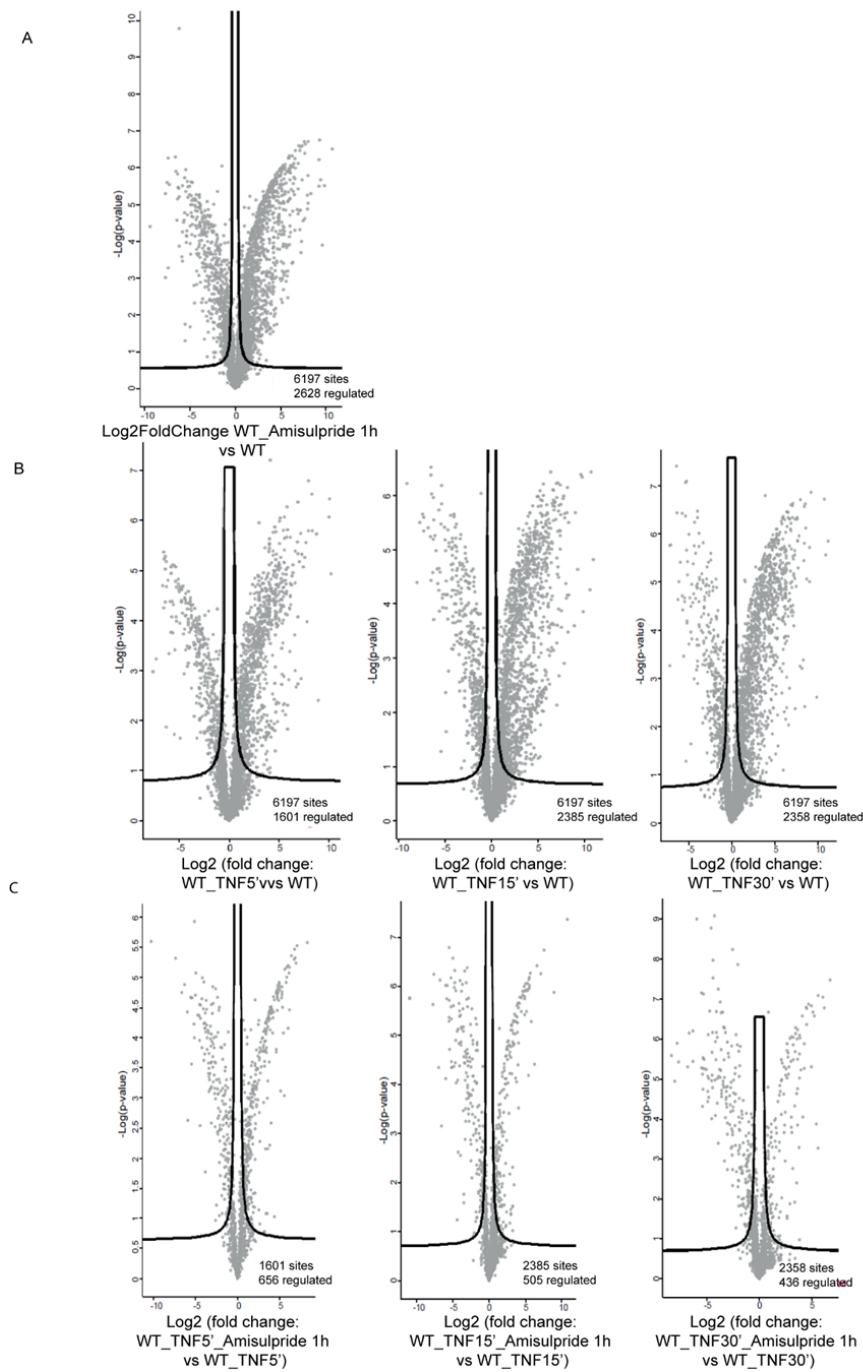

Figure 18 A. Volcano plot illustrating phosphorylations that are up and down- regulated upon Amisulpride treatment with significance cut-off = 0.05 indicated by lines. B. Volcano plots indicating the deregulation of phosphoproteome on hTNF stimulated WT SFs, when treated with Amisulpride. The samples were gathered on the three indicated timepoints of 5', 15' and 30' after hTNF stimulation and were compared to untreated control. C. Deregulated phosphorylations upon TNF treatment, identified in B, were used as input to compare corresponding inhibitor treatment.
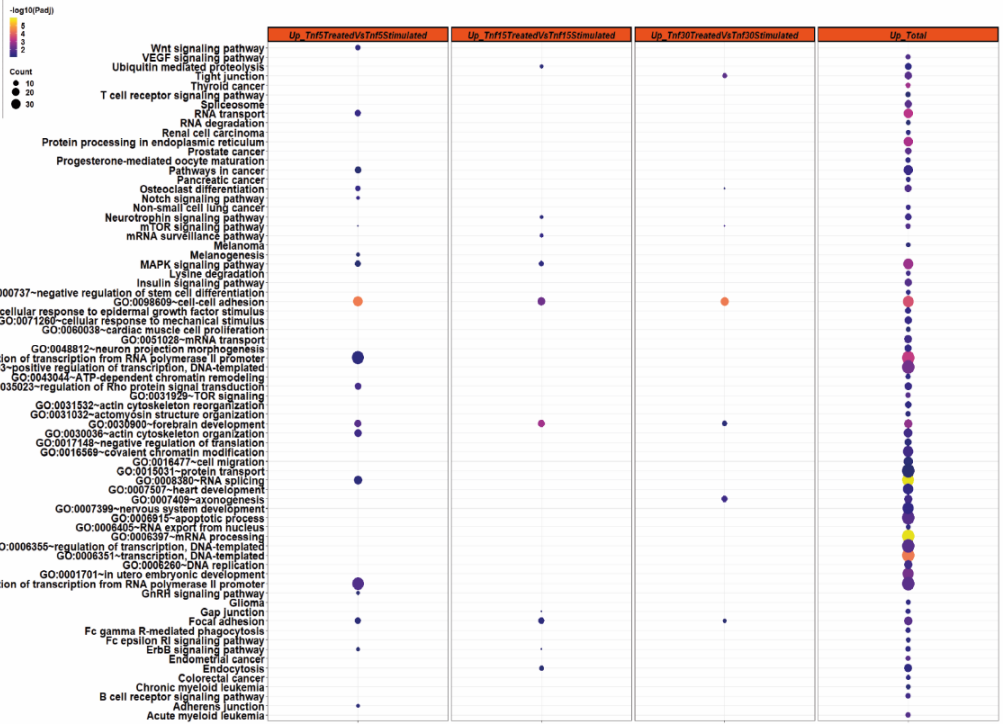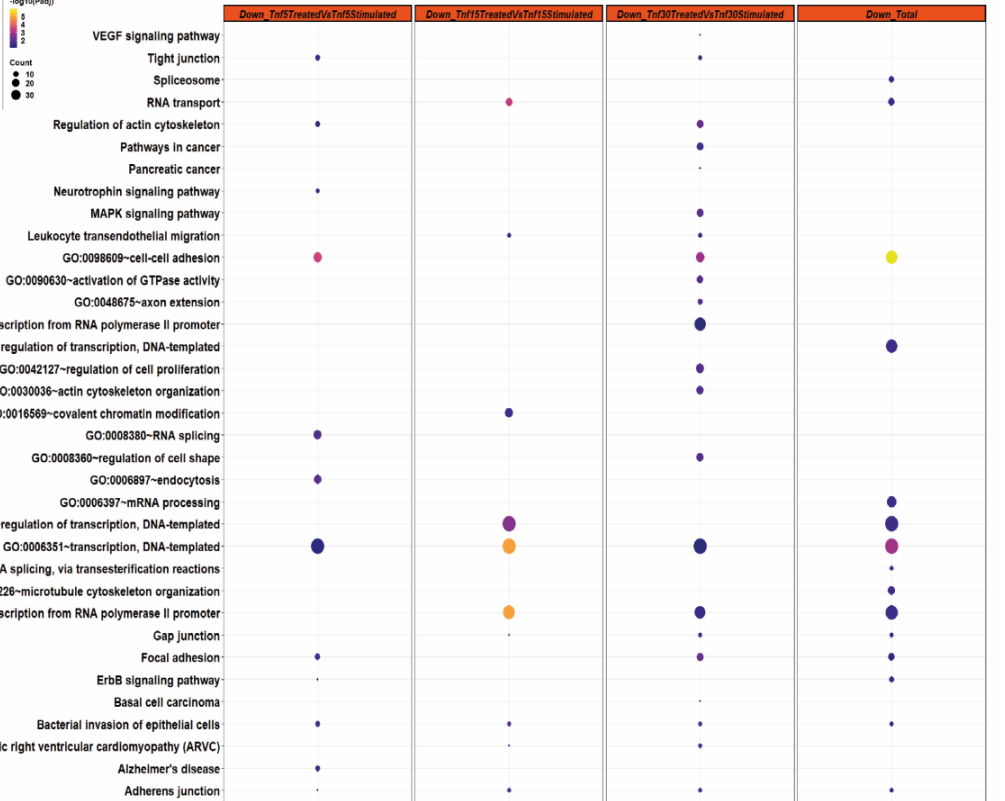
Figure 19 Phosphoproteomics analysis of intraarticular SFs treated with Amisulrpide reveal pathways that are regulated upon the drug treatment. A. Heatmap based on hierarchical clustering analysis of t-test significantly regulated phosphosites comparing Ami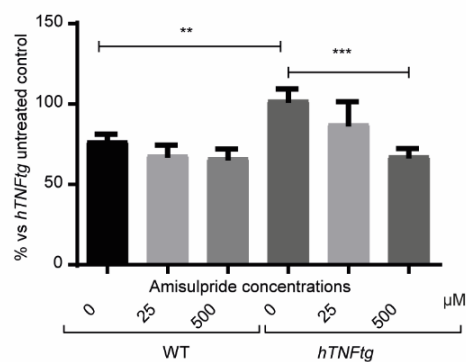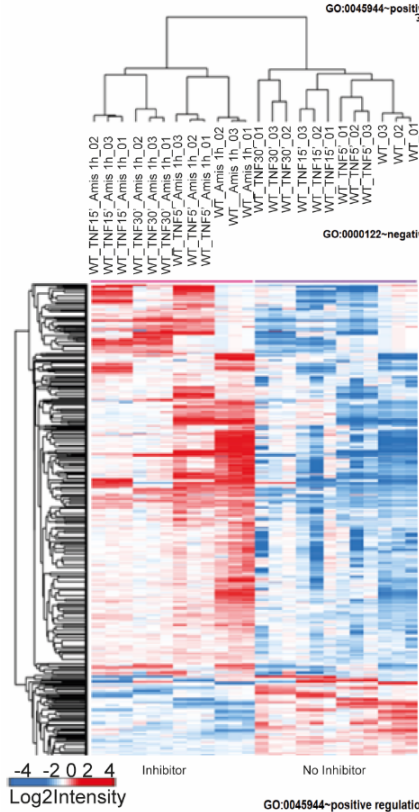sulpride treated and untreated (significance cut-off 0.05) reveals clearly distinguishable row-clusters depending on inhibitor-effect. B. Kegg pathways and GO terms enrichment analysis for upregulated phosphorylations upon Amisulpride treatment. C. Kegg pathways and GO terms enrichment analysis for downregulated phosphorylations upon Amisulpride treatment. D. Amisulpride downregulates the adherence of activated *hTNFtg* SFs. (* p-value < 0.05; ** p-value < 0.01; *** p-value ≤ 0.0001, all data are shown as mean ± SEM and all comparisons were made against *hTNFtg* vehicle treated sample)

4.2.6   Study of Amisulpride as a modifier of arthritogenic fibroblasts' activation

Conclusively, we have identified Amisulpride, a known antipsychotic agent known to inhibit dopamine and serotonin receptors, as a modifier of arthritic fibroblasts' activation and mouse polyarthritis disease, starting from transcriptomic signature matching.

RA is characterized by joints' sensory nerve fibers accumulation that can respond to antidepressants agents[255]. Although neurotransmitters are considered as key role molecules in signal transduction of nervous system, they have been also implicated in immune cells' regulation[256]. In this context, anti-dopamine drugs have been used to supress sepsis[257], stress-induced neuroinflammation[258] and proinflammatory cytokines production in lipopolysaccharide (LPS)-induced macrophages[259], while they have exhibited differential results in several RA *in vivo* studies[260].

Amisulpride is widely used in high doses to treat schizophrenia and in low doses for treating depressive disorders. In the present study, it has been demonstrated that low doses of the drug exert, additionally, an anti-rheumatic potential. The new activity of the drug *in vivo* could be synergistic. It could first be ascribed to DRD2, DRD3 and HTR7 blocking (Amisulpride known targets) on macrophage lineage and their consequent response to dopamine expressed by joints SFs[261]. Furthermore, it could be due to the modification of function of the five newly identified drug off-targets on arthritogenic fibroblasts, two of which (ASCC3 and SEC62) have been validated to support the drug's anti-inflammatory effect. This dual role underlines the high potential of this specific drug to be repurposed. Given that the traditional *de novo* identification of new drugs against RA is highly costly and time consuming, the drug repositioning research area consists a tractable and favourable alternative in drug discovery process since essential component issues such as bioavailability, toxicity and manufacturing routes are already known and established[116].

Regarding, the new drug targets validated to support the anti-inflammatory function of Amisulpride, ASCC3 is the largest subunit of ASC1 (or ASCC) complex, where it functions as a 3'-5' DNA helicase, together with ASCC1, ASCC2 and ASC1/ TRIP4[247,262]. Inhibitors targeting DNA/ RNA helicases have been proposed to regulate viral, bacterial or cancer cells' proliferation and responses[263]. ASCC3 is believed to participate in DNA repair pathways, as it prepares single-stranded DNA for AlkBH3 to proceed in de-alkylation repair[247] and it resolves stalled ribosomes[264,265]. ASCC3, among other helicases, has also been connected with cancer biology since deletion of ASCC3 suppressed human cancer cells' proliferation[247], while it has also been implicated in viral defense[266]. ASC1 complex has been additionally involved in transcriptional regulation, being associated with transcription integrators SRC-1 and CBP-p300, that co-activate several transcription factors such as CREB, STATs, AP-1 and NF-κB[267]. Moreover, ASC1 complex has been itself implicated in the regulation of AP-1, NF-κB, and SRF, and thus it can also be characterized as a transcription integrator[262]. ASCC3 involvement in the regulation of these inflammation-related transcription factors[268] can be further substantiated by the findings of the present study, where *Ascc3* downregulation is able to cause a significant reduction of the proinflammatory CCL20 secretion in TNF- activated SFs.

The translocation protein SEC62, on the other hand, is a part of the dimeric SEC62/SEC63 complex, that along with Sec61 is located in the membrane of the endoplasmic reticulum (ER), facilitating the translocation of nascent polypeptides into the ER and the cell calcium homeostasis[252,269,270]. Additionally, SEC62 has been described to play a crucial role in the successful ER-stress response process, as it favours the release of the accumulated ER chaperones driving cell physiological homeostasis[270]. Notably, SEC62 has been reported as oncogenic, being overexpressed in a variety of tumours, supporting the migration but not the proliferation of several cancer cell lines[271]. The supportive effect of SEC62 in tumour metastasis can be attributed either to the deregulated translocation of migration-related precursor proteins at the ER or to the inhibition of Ca^{2+} homeostasis along with the attributed ER stress tolerance[252]. In particular, no SEC62 specific inhibitors have been reported to date, but inhibition of SEC62 function through antagonizing cellular Ca^{2+} homeostasis by CaM antagonists (such as the antipsychotic drug trifluoperazine) has been proven to mimic *Sec62* deletion *in vitro* by inhibiting migration and proliferation of human tumor cells[271,272]. Targeting of SEC62 could also be beneficial in RA, since SEC62 has been found to be induced in a human RA synovial tissue study, and especially in a patients' cohort that is characterized by expansion of FLS and not by predominance of myeloid/lymphoid compartment before receiving any

treatment[273]. This subgroup of patients can be probably imitated by *hTNFtg* mice where TNF signalling in fibroblasts specifically is sufficient and necessary to initiate disease[64,69].

Psychiatric disorders are common comorbidities of RA and almost 19% of RA patients do develop depression, a percentage much higher than the one met in the general population[274]. This comorbidity affects not only patients' daily life but also the physical aspects of the disease as well as response to therapies[275,276]. A common association of RA with its comorbid depression could be the fatigue and pain that patients suffering from chronic inflammation can face[277,278]. Although this might be the case, it has also been proven that the immune system itself can mediate depression pathogenesis, as circulating cytokines, such as IL6 and TNF, can activate endothelial cells of blood brain barrier, thus enabling the circulating mediators to enter in the central nervous system and to cause several mental disabilitites[279]. These two theories can in fact intersect since pain and fatigue, common symptoms of RA, can also activate immune response which can in turn cause dysthymia pathology[280,281]. Of note, anti-TNF biologics have been proposed for alleviating both RA and depression symptoms[278]. However, biologics prescription is approved only in severe cases of RA and not all patients respond to them, thereby necessitating the frequent prescription of additional antidepressants[282].

Consequently, patients suffering from RA and comorbid depression may be highly benefited by the use of Amisulpride. Importantly, clinical use of several dopamine receptor antagonists in schizophrenia patients has been associated with a much lower incidence of RA compared with the one met in the general population[283]. Accordingly, studying RA patients, who have been under Amisulpride treatment prescribed for their depression symptoms, for possible beneficial clinical and histological RA outcome might provide valuable knowledge for the anti-arthritic effects of the drug, related to the dampening of fibroblasts' pathogenicity. In parallel, further preclinical studies of the *in vivo* inhibition of ASCC3 and SEC62 would further corroborate the use of Amisulpride as a repurposing candidate and render it as a promising lead compound for the development of novel and potent anti-rheumatic therapeutics.

4.3 Use of Amisulpride as a lead compound to identify novel, more potent inhibitors of fibroblasts 'activation

Having confirmed the suppressive effect of Amisulpride on TNF-induced pathogenic mechanisms, we aimed to design, synthesize and evaluate pharmacologically bioactive small molecules, using Amisulpride as a scaffold.
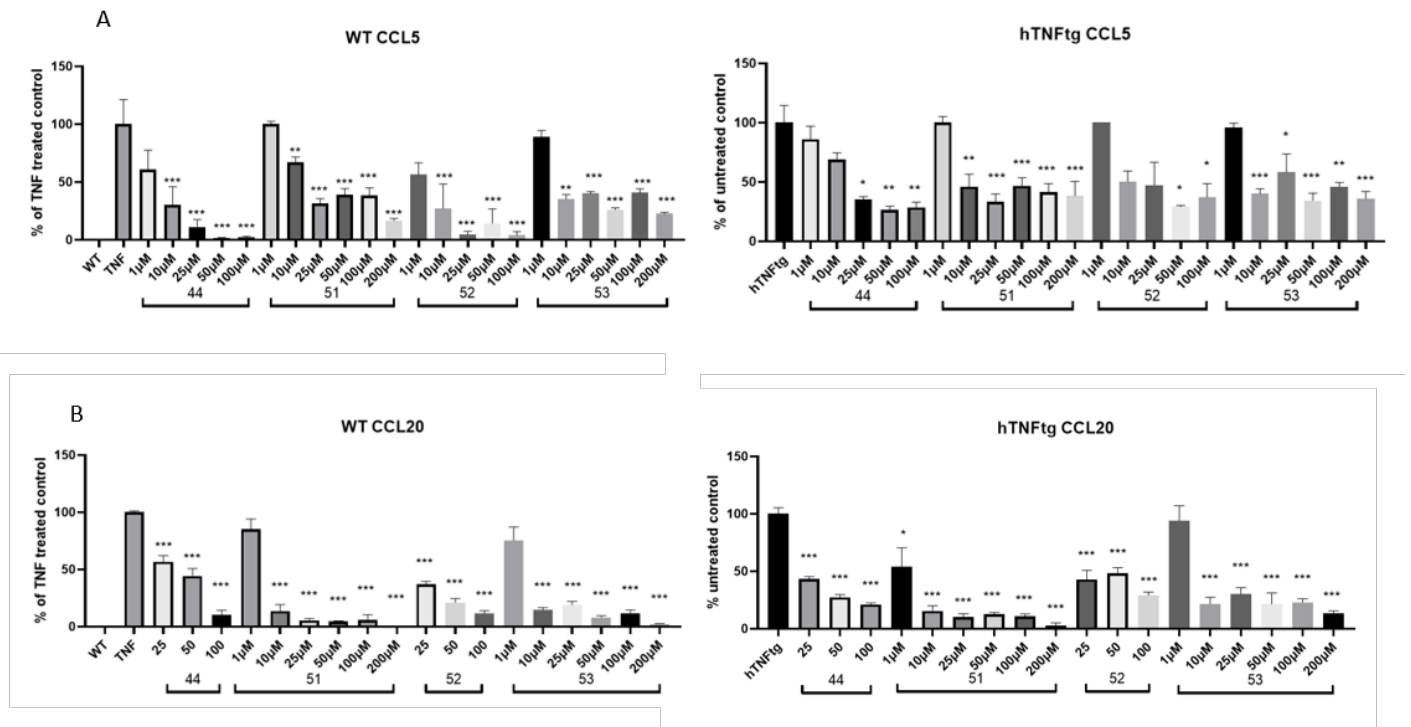
A series of more than a hundred compounds were tested in a dose dependent manner on activated SFs and macrophages.

4.3.1 The test compounds exhibit an anti-inflammatory potential on activated SFs

The *in vitro* effect of the novel compounds was firstly evaluated on activated synovial fibroblasts, in order to examine if the test compounds maintain their ability, as they are based on Amisulpride scaffold, to downregulate the elevated levels of chemokines CCL5 and CCL20.

Repetitive screening in a dose dependent manner resulted in the identification of the most efficient compounds, namely here 44, 51, 52 and 53. The results of the compounds' effect together with a table presenting the relevant IC50 values and their cytotoxicity data are presented in Figure 20, below. Interestingly, the novel compounds seemed almost 100fold more efficient than the original scaffold, Amisulpride (comparison with Figure 11A and 11B).

As the novel structures seemed quite promising according to their aforementioned IC50 values, the anti-inflammatory potential of the most efficient test compounds 51, 52, 53 was further assessed using the Mouse proinflammatory chemokine panel from Legendplex, that allows the simultaneous detection of 13 Mouse chemokines. The effect of compound 51 on SFs was assessed at a dose of 25μM, while the effect of the test compounds 52 and 53 was assessed at a dose of 10μM. The test compounds ameliorated the levels of the secreted chemokines EOTAXIN, KC, LIX and MCP1 as shown in Table 4. Numbers represent percentages of the chemokines' levels secreted from the treated SFs compared to 100% levels of the chemokines detected in the untreated cells (i.e. either *hTNFtg* SFs or hTNF-activated WT SFs).

Figure 20 Test compounds effectively downregulate elevated levels of A. CCL5 and B. CCL20 in both hTNF stimulated WT and *hTNFtg* joint activated fibroblasts. C. Conclusive table of IC50 values of data presented in A and B, along with the respective compounds' cytoxicity data.

Thus, the tested compounds can downregulate more efficiently than Amisulpride (Table 4 in comparison with Figure 12B) the levels of several inflammatory chemokines secreted from activated SFs, supporting further that the compounds may have a therapeutic effect on *hTNFtg* polyarthritis.

	hTNFtg				WT			
Chemokine	untreated	51	52	53	untreated	51	52	53
EOTAXIN	100	24	6	9	100	7	26	59
KC	100	80	49	49	100	41	34	68
LIX	100	22	48	40	100	3	23	24
MCP1	100	89	55	49.5	100	59	40	57

Table 4 Summary of the effect of the test compounds 51, 52 and 53 on the inflammatory chemokines secreted by activated SFs.

4.3.2 Novel compounds alleviate the increased wound healing potential of activated SFs

Focusing on the most efficient compounds, according to Figure 20C, we assessed the effect of compound 51, 52, 53 on the adhesion of *hTNFtg* SFs. Notably, although the novel structures were based on Amisulpride scaffold, the adhesion potential of *hTNFtg* SFs was not strongly affected upon their addition, as expected (comparison of Figure 19D with Figure 21A). This was an indication that the new compounds, probably due to several chemical modifications that they bear, may have different properties and targets than Amisulpride on arthritogenic SFs.

For instance, and based on a wound healing assay, compounds 52 and 53, used at 10μM, managed to downregulate the increased arthritogenic SFs' wound healing potential (assessing proliferation and migration)[67], while Amisulpride was not efficient in the same assay (Figure 21).
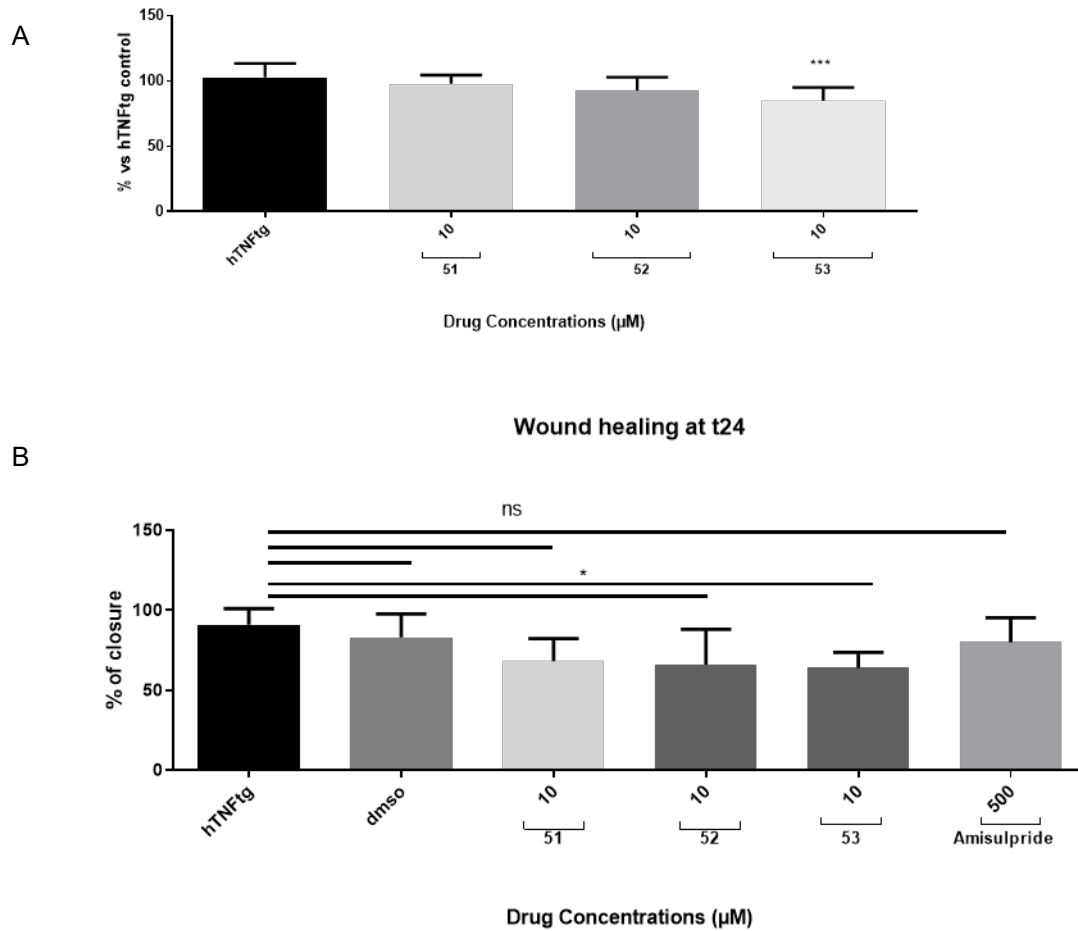
Figure 21 Novel compounds bear different properties than Amisulpride on arthritogenic SFs. A. Only compound 53 slightly alter the adhesion property of *hTNFtg* SFs. B. Compounds 52 and 53 do affect the wound healing potential of arthritic SFs indicating that the novel structures can play a role in migration and proliferation of activated fibroblasts. (* p-value < 0.05; ** p-value < 0.01; *** p-value ≤ 0.0001, all data are shown as mean ± SEM and all comparisons were made against *hTNFtg* sample using Student's t test.)

4.3.3   Novel compounds do not influence *hTNFtg* SFs' proliferation

In order to investigate further the wound healing assay result, and discriminate whether proliferation or migration of the cells is mainly affected, Propidium Iodide (PI) staining was used in both WT and *hTNFtg* SFs with or without the compounds addition (at concentration of 10μM). PI was used as a DNA binding dye to evaluate if our compounds influence the Cell Cycle progression, by causing an S phase arrest. Cells (WT or *hTNFtg* SFs) were fixed with 70% ethanol to allow entry of the dye inside the cell. The cells were also treated with ribonuclease, to ensure that only DNA and not RNA is stained. PI staining was measured by Flow cytometry and analysed using Flowjo DNA/ Cell Cycle interface. Cells that are in S phase have more DNA than cells in G0/G1 phase, thus they will take up proportionally more dye and will fluorescent

more brightly until their DNA content will be doubled. The cells in G2 phase will be approximately twice as bright as cells in G1. The compounds seemed not to influence significantly the proliferation capacity of the cells as they do not influence the cell cycle progression in either the WT or the *hTNFtg* cells (Figure 22). Thus, the result of compounds 52 and 53 in the wound healing assay (Figure 21B) is probably due to the effect of the compounds in *hTNFtg* SFs' migration property.
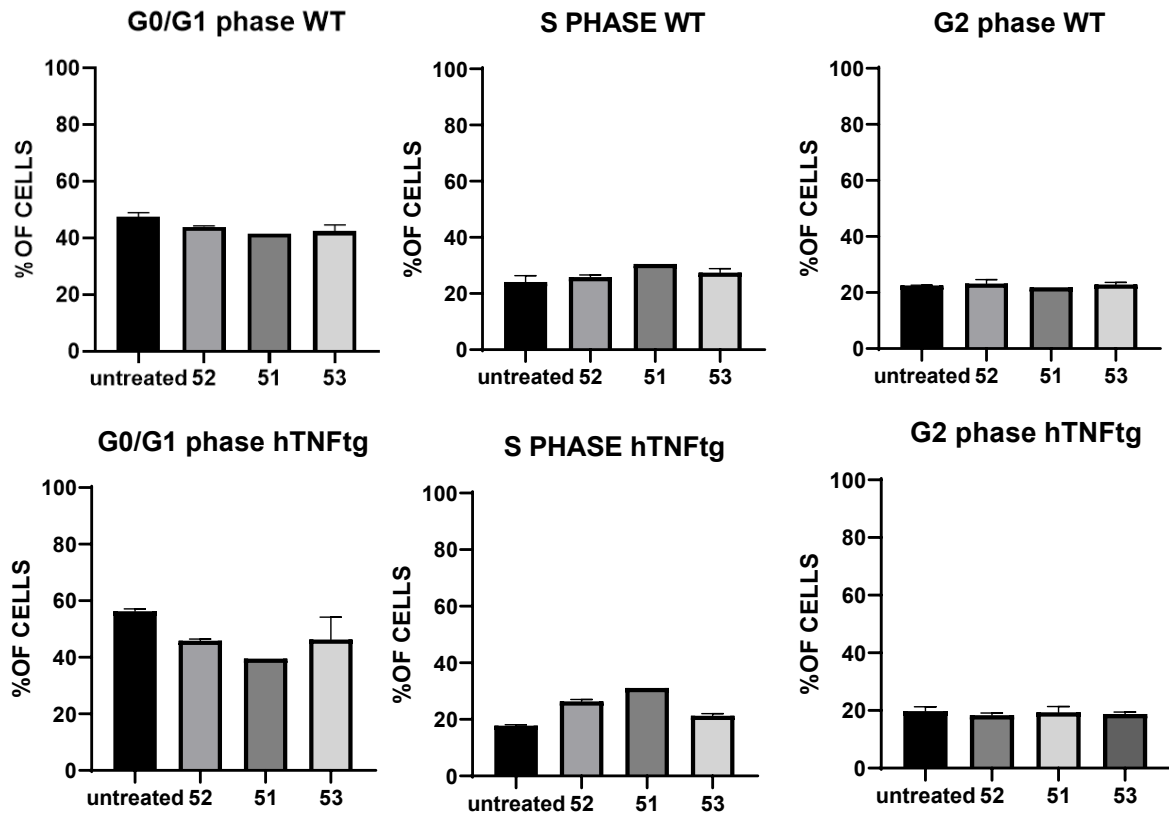
Figure 22 The novel compounds do not influence the cell cycle progression of both the *hTNFtg* and WT SFs.

4.3.4   Novel compounds do not induce death pathways in SFs

Since it is known that TNFR signalling is implicated in cellular survival, apoptosis and necroptosis[27] we investigated whether the novel compounds influence SFs' death pathways regulation. Annexin V staining was performed, as it has a strong affinity for Phosphatidylserine (PS) residues, that are located in the cytoplasmic phase of plasma membrane and during apoptosis they are translocated on the surface of the cell. Thus, an Annexin FITC conjugated antibody has been used to measure the Annexin binding through Flow Cytometry Analysis. Another characteristic of apoptotic cells is the loss of membrane integrity, that follows the PS

residues' translocation. Thus, Annexin staining is usually combined with Propidium Iodide staining (PI), as the latter can enter through the permeable membranes of damaged cells. Healthy cells are both Annexin V and PI negative. Annexin V positive and PI negative signal indicates early apoptosis with intact membranes, while positive signal for both Annexin V and PI indicates necroptotic cell death. As seen in Figure 23, no significant apoptosis/ necroptosis induction was detected upon the compounds addition.
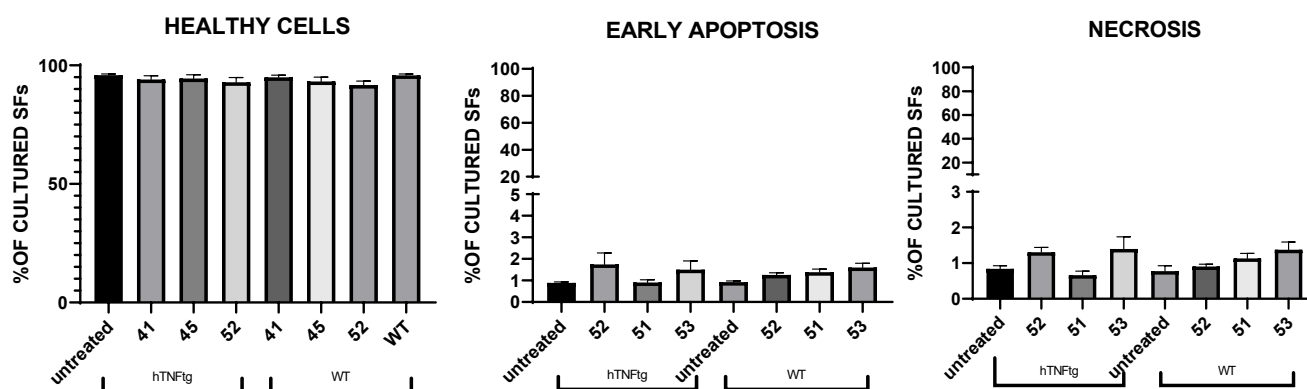
Figure 23 No significant regulation of death pathways (apoptosis and necroptosis) was detected upon compounds' addition on joint SFs.

4.3.5   Novel compounds' anti-inflammatory potential is not limited in fibroblasts

Finally, in order to assess if the compounds possess a broader anti-inflammatory profile, their ability to reduce the levels of secreted cytokines and chemokines from endoperitoneal elicited activated macrophages was measured. Test compounds 51, 52 and 53 were tested at a dose of 10μM on LPS induced thioglycolate derived peritoneal macrophages. Chemokines and cytokines analyses were performed using the 13plex mouse panels from Legendplex and their levels are presented as a percentage of the levels detected in the untreated control cells (Table 5A and B, respectively).

A

Chemokines	untreated	51	52	53
MCP1	100	27	28	75
MIP1α	100	No effect	No effect	60
MIP1β	100	90	51	67
CCL5	100	No effect	No effect	22
MDC	100	No effect	No effect	52

B

Cytokines	untreated	51	52	53
IL1α	100	36	9	30
IL12p70	100	54	23	18
IL6	100	44	7	15
IL27	100	77	19	75
GMCSF	100	80	36	38

Table 5 Data showing that the tested compounds can effectively ameliorate inflammatory cytokines and chemokines secreted from activated macrophages, thus supporting that they may play a broad anti-inflammatory role.

4.3.6 Novel compound 53 ameliorates LPS induced acute sepsis, downregulating the elevated mTNF serum levels

In order to test if novel compounds show a potential in downregulating inflammation *in vivo*, we administered the most promising compound (53) in the LPS acute sepsis model, *per os*. The compound retained its anti-inflammatory properties, by downregulating the LPS induced elevated mTNF levels, in serum of mice challenged with 1μg LPS (Figure 24A). Administration in chronic models, such as in *hTNFtg* polyarthritis model, will be tested after succeeding in a more massive synthesis of the compound 53 and more importantly after studying its pharmacokinetic and pharmacodynamic profile.

4.3.7   Identification of potential targets of novel compound 53

Lastly, in order to search for compound 53 potential targets, we applied the "click chemistry" approach in the *hTNFtg* activated SFs, as in the case of Amisulpride. We started with two similar structures (53a and 53b), which were used as scaffolds for the synthesis of two different "click compounds" (click1 and click 2, respectively), bearing an alkyne in different positions (Figure 24B).
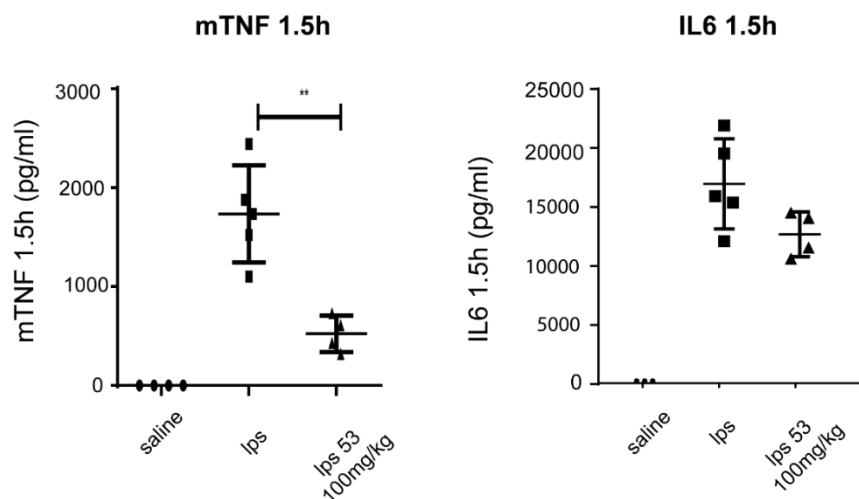
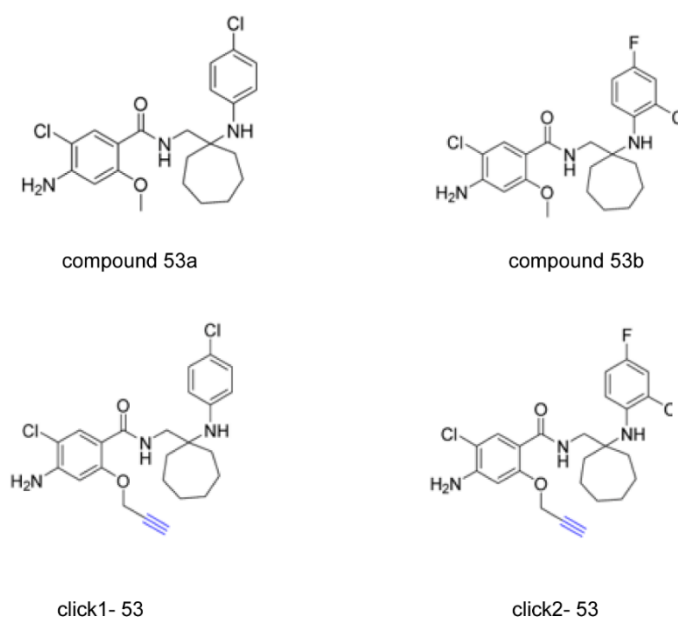**Figure 24** A. Compound 53 significanlty downregulates the elevated levels of mTNF in the serum of LPS challenged mice B. Two similar structures of compound 53 (a and b) were used as a scaffold for the creation of two different click molecules.

Interestingly, as shown in Figure 25A, 3 proteins were identified significantly enhanced in both the "click" treated samples, in comparison with the DMSO control (COX5a, HYOU1, ANXA2). Importantly, two out of the three proteins (COX5a, HYOU1) were also identified significantly upregulated in the "click" treated samples when compared with the relevant competition controls (Figure 25B).

Notably, COX5a is a subunit of the cytochrome c oxidase complex, which is the last enzyme used during the mitochondrial electron transport chain. COX5a along with its partner COX5b have been implicated in the regulation of cancer cell metabolism via non-canonical Bcl-2 pathway, amplifying cytochrome c oxidase activity in tumour cells, resulting in their resistance to apoptosis[284]. A similar mechanism of COX5a activity, targeted by compound 53, could also be the case in *hTNFtg* activated SFs, as they are known to be resistant to apoptosis[69], while Bcl2 has been notably found to regulate survival of RA FLS[285].

Moreover, HYOU1 is a protein localized in the lumen of the ER, participating in protein folding and secretion. Its function has also been related to apoptosis, as it has been found to regulate ER related stress, protecting cells from hypoxia-induced apoptosis. Interestingly, proteins involved in the ER stress have been found modulated in synovial tissue of RA patients, being correlated with the histological inflammatory score[286]. Finally, HYOU1 is highly expressed in cancer samples, such as breast tumors, suggesting an important role in tumorigenesis[287]. Expression of *Hyou1* also accelerated wound healing potential of tumor cells by modulating intracellular VEGF transport, increasing angiogenesis[288]. Thus, potential antagonistic targeting of HYOU1 by compound 53 could lead *hTNFtg* SFs to decreased wound healing properties (validated already as shown in Figure 21B), leading probably to reduced synovitis of *hTNFtg* mice.

Experimental validation of COX5a and HYOU1, as targets of compound 53, through shRNA mediated deletion of the relevant genes, will validate their effectiveness on downregulating inflammatory and wound healing potential of *hTNFtg* activated SFs, indicating a future therapeutic use of the compound in chronic inflammation.
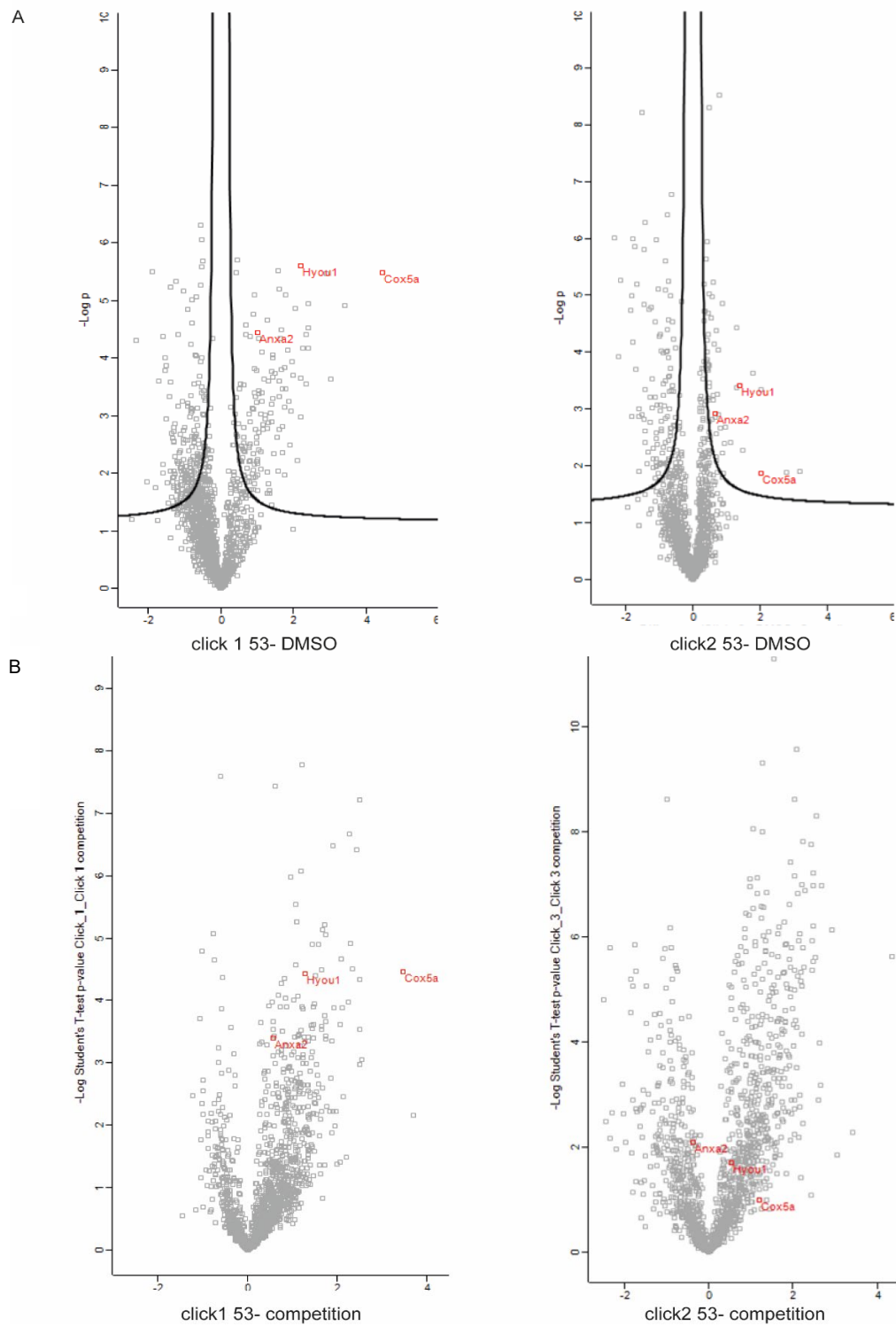
Figure 25 A. Volcano plot highlighting proteins commonly identified in the "click" treated samples in comparison with the untreated dmso controls B. Cox5a and Hyou1 are also significantly upregulated in the "click" treated samples when compared with the relevant competition controls.

5. Conclusion

In this research project we focused in identifying new small molecule inhibitors that could be used as therapeutics for chronic inflammatory diseases. Thus, in order to discover potential candidates, we followed three different ways of identification (Graphical abstract, Image 11), described below.
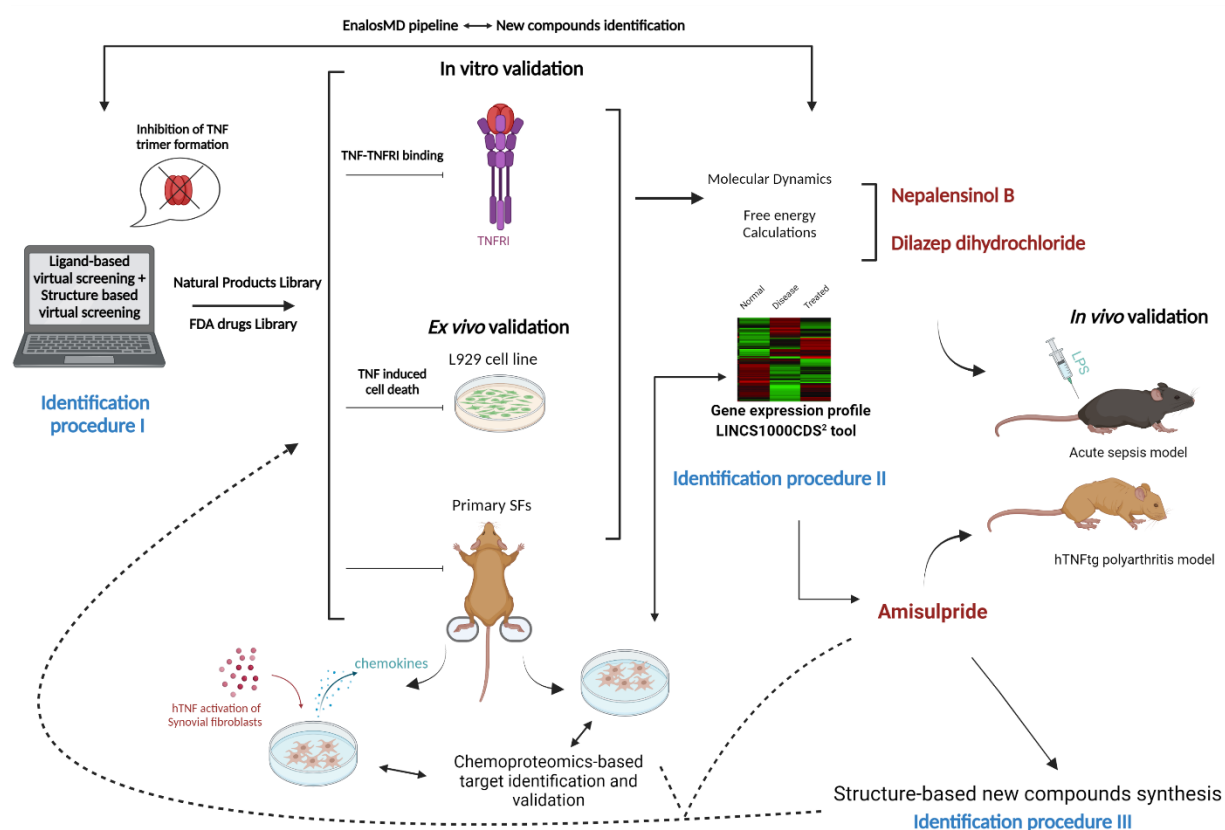
Image 11 Graphical abstract of the screening pipeline used, describing the three different identification procedures followed.

- The first identification procedure included a molecular docking approach, that aimed to identify direct inhibitors of TNF, an etiopathogenic cytokine of several chronic inflammatory diseases, such as RA and CD. We used as a scaffold the crystal structure of the complex of TNF with SPD304, which is known to directly inhibit TNF[31], searching for compounds that could bind similarly in two different libraries. The first library included NPs, where we additionally followed a similarity principle, looking for molecules that would act similarly but more potently than Ampelopsin-H, previously identified as a direct inhibitor of TNF trimerization[35]. The second library included FDA approved drugs, which were further filtered out according to their current use.

Although the most successful compound of each library, namely Nepalensinol B and Dilazep dihydrochloride, respectively, showed promising *ex vivo* results, in both the TNF induced death assay in L929 cell line, but also in reducing the proinflammatory responses of hTNF activated primary joint fibroblasts, being validated to interrupt TNF binding to its main receptor, TNFR1, we acquired unfavourable results in *in vivo* experiments.

- Intending to identify candidate compounds starting from a more biologically relevant approach, we applied a signature matching strategy. In our study, we used the gene expression profile of *hTNFtg* SFs, which are key pathogenic drivers in RA development and their *in vivo* activation by TNF is sufficient to orchestrate full arthritic pathogenesis in animal models. Thus, we aimed to find small molecules, that could potentially mimic the expression profile of arthritogenic SFs, when treated with an anti-TNF biologic, or reverse their pathogenic expression signature.

  We identified a neuroleptic drug, named Amisulpride, which was validated to reduce SFs' inflammatory and adhesive potential while decreasing also the clinical score of *hTNFtg* polyarthritis.

  Although signature matching approach can propose candidates that can regulate the disease gene profile of interest, it does not specify the compounds' target proteins. Notably, we found that Amisulpride did not exert its biological activities neither through its known targets, DRD2, DRD3 and HTR7, nor through TNF-TNFR1 binding inhibition. By applying a click chemistry approach, novel potential targets of Amisulpride were identified, which were further validated to repress *hTNFtg* SFs' inflammatory potential (ASCC3 and SEC62).

  Conclusively, our data support that Amisulpride could provide a combinatorial beneficial effect to patients suffering from RA and comorbid dysthymia, as it may reduce SFs pathogenicity in parallel with its anti-depressive activity.

- Amisulpride was used in high concentration (IC50 ≈ 250μM) to produce an anti-inflammatory effect in *hTNFtg* SFs, while it produced a significant, but not complete, amelioration of *hTNFtg in vivo* polyarthritis phenotype and histological score. Consequently, we used Amisulpride, as a scaffold for the synthesis of novel, more potent therapeutics against chronic inflammatory diseases.

  Hence, we screened over a hundred of newly synthesized compounds, dose dependently, using CCL5 and CCL20 levels as an indication of the compounds' anti-inflammatory properties.

We present here an example of a successful candidate, namely compound 53, which presented a 100fold less IC50 value in downregulating the elevated levels of both aforementioned chemokines in hTNF activated mouse joint SFs.

However, both cellular properties of compound 53 but more importantly its targets on *hTNFtg* SFs seem different than these of the original scaffold, Amisulpride, indicating a different mode of action. Compound 53 produced promising results in LPS acute sepsis model *in vivo*, however further validation of its targets and *in vivo* administration in further disease models is required for evaluating its potential use in the context of chronic inflammation.

6. Summary of the PhD thesis

In this work we aimed to identify new potential therapeutics against chronic inflammatory diseases, by developing of a novel screening pipeline, as current treatments are characterized by low patients' response, invasive administration and a plethora of side effects.

Initially, we considered a molecular docking approach searching for direct inhibitors of TNF trimerization, by using the Enalos *Asclepios in silico* pipeline, which has been used for identification of new therapeutics against TNF-mediated chronic inflammatory diseases, providing state-of-the-art insight on their binding mode.

Focusing on a NPs library, we propose that Nepalensinol B, a stilbenoid that belongs to resveratrol dimers, characterized by low free energy of binding and by a high number of hydrogen bonds with TNF, qualifies as a potential lead compound for TNF inhibitors' drug development, as it shows promising results in relevant *ex vivo* assays and it effectively interrupts TNF-TNFR1 binding.

A similar molecular docking approach for identification of potential PPI inhibitors of TNF was applied in a library of FDA approved drugs. Pharmacological testing of the selected compounds, along with the application of the Enalos Asclepios pipeline, concluded in proposing Dilazep Dihydrochloride as a potent compound to down-regulate proinflammatory responses of *hTNFtg* pathogenic synovial fibroblasts and TNF induced necroptosis on L929 cells, while interrupting the TNF-TNFR1 binding.

Because of non-consistent *in vivo* results, we then aimed to identify compounds starting from a more biologically relevant perspective, searching for compounds that could reverse deregulated gene expression signature of *hTNFtg* joints' SFs. We identified that a neuroleptic medication, namely Amisulpride, could downregulate *hTNFtg* SFs' activation and *hTNFtg* polyarthritis *in vivo*. Importantly, the molecular mechanism of the drug was not dependent on its main known receptors DRD2, DRD3 and HTR7. By applying a click chemistry approach, we identified two novel targets of the drug, namely ASCC3 and SEC62, which were further validated to repress *hTNFtg* SFs' inflammatory potential. Thus, Amisulpride is proposed as a candidate for offering a combinatorial advantage to patients suffering from RA and comorbid depression.

Finally, Amisulpride served as a lead compound for identification of novel, more potent therapeutics for chronic inflammatory disorders, which showed promising results *ex vivo* and *in vivo*.

In conclusion, the pipeline we developed includes a combination of identification methods searching for new potential small molecule therapeutics, with a plethora of assays confirming the inhibitors' action *in silico*, via the Enalos Asclepios pipeline, *ex vivo* in cell lines and primary cells, and *in vivo* in acute and chronic inflammation animal models. Potential targets of the compounds can be further identified following a click chemoproteomics approach.

7. Περίληψη της παρούσας διδακτορικής διατριβής στην ελληνική

Σε αυτή τη διδακτορική διατριβή στοχεύσαμε στον εντοπισμό νέων πιθανών θεραπευτικών μορίων κατά των χρόνιων φλεγμονωδών νόσων, αναπτύσσοντας μία προτυποποιημένη διαδικασία ελέγχου, καθώς οι τρέχουσες θεραπείες χαρακτηρίζονται από χαμηλή ανταπόκριση ασθενών, επεμβατική χορήγηση και πληθώρα παρενεργειών.

Αρχικά, εξετάσαμε μια υπολογιστική προσέγγιση μοριακής σύνδεσης για την αναζήτηση άμεσων αναστολέων του τριμερισμού του Παράγοντα Νέκρωσης όγκων (TNF), χρησιμοποιώντας το «Enalos Asclepios pipeline». Το τελευταίο έχει χρησιμοποιηθεί για τον εντοπισμό νέων θεραπευτικών μορίων κατά των χρόνιων φλεγμονωδών νόσων που διέπονται από την απορρύθμιση του TNF, παρέχοντας τελευταίας τεχνολογίας πληροφορίες σχετικά με τον τρόπο δράσης τους.

Εστιάζοντας σε μια βιβλιοθήκη φυσικών προϊόντων, προτείνουμε ότι το Nepalensinol B, ένα στιλβενοειδές που ανήκει στα διμερή της ρεσβερατρόλης, που χαρακτηρίζεται από χαμηλή ελεύθερη ενέργεια δέσμευσης και μεγάλο αριθμό δεσμών υδρογόνου με τον TNF, μπορεί να χαρακτηριστεί ως πιθανή ένωση οδηγός προς την ανάπτυξη αντι-TNF μορίων, καθώς παρουσιάζει δράση σε σχετικές δοκιμασίες κυττάρων αλλά και στη δοκιμασία δέσμευσης του TNF με τον κύριο υποδοχέα του, TNFR1.

Μια παρόμοια προσέγγιση μοριακής σύνδεσης για ανεύρεση αναστολέων του TNF εφαρμόστηκε επιπλέον και σε μια βιβλιοθήκη φαρμάκων, εγκεκριμένων από τον Οργανισμό Υγείας των Η.Π.Α (FDA). Ο φαρμακολογικός έλεγχος των επιλεγμένων ενώσεων, μαζί με την εφαρμογή της «Enalos Asclepios» διαδικασίας ελέγχου, κατέληξε στην πρόταση του Dilazep Dihydrochloride ως μια ένωση ικανή να μειώσει τις προφλεγμονώδεις αποκρίσεις των παθογόνων αρθρικών ινοβλαστών *hTNFtg* και την επαγώμενη από τον TNF νεκρόπτωση στα κύτταρα L929, παρεμποδίζοντας τη δημιουργία του συμπλόκου TNF-TNFR1.

Λόγω μη επιτυχών αποτελεσμάτων των προαναφερθέντων ενώσεων σε ζωικά πρότυπα, στοχεύσαμε, στη συνέχεια, να αναζητήσουμε πιθανά θεραπευτικά μικρά μόρια, ακολουθώντας μία πιο σχετική βιολογική προσέγγιση, με σκοπό την εύρεση δομών που θα μπορούσαν να αντιστρέψουν την απορυθμισμένη γονιδιακή έκφραση των παθογόνων αρθρικών *hTNFtg* ινοβλαστών. Εντοπίσαμε ότι ένα νευροληπτικό φάρμακο, ονόματι Amisulpride, μπόρεσε να μειώσει την ενεργοποίηση των αρθριτικών *hTNFtg* ινοβλαστών καθώς και την πολυαρθρίτιδα *hTNFtg in vivo*, ενώ είναι σημαντικό ότι ο μηχανισμός δράσης του δε στηρίζεται στους κύριους γνωστούς υποδοχείς του φαρμάκου, DRD2, DRD3 και HTR7. Εφαρμόζοντας μια προσέγγιση χημείας «κλικ», εντοπίσαμε δύο νέους στόχους του φαρμάκου, συγκεκριμένα τους ASCC3 και SEC62, οι οποίοι επικυρώθηκαν περαιτέρω ως ικανοί να προκαλέσουν καταστολή του φλεγμονώδους δυναμικού των *hTNFtg* ινοβλαστών. Συμπερασματικά, η θεραπεία με Amisulpride θα μπορούσε να προσφέρει ένα συνδυαστικό πλεονέκτημα σε ασθενείς που πάσχουν από Ρευματοειδή αρθρίτιδα και συννοσηρότητα κατάθλιψης.

Τέλος, η δομή του Amisulpride χρησίμευσε ως βασική ένωση για την ανακάλυψη νέων, πιο ισχυρών θεραπευτικών μορίων έναντι χρόνιων φλεγμονώδων διαταραχών, οι οποίες σε προκαταρκτικά πειράματα έδειξαν υποσχόμενα αποτελέσματα *ex vivo* και *in vivo*.

Συμπερασματικά, η διαδικασία ελέγχου που αναπτύξαμε περιλαμβάνει συνδυασμό μεθόδων ανίχνευσης νέων πιθανών μικρών μορίων αναστολέων, και επιβεβαίωση δράσης αυτών υπολογιστικά, μέσω της «Enalos Asclepios» διαδικασίας ελέγχου, *ex vivo*, σε κυτταρικές σειρές και σε πρωτογενή κύτταρα και *in vivo* σε ζωικά πρότυπα οξείας και χρόνιας φλεγμονής. Οι πιθανοί στόχοι των ενώσεων μπορούν να εντοπιστούν περαιτέρω ακολουθώντας μια προσέγγιση χημειοπρωτεϊνικής μέσω «κλικ» μορίων.

8. References

1.   Hayden, M. S. & Ghosh, S. Regulation of NF-κB by TNF family cytokines. *Seminars in Immunology* (2014). doi:10.1016/j.smim.2014.05.004

2.   Neumann, E., Lefèvre, S., Zimmermann, B., Gay, S. & Müller-Ladner, U. Rheumatoid arthritis progression mediated by activated synovial fibroblasts. *Trends Mol. Med.* **16**, 458–468 (2010).

3.   Tobón, G. J., Youinou, P. & Saraux, A. The environment, geo-epidemiology, and autoimmune disease: Rheumatoid arthritis. *J. Autoimmun.* (2010). doi:10.1016/j.jaut.2009.12.009

4.   Ngo, S. T., Steyn, F. J. & McCombe, P. A. Gender differences in autoimmune disease. *Frontiers in Neuroendocrinology* (2014). doi:10.1016/j.yfrne.2014.04.004

5.   López-Mejías, R. *et al.* Cardiovascular risk assessment in patients with rheumatoid arthritis: The relevance of clinical, genetic and serological markers. *Autoimmunity Reviews* (2016). doi:10.1016/j.autrev.2016.07.026

6.   Firestein, G. S. & McInnes, I. B. Immunopathogenesis of Rheumatoid Arthritis. *Immunity* (2017). doi:10.1016/j.immuni.2017.02.006

7.   Smolen, J. S. *et al.* Rheumatoid arthritis. *Nat. Rev. Dis. Prim.* **4**, (2018).

8.   Dennis, G. *et al.* Synovial phenotypes in rheumatoid arthritis correlate with response to biologic therapeutics. *Arthritis Res. Ther.* (2014). doi:10.1186/ar4555

9.   Malmström, V., Catrina, A. I. & Klareskog, L. The immunopathogenesis of seropositive rheumatoid arthritis: From triggering to targeting. *Nature Reviews Immunology* (2017). doi:10.1038/nri.2016.124

10.   Eyre, S. *et al.* High-density genetic mapping identifies new susceptibility loci for rheumatoid arthritis. *Nat. Genet.* (2012). doi:10.1038/ng.2462

11.   McInnes, I. B., Buckley, C. D. & Isaacs, J. D. Cytokines in rheumatoid arthritis-shaping the immunological landscape. *Nature Reviews Rheumatology* (2016). doi:10.1038/nrrheum.2015.171

12.   Hunter, C. A. & Jones, S. A. IL-6 as a keystone cytokine in health and disease. *Nature Immunology* (2015). doi:10.1038/ni.3153

13. Tanaka, T., Narazaki, M. & Kishimoto, T. Il-6 in inflammation, Immunity, And disease. *Cold Spring Harb. Perspect. Biol.* (2014). doi:10.1101/cshperspect.a016295

14. Biggioggero, M., Crotti, C., Becciolini, A. & Favalli, E. G. Tocilizumab in the treatment of rheumatoid arthritis: An evidence-based review and patient selection. *Drug Design, Development and Therapy* (2019). doi:10.2147/DDDT.S150580

15. Benedetti, G. & Miossec, P. Interleukin 17 contributes to the chronicity of inflammatory diseases such as rheumatoid arthritis. *Eur. J. Immunol.* (2014). doi:10.1002/eji.201344184

16. Garlanda, C., Dinarello, C. A. & Mantovani, A. The Interleukin-1 Family: Back to the Future. *Immunity* (2013). doi:10.1016/j.immuni.2013.11.010

17. Schett, G., Dayer, J. M. & Manger, B. Interleukin-1 function and role in rheumatic disease. *Nature Reviews Rheumatology* (2016). doi:10.1038/nrrheum.2016.166

18. Vignali, D. A. A. & Kuchroo, V. K. IL-12 family cytokines: immunological playmakers. *Nature Immunology* (2012). doi:10.1038/ni.2366

19. Rönnblom, L. & Eloranta, M. L. The interferon signature in autoimmune diseases. *Current Opinion in Rheumatology* (2013). doi:10.1097/BOR.0b013e32835c7e32

20. van Nieuwenhuijze, A. *et al.* GM-CSF as a therapeutic target in inflammatory diseases. *Molecular Immunology* (2013). doi:10.1016/j.molimm.2013.05.002

21. Burmester, G. R. *et al.* Efficacy and safety of mavrilimumab in subjects with rheumatoid arthritis. *Ann. Rheum. Dis.* (2013). doi:10.1136/annrheumdis-2012-202450

22. Beutler, B., Milsark, I. W. & Cerami, A. C. Passive immunization against cachectin/tumor necrosis factor protects mice from lethal effect of endotoxin. *Science (80-.).* (1985). doi:10.1126/science.3895437

23. Eck, M. J. & Sprang, S. R. The structure of tumor necrosis factor-α at 2.6 Å resolution. Implications for receptor binding. *J. Biol. Chem.* (1989). doi:10.2210/pdb1tnf/pdb

24. Bertrand, M. J. M. *et al.* cIAP1 and cIAP2 Facilitate Cancer Cell Survival by Functioning as E3 Ligases that Promote RIP1 Ubiquitination. *Mol. Cell* (2008). doi:10.1016/j.molcel.2008.05.014

25. Kanayama, A. *et al.* TAB2 and TAB3 activate the NF-κB pathway through binding to

polyubiquitin chains. *Mol. Cell* (2004). doi:10.1016/j.molcel.2004.08.008

26. Ghosh, S. & Hayden, M. S. Celebrating 25 years of NF-κB research. *Immunological Reviews* (2012). doi:10.1111/j.1600-065X.2012.01111.x

27. Brenner, D., Blaser, H. & Mak, T. W. Regulation of tumour necrosis factor signalling: Live or let die. *Nature Reviews Immunology* (2015). doi:10.1038/nri3834

28. Sun, S. C. The non-canonical NF-κB pathway in immunity and inflammation. *Nature Reviews Immunology* (2017). doi:10.1038/nri.2017.52

29. Rauert, H. *et al.* Membrane Tumor Necrosis Factor (TNF) induces p100 processing via TNF receptor-2 (TNFR2). *J. Biol. Chem.* (2010). doi:10.1074/jbc.M109.037341

30. Reinhard, C., Shamoon, B., Shyamala, V. & Williams, L. T. Tumor necrosis factor α-induced activation of c-jun N-terminal kinase is mediated by TRAF2. *EMBO J.* **16**, 1080–1092 (1997).

31. He, M. M. *et al.* Small-molecule inhibition of TNF-alpha. *Science* **310**, 1022–5 (2005).

32. Atretkhany, K. S. N., Gogoleva, V. S., Drutskaya, M. S. & Nedospasov, S. A. Distinct modes of TNF signaling through its two receptors in health and disease. *Journal of Leukocyte Biology* (2020). doi:10.1002/JLB.2MR0120-510R

33. Willrich, M. A. V., Murray, D. L. & Snyder, M. R. Tumor necrosis factor inhibitors: Clinical utility in autoimmune diseases. *Translational Research* (2015). doi:10.1016/j.trsl.2014.09.006

34. Sfikakis, P. P. The first decade of biologic TNF antagonists in clinical practice: Lessons learned, unresolved issues and future directions. *Current Directions in Autoimmunity* **11**, 180–210 (2010).

35. Melagraki, G. *et al.* In silico discovery of plant-origin natural product inhibitors of tumor necrosis factor (TNF) and receptor activator of NF-κB ligand (RANKL). *Front. Pharmacol.* (2018). doi:10.3389/fphar.2018.00800

36. Davis, J. M. & Colangelo, J. Small-molecule inhibitors of the interaction between TNF and TNFR. *Future Medicinal Chemistry* (2013). doi:10.4155/fmc.12.192

37. Richmond, V., Michelini, F., Bueno, C., Alche, L. & Ramirez, J. Small Molecules as Anti-TNF Drugs. *Curr. Med. Chem.* (2015). doi:10.2174/0929867322666150729115553

38. Dietrich, J. D. *et al.* Development of Orally Efficacious Allosteric Inhibitors of TNFα via Fragment-Based Drug Design. *J. Med. Chem.* (2021). doi:10.1021/acs.jmedchem.0c01280

39. Steeland, S., Libert, C. & Vandenbroucke, R. E. A new venue of TNF targeting. *International Journal of Molecular Sciences* (2018). doi:10.3390/ijms19051442

40. Rothe, J. *et al.* Mice lacking the tumour necrosis factor receptor 1 are resistant to IMF-mediated toxicity but highly susceptible to infection by Listeria monocytogenes. *Nature* (1993). doi:10.1038/364798a0

41. Pfeffer, K. *et al.* Mice deficient for the 55 kd tumor necrosis factor receptor are resistant to endotoxic shock, yet succumb to L. monocytogenes infection. *Cell* (1993). doi:10.1016/0092-8674(93)90134-C

42. Alexopoulou, L. *et al.* Transmembrane TNF protects mutant mice against intracellular bacterial infections, chronic inflammation and autoimmunity. *Eur. J. Immunol.* (2006). doi:10.1002/eji.200635921

43. Tumanov, A. V. *et al.* Cellular source and molecular form of TNF specify its distinct functions in organization of secondary lymphoid organs. *Blood* (2010). doi:10.1182/blood-2009-10-249177

44. Kuprash, D. V. *et al.* Novel tumor necrosis factor-knockout mice that lack Peyer's patches. *Eur. J. Immunol.* (2005). doi:10.1002/eji.200526119

45. Tsakiri, N., Papadopoulos, D., Denis, M. C., Mitsikostas, D. D. & Kollias, G. TNFR2 on non-haematopoietic cells is required for Foxp3 + Treg-cell function and disease suppression in EAE. *Eur. J. Immunol.* (2012). doi:10.1002/eji.201141659

46. Taoufik, E. *et al.* Transmembrane tumour necrosis factor is neuroprotective and regulates experimental autoimmune encephalomyelitis via neuronal nuclear factor-κB. *Brain* (2011). doi:10.1093/brain/awr203

47. Williams, S. K. *et al.* Anti-TNFR1 targeting in humanized mice ameliorates disease in a model of multiple sclerosis. *Sci. Rep.* (2018). doi:10.1038/s41598-018-31957-7

48. Keffer, J. *et al.* Transgenic mice expressing human tumour necrosis factor: A predictive genetic model of arthritis. *EMBO J.* (1991). doi:10.1002/j.1460-2075.1991.tb04978.x

49.   Kollias, G. *et al.* Animal models for arthritis: Innovative tools for prevention and treatment. *Annals of the Rheumatic Diseases* (2011). doi:10.1136/ard.2010.148551

50.   Holmdahl, R. *et al.* Arthritis induced in rats with non-immunogenic adjuvants as models for rheumatoid arthritis. *Immunol. Rev.* **184**, 184–202 (2001).

51.   Wooley, P. H., Seibold, J. R., Whalen, J. D. & Chapdelaine, J. M. Pristane-induced arthritis. the immunologic and genetic features of an experimental murine model of autoimmune disease. *Arthritis Rheum.* (1989). doi:10.1002/anr.1780320812

52.   Frasnelli, M. E., Tarussio, D., Chobaz-Péclat, V., Busso, N. & So, A. TLR2 modulates inflammation in zymosan-induced arthritis in mice. *Arthritis Res. Ther.* (2005).

53.   Trentham, D. E., Townes, A. S. & Kang, A. H. Autoimmunity to type II collagen: An experimental model of arthritis*. *J. Exp. Med.* (1977). doi:10.1084/jem.146.3.857

54.   Holmdahl, R., Jansson, L., Andersson, M. & Jonsson, R. Genetic, hormonal and behavioural influence on spontaneously developing arthritis in normal mice. *Clin. Exp. Immunol.* (1992). doi:10.1111/j.1365-2249.1992.tb06473.x

55.   Holmdahl, R., Rubin, K., Klareskog, L., Larsson, E. & Wigzell, H. Characterization of the antibody response in mice with type II collagen–induced arthritis, using monoclonal anti–type II collagen antibodies. *Arthritis Rheum.* (1986). doi:10.1002/art.1780290314

56.   Nandakumar, K. S., Svensson, L. & Holmdahl, R. Collagen Type II-Specific Monoclonal Antibody-Induced Arthritis in Mice: Description of the Disease and the Influence of Age, Sex, and Genes. *Am. J. Pathol.* (2003). doi:10.1016/S0002-9440(10)63542-0

57.   Christianson, C. A., Corr, M., Yaksh, T. L. & Svensson, C. I. K/BxN serum transfer arthritis as a model of inflammatory joint pain. *Methods Mol. Biol.* (2012). doi:10.1007/978-1-61779-561-9_19

58.   Geiler, T., Kriegsmann, Jöu., Keyszer, G. M., Gay, R. E. & Gay, S. A new model for rheumatoid arthritis generated by engraftment of rheumatoid synovial tissue and normal human cartilage into scid mice. *Arthritis Rheum.* (1994). doi:10.1002/art.1780371116

59.   Monach, P. A., Mathis, D. & Benoist, C. The K/BxN arthritis model. *Current Protocols in Immunology* (2008). doi:10.1002/0471142735.im1522s81

60. Horai, R. *et al.* Development of chronic inflammatory arthropathy resembling rheumatoid arthritis in interleukin I receptor antagonist-deficient mice. *J. Exp. Med.* (2000). doi:10.1084/jem.191.2.313

61. Sakaguchi, N. *et al.* Altered thymic T-cell selection due to a mutation of the ZAP-70 gene causes autoimmune arthritis in mice. *Nature* (2003). doi:10.1038/nature02119

62. Hashimoto, M. *et al.* Complement drives Th17 cell differentiation and triggers autoimmune arthritis. *J. Exp. Med.* (2010). doi:10.1084/jem.20092301

63. Kontoyiannis, D., Pasparakis, M., Pizarro, T. T., Cominelli, F. & Kollias, G. Impaired On/Off Regulation of TNF Biosynthesis in Mice Lacking TNF AU-Rich Elements. *Immunity* **10**, 387–398 (1999).

64. Armaka, M. *et al.* Mesenchymal cell targeting by TNF as a common pathogenic principle in chronic inflammatory joint and intestinal diseases. *J. Exp. Med.* (2008). doi:10.1084/jem.20070906

65. Zucker, S. *et al.* Measurement of matrix metalloproteinases and tissue inhibitors of metalloproteinases in blood and tissues. Clinical and experimental applications. in *Annals of the New York Academy of Sciences* (1999). doi:10.1111/j.1749-6632.1999.tb07687.x

66. Ntougkos, E. *et al.* Genomic Responses of Mouse Synovial Fibroblasts During Tumor Necrosis Factor–Driven Arthritogenesis Greatly Mimic Those in Human Rheumatoid Arthritis. *Arthritis Rheumatol.* **69**, 1588–1600 (2017).

67. Vasilopoulos, Y., Gkretsi, V., Armaka, M., Aidinis, V. & Kollias, G. Actin cytoskeleton dynamics linked to synovial fibroblast activation as a novel pathogenic principle in TNF-driven arthritis. in *Annals of the Rheumatic Diseases* (2007). doi:10.1136/ard.2007.079822

68. Aidinis, V. *et al.* Functional analysis of an arthritogenic synovial fibroblast. *Arthritis Res. Ther.* **5**, R140-57 (2003).

69. Armaka, M., Ospelt, C., Pasparakis, M. & Kollias, G. The p55TNFR-IKK2-Ripk3 axis orchestrates arthritis by regulating death and inflammatory pathways in synovial fibroblasts. *Nat. Commun.* (2018). doi:10.1038/s41467-018-02935-4

70. Douni, E. *et al.* Transgenic and knockout analyses of the role of TNF in immune regulation and disease pathogenesis. in *Journal of Inflammation* (1995).

71.	Probert, L., Plows, D., Kontogeorgos, G. & Kollias, G. The type I interleukin-1 receptor acts in series with tumor necrosis factor (TNF) to induce arthritis in TNF-transgenic mice. *Eur. J. Immunol.* (1995). doi:10.1002/eji.1830250647

72.	Alonzi, T. *et al.* Interleukin 6 is required for the development of collagen-induced arthritis. *J. Exp. Med.* (1998). doi:10.1084/jem.187.4.461

73.	Ntari, L. *et al.* Comorbid TNF-mediated heart valve disease and chronic polyarthritis share common mesenchymal cell-mediated aetiopathogenesis. *Ann. Rheum. Dis.* (2018). doi:10.1136/annrheumdis-2017-212597

74.	Koliaraki, V., Prados, A., Armaka, M. & Kollias, G. The mesenchymal context in inflammation, immunity and cancer. *Nature Immunology* (2020). doi:10.1038/s41590-020-0741-2

75.	Davidson, S. *et al.* Fibroblasts as immune regulators in infection, inflammation and cancer. *Nature Reviews Immunology* (2021). doi:10.1038/s41577-021-00540-z

76.	Buechler, M. B. *et al.* Cross-tissue organization of the fibroblast lineage. *Nature* (2021). doi:10.1038/s41586-021-03549-5

77.	Smillie, C. S. *et al.* Intra- and Inter-cellular Rewiring of the Human Colon during Ulcerative Colitis. *Cell* (2019). doi:10.1016/j.cell.2019.06.029

78.	Zepp, J. A. *et al.* Distinct Mesenchymal Lineages and Niches Promote Epithelial Self-Renewal and Myofibrogenesis in the Lung. *Cell* (2017). doi:10.1016/j.cell.2017.07.034

79.	Muller-Ladner, U. *et al.* Synovial fibroblasts of patients with rheumatoid arthritis attach to and invade normal human cartilage when engrafted into SCID mice. *Am J Pathol* **149**, 1607–1615 (1996).

80.	Lefèvre, S. *et al.* Synovial fibroblasts spread rheumatoid arthritis to unaffected joints. *Nat. Med.* (2009). doi:10.1038/nm.2050

81.	Croft, A. P. *et al.* Distinct fibroblast subsets drive inflammation and damage in arthritis. *Nature* (2019). doi:10.1038/s41586-019-1263-7

82.	Wynn, T. A. Two types of fibroblast drive arthritis. *Nature* (2019). doi:10.1038/d41586-019-01594-9

83.	Culemann, S. *et al.* Locally renewing resident synovial macrophages provide a protective barrier for the joint. *Nature* (2019). doi:10.1038/s41586-019-1471-1

84. Wei, K. *et al.* Notch signalling drives synovial fibroblast identity and arthritis pathology. *Nature* (2020). doi:10.1038/s41586-020-2222-z

85. Armaka, M. *et al.* Single - cell multimodal analysis identifies common regulatory programs in synovial fibroblasts of rheumatoid arthritis patients and modeled TNF - driven arthritis. *Genome Med.* 1–25 (2022). doi:10.1186/s13073-022-01081-3

86. Smith, M. *et al.* Heterogeneity of Inflammation-associated Synovial Fibroblasts in Rheumatoid Arthritis 2 and Its Drivers. *bioRxiv* 1–40 (2022).

87. Smolen, J. S. *et al.* EULAR recommendations for the management of rheumatoid arthritis with synthetic and biological disease-modifying antirheumatic drugs: 2019 update. *Ann. Rheum. Dis.* (2020). doi:10.1136/annrheumdis-2019-216655

88. Roskoski, R. Classification of small molecule protein kinase inhibitors based upon the structures of their drug-enzyme complexes. *Pharmacological Research* (2016). doi:10.1016/j.phrs.2015.10.021

89. Goel, N. & Stephens, S. Certolizumab pegol. *MAbs* **2**, 137–147 (2010).

90. Mazumdar, S. & Greenwald, D. Golimumab. *mAbs* **1**, 420–429 (2009).

91. Gu, T., Shah, N., Deshpande, G., Tang, D. H. & Eisenberg, D. F. Comparing Biologic Cost Per Treated Patient Across Indications Among Adult US Managed Care Patients: A Retrospective Cohort Study. *Drugs - Real World Outcomes* (2016). doi:10.1007/s40801-016-0093-2

92. Steenholdt, C. *et al.* Acute and delayed hypersensitivity reactions to infliximab and adalimumab in a patient with Crohn's disease. *J. Crohn's Colitis* (2012). doi:10.1016/j.crohns.2011.08.001

93. Ben-Horin, S., Kopylov, U. & Chowers, Y. Optimizing anti-TNF treatments in inflammatory bowel disease. *Autoimmunity Reviews* (2014). doi:10.1016/j.autrev.2013.06.002

94. Murdaca, G. *et al.* Immunogenicity of infliximab and adalimumab: What is its role in hypersensitivity and modulation of therapeutic efficacy and safety? *Expert Opinion on Drug Safety* (2016). doi:10.1517/14740338.2016.1112375

95. Melagraki, G. *et al.* Current Status and Future Prospects of Small–molecule Protein–protein Interaction (PPI) Inhibitors of Tumor Necrosis Factor (TNF) and Receptor

Activator of NF-κB Ligand (RANKL). *Curr. Top. Med. Chem.* (2018). doi:10.2174/1568026618666180607084430

96. Rees, H. *Supply Chain Management in the Drug Industry: Delivering Patient Value for Pharmaceuticals and Biologics*. *Supply Chain Management in the Drug Industry* (2011).

97. Ridgley, L. A., Anderson, A. E. & Pratt, A. G. What are the dominant cytokines in early rheumatoid arthritis? *Current Opinion in Rheumatology* (2018). doi:10.1097/BOR.0000000000000470

98. Hawking, F. Suramin: With Special Reference to Onchocerciasis. *Adv. Pharmacol.* (1978). doi:10.1016/S1054-3589(08)60486-X

99. Grazioli, L. *et al.* Inhibitory effect of suramin on receptor binding and cytotoxic activity of tumor necrosis factor α. *Int. J. Immunopharmacol.* (1992). doi:10.1016/0192-0561(92)90125-5

100. Mancini, F. *et al.* Inhibition of tumor necrosis factor-α (TNF-α)/TNF-α receptor binding by structural analogues of suramin. *Biochem. Pharmacol.* (1999). doi:10.1016/S0006-2952(99)00150-1

101. Papaneophytou, C. P., Mettou, A. K., Rinotas, V., Douni, E. & Kontopidis, G. A. Solvent selection for insoluble ligands, a challenge for biological assay development: A TNF-α/SPD304 study. *ACS Med. Chem. Lett.* (2013). doi:10.1021/ml300380h

102. Mascret, A. *et al.* New contributions to the drug profile of TNFα inhibitor SPD304: Affinity, selectivity and ADMET considerations. *Eur. J. Pharmacol.* (2021). doi:10.1016/j.ejphar.2021.174285

103. Shah, B. A. *et al.* Saponins as novel TNF-α inhibitors: Isolation of saponins and a nor-pseudoguaianolide from Parthenium hysterophorus. *Org. Biomol. Chem.* (2009). doi:10.1039/b902041a

104. O'Connell, J. *et al.* Small molecules that inhibit TNF signalling by stabilising an asymmetric form of the trimer. *Nat. Commun.* (2019). doi:10.1038/s41467-019-13616-1

105. Mouhsine, H. *et al.* Identification of an in vivo orally active dual-binding protein-protein interaction inhibitor targeting TNFα through combined in silico/in vitro/in vivo screening. *Sci. Rep.* (2017). doi:10.1038/s41598-017-03427-z

106. Leung, C. H. *et al.* Structure-based repurposing of FDA-approved drugs as TNF-α inhibitors. *ChemMedChem* **6**, 765–768 (2011).

107. Blevitt, J. M. *et al.* Structural Basis of Small-Molecule Aggregate Induced Inhibition of a Protein-Protein Interaction. *J. Med. Chem.* (2017). doi:10.1021/acs.jmedchem.6b01836

108. Xiao, H. Y. *et al.* Biologic-like in Vivo Efficacy with Small Molecule Inhibitors of TNFα Identified Using Scaffold Hopping and Structure-Based Drug Design Approaches. *J. Med. Chem.* (2020). doi:10.1021/acs.jmedchem.0c01732

109. Rodrigues, T., Reker, D., Schneider, P. & Schneider, G. Counting on natural products for drug design. *Nature Chemistry* (2016). doi:10.1038/nchem.2479

110. Hassan Baig, M. *et al.* Computer Aided Drug Design: Success and Limitations. *Curr. Pharm. Des.* (2016). doi:10.2174/1381612822666151125000550

111. Choi, H., Lee, Y., Park, H. & Oh, D. S. Discovery of the inhibitors of tumor necrosis factor alpha with structure-based virtual screening. *Bioorganic Med. Chem. Lett.* (2010). doi:10.1016/j.bmcl.2010.08.116

112. Saddala, M. S. & Huang, H. Identification of novel inhibitors for TNFα, TNFR1 and TNFα-TNFR1 complex using pharmacophore-based approaches. *J. Transl. Med.* (2019). doi:10.1186/s12967-019-1965-5

113. Melagraki, G. *et al.* Cheminformatics-aided discovery of small-molecule Protein-Protein Interaction (PPI) dual inhibitors of Tumor Necrosis Factor (TNF) and Receptor Activator of NF-κB Ligand (RANKL). *PLoS Comput. Biol.* (2017). doi:10.1371/journal.pcbi.1005372

114. Afantitis, A., Tsoumanis, A. & Melagraki, G. Enalos Suite of Tools: Enhancing Cheminformatics and Nanoinfor - matics through KNIME. *Curr. Med. Chem.* (2020). doi:10.2174/0929867327666200727114410

115. Pushpakom, S. *et al.* Drug repurposing: Progress, challenges and recommendations. *Nature Reviews Drug Discovery* (2018). doi:10.1038/nrd.2018.168

116. Breckenridge, A. & Jacob, R. Overcoming the legal and regulatory barriers to drug repurposing. *Nature Reviews Drug Discovery* (2018). doi:10.1038/nrd.2018.92

117. Ashburn, T. T. & Thor, K. B. Drug repositioning: Identifying and developing new uses

for existing drugs. *Nature Reviews Drug Discovery* (2004). doi:10.1038/nrd1468

118. Singhal, S. *et al.* Antitumor Activity of Thalidomide in Refractory Multiple Myeloma. *N. Engl. J. Med.* (1999). doi:10.1056/nejm199911183412102

119. Molina, D. M. *et al.* Monitoring drug target engagement in cells and tissues using the cellular thermal shift assay. *Science (80-.).* (2013). doi:10.1126/science.1233606

120. Su, Y. *et al.* Target identification of biologically active small molecules via in situ methods. *Current Opinion in Chemical Biology* (2013). doi:10.1016/j.cbpa.2013.06.005

121. Apostolaki, M., Armaka, M., Victoratos, P. & Kollias, G. Cellular mechanisms of TNF function in models of inflammation and autoimmunity. in *TNF Pathophysiology: Molecular and Cellular Mechanisms* **11**, 1–26 (2010).

122. Kingsmore, K. M., Grammer, A. C. & Lipsky, P. E. Drug repurposing to improve treatment of rheumatic autoimmune inflammatory diseases. *Nature Reviews Rheumatology* (2020). doi:10.1038/s41584-019-0337-0

123. Brown, P. M., Pratt, A. G. & Isaacs, J. D. Mechanism of action of methotrexate in rheumatoid arthritis, and the search for biomarkers. *Nature Reviews Rheumatology* (2016). doi:10.1038/nrrheum.2016.175

124. Cuellar, M. L. & Espinoza, L. R. Methotrexate use in psoriasis and psoriatic arthritis. *Rheum. Dis. Clin. North Am.* (1997). doi:10.1016/S0889-857X(05)70361-6

125. Hardy, R. S., Raza, K. & Cooper, M. S. Therapeutic glucocorticoids: mechanisms of actions in rheumatic diseases. *Nature Reviews Rheumatology* (2020). doi:10.1038/s41584-020-0371-y

126. Present, D. H. *et al.* Infliximab for the Treatment of Fistulas in Patients with Crohn's Disease. *N. Engl. J. Med.* (1999). doi:10.1056/nejm199905063401804

127. Lipsky, P. E. *et al.* Infliximab and Methotrexate in the Treatment of Rheumatoid Arthritis. *N. Engl. J. Med.* (2000). doi:10.1056/nejm200011303432202

128. Davis, J. C. *et al.* Recombinant Human Tumor Necrosis Factor Receptor (Etanercept) for Treating Ankylosing Spondylitis: A Randomized, Controlled Trial. *Arthritis Rheum.* (2003). doi:10.1002/art.11325

129. Yuan, K., Huang, G., Sang, X. & Xu, A. Baricitinib for systemic lupus erythematosus.

The Lancet (2019). doi:10.1016/S0140-6736(18)32763-6

130. Wells, J. A. & McClendon, C. L. Reaching for high-hanging fruit in drug discovery at protein-protein interfaces. *Nature* **450**, 1001–1009 (2007).

131. Clackson, T. & Wells, J. A. A hot spot of binding energy in a hormone-receptor interface. *Science (80-.).* (1995). doi:10.1126/science.7529940

132. Berg, T. Modulation of protein-protein interactions with small organic molecules. *Angewandte Chemie - International Edition* (2003). doi:10.1002/anie.200200558

133. Jones, S. & Thornton, J. M. Principles of protein-protein interactions. *Proceedings of the National Academy of Sciences of the United States of America* (1996). doi:10.1073/pnas.93.1.13

134. Sheng, C., Dong, G., Miao, Z., Zhang, W. & Wang, W. State-of-the-art strategies for targeting protein-protein interactions by small-molecule inhibitors. *Chemical Society Reviews* (2015). doi:10.1039/c5cs00252d

135. Magkrioti, C. *et al.* Structure-based discovery of novel chemical classes of autotaxin inhibitors. *Int. J. Mol. Sci.* (2020). doi:10.3390/ijms21197002

136. Mouchlis, V. D. *et al.* Advances in de novo drug design: From conventional to machine learning methods. *International Journal of Molecular Sciences* (2021). doi:10.3390/ijms22041676

137. Mouchlis, V. D., Melagraki, G., Zacharia, L. C. & Afantitis, A. Computer-aided drug design of β-secretase, γ- secretase and anti-tau inhibitors for the discovery of novel alzheimer's therapeutics. *International Journal of Molecular Sciences* (2020). doi:10.3390/ijms21030703

138. Melagraki, G. *et al.* In silico discovery of plant-origin natural product inhibitors of tumor necrosis factor (TNF) and receptor activator of NF-κB ligand (RANKL). *Front. Pharmacol.* **9**, 1–12 (2018).

139. Papadopoulou, D. *et al.* In silico identification and evaluation of natural products as potential tumor necrosis factor function inhibitors using advanced enalos asclepios KNIME nodes. *Int. J. Mol. Sci.* (2021). doi:10.3390/ijms221910220

140. Vanlangenakker, N., Bertrand, M. J. M., Bogaert, P., Vandenabeele, P. & Vanden Berghe, T. TNF-induced necroptosis in L929 cells is tightly regulated by multiple

TNFR1 complex i and II members. *Cell Death Dis.* (2011). doi:10.1038/cddis.2011.111

141. Duan, Q. *et al.* L1000CDS2: LINCS L1000 characteristic direction signatures search engine. *npj Syst. Biol. Appl.* **2**, 16015 (2016).

142. Lee, J. *et al.* Withaferin A is a leptin sensitizer with strong antidiabetic properties in mice. *Nat. Med.* (2016). doi:10.1038/nm.4145

143. Armaka, M., Gkretsi, V., Kontoyiannis, D. & Kollias, G. A standardized protocol for the isolation and culture of normal and arthritogenic murine synovial fibroblasts. *Protoc. Exch.* 2–5 (2009). doi:10.1038/nprot.2009.102

144. Feoktistova, M., Geserick, P. & Leverkus, M. Crystal violet assay for determining viability of cultured cells. *Cold Spring Harb. Protoc.* (2016). doi:10.1101/pdb.prot087379

145. Mould, A. W. *et al.* Vegfb gene knockout mice display reduced pathology and synovial angiogenesis in both antigen-induced and collagen-induced models of arthritis. *Arthritis Rheum.* (2003). doi:10.1002/art.11232

146. Anders, S. & Huber, W. Differential expression analysis for sequence count data. *Genome Biol.* (2010). doi:10.1186/gb-2010-11-10-r106

147. Moulos, P. & Hatzis, P. Systematic integration of RNA-Seq statistical algorithms for accurate detection of differential gene expression patterns. *Nucleic Acids Res.* (2015). doi:10.1093/nar/gku1273

148. RCoreTeam, R. *R: a Language and Environment for Statistical Computing.* http://www.R-project.org/ (2008).

149. Heberle, H., Meirelles, V. G., da Silva, F. R., Telles, G. P. & Minghim, R. InteractiVenn: A web-based tool for the analysis of sets through Venn diagrams. *BMC Bioinformatics* (2015). doi:10.1186/s12859-015-0611-3

150. Chen, E. Y. *et al.* Enrichr: Interactive and collaborative HTML5 gene list enrichment analysis tool. *BMC Bioinformatics* (2013). doi:10.1186/1471-2105-14-128

151. Chen, Y. C. & Zhang, C. A chemoproteomic method for identifying cellular targets of covalent kinase inhibitors. *Genes and Cancer* (2016). doi:10.18632/genesandcancer.106

152. Center, M. A. C. 4 × Lentivirus Concentrator Solution. *Internal* 4–6

153. Bekker-Jensen, D. B. *et al.* A compact quadrupole-orbitrap mass spectrometer with FAIMS interface improves proteome coverage in short LC gradients. *Mol. Cell. Proteomics* (2020). doi:10.1074/mcp.TIR119.001906

154. Martinez-Val, A. *et al.* Spatial-proteomics reveals phospho-signaling dynamics at subcellular resolution. *Nat. Commun. 2021 121* (2021).

155. Bekker-Jensen, D. B. *et al.* Rapid and site-specific deep phosphoproteome profiling by data-independent acquisition without the need for spectral libraries. *Nat. Commun.* (2020). doi:10.1038/s41467-020-14609-1

156. Cox, J. & Mann, M. MaxQuant enables high peptide identification rates, individualized p.p.b.-range mass accuracies and proteome-wide protein quantification. *Nat. Biotechnol.* (2008). doi:10.1038/nbt.1511

157. Cox, J. *et al.* Andromeda: A peptide search engine integrated into the MaxQuant environment. *J. Proteome Res.* (2011). doi:10.1021/pr101065j

158. Wieczorek, S. *et al.* DAPAR & ProStaR: Software to perform statistical analyses in quantitative discovery proteomics. *Bioinformatics* (2017). doi:10.1093/bioinformatics/btw580

159. Huang, D. W., Sherman, B. T. & Lempicki, R. A. Systematic and integrative analysis of large gene lists using DAVID bioinformatics resources. *Nat. Protoc.* (2009). doi:10.1038/nprot.2008.211

160. Huang, D. W., Sherman, B. T. & Lempicki, R. A. Bioinformatics enrichment tools: Paths toward the comprehensive functional analysis of large gene lists. *Nucleic Acids Res.* (2009). doi:10.1093/nar/gkn923

161. Lynn, D. J. *et al.* InnateDB: Facilitating systems-level analyses of the mammalian innate immune response. *Mol. Syst. Biol.* (2008). doi:10.1038/msb.2008.55

162. Jimenez-Garcia, L., Herranz, S., Luque, A. & Hortelano, S. Thioglycollate-elicited Peritoneal Macrophages Preparation and Arginase Activity Measurement in IL-4 Stimulated Macrophages. *BIO-PROTOCOL* (2015). doi:10.21769/bioprotoc.1585

163. Varsou, D. D., Nikolakopoulos, S., Tsoumanis, A., Melagraki, G. & Afantitis, A. ENALOS+ KNIME nodes: New cheminformatics tools for drug discovery. in *Methods in Molecular Biology* (2018). doi:10.1007/978-1-4939-8630-9_7

164. Klopmand, G. Concepts and applications of molecular similarity, by Mark A. Johnson and Gerald M. Maggiora, eds., John Wiley & Sons, New York, 1990, 393 pp. Price: $65.00. *J. Comput. Chem.* (1992). doi:10.1002/jcc.540130415

165. Willett, P., Barnard, J. M. & Downs, G. M. Chemical similarity searching. *J. Chem. Inf. Comput. Sci.* (1998). doi:10.1021/ci9800211

166. Ruiz-Carmona, S. *et al.* rDock: A Fast, Versatile and Open Source Program for Docking Ligands to Proteins and Nucleic Acids. *PLoS Comput. Biol.* (2014). doi:10.1371/journal.pcbi.1003571

167. Atanasov, A. G. *et al.* Discovery and resupply of pharmacologically active plant-derived natural products: A review. *Biotechnology Advances* (2015). doi:10.1016/j.biotechadv.2015.08.001

168. Feher, M. & Schmidt, J. M. Property distributions: Differences between drugs, natural products, and molecules from combinatorial chemistry. *J. Chem. Inf. Comput. Sci.* (2003). doi:10.1021/ci0200467

169. Barnes, E. C., Kumar, R. & Davis, R. A. The use of isolated natural products as scaffolds for the generation of chemically diverse screening libraries for drug discovery. *Natural Product Reports* (2016). doi:10.1039/c5np00121h

170. Li, J. W. H. & Vederas, J. C. Drug discovery and natural products: End of an era or an endless frontier? *Science* (2009). doi:10.1126/science.1168243

171. Clardy, J. & Walsh, C. Lessons from natural molecules. *Nature* (2004). doi:10.1038/nature03194

172. Moffat, J. G., Vincent, F., Lee, J. A., Eder, J. & Prunotto, M. Opportunities and challenges in phenotypic drug discovery: An industry perspective. *Nature Reviews Drug Discovery* (2017). doi:10.1038/nrd.2017.111

173. Atanasov, A. G. *et al.* Natural products in drug discovery: advances and opportunities. *Nature Reviews Drug Discovery* (2021). doi:10.1038/s41573-020-00114-z

174. Harrison, C. Patenting natural products just got harder. *Nature biotechnology* (2014). doi:10.1038/nbt0514-403a

175. Wu, M. *et al.* An update on phytochemistry and biological activities of Cinnamomum. *Records of Natural Products* (2022). doi:10.25135/rnp.245.21.03.2000

176. Niesen, D. B., Hessler, C. & Seeram, N. P. Beyond resveratrol: A review of natural stilbenoids identified from 2009-2013. *Journal of Berry Research* (2013). doi:10.3233/JBR-130062

177. Li, W. W., Li, B. G. & Chen, Y. Z. Flexuosol A, a new tetrastilbene from Vitis flexuosa. *J. Nat. Prod.* (1998). doi:10.1021/np970457v

178. Yamada, M. *et al.* Stilbenoids of Kobresia nepalensis (Cyperaceae) exhibiting DNA topoisomerase II inhibition. *Phytochemistry* (2006). doi:10.1016/j.phytochem.2005.11.001

179. Silva, A. A. *et al.* Resveratrol-derived stilbenoids and biological activity evaluation of seed extracts of Cenchrus echinatus L. *Nat. Prod. Res.* (2012). doi:10.1080/14786419.2011.561538

180. Keylor, M. H. *et al.* Synthesis of resveratrol tetramers via a stereoconvergent radical equilibrium. *Science (80-.).* (2016). doi:10.1126/science.aaj1597

181. Mattivi, F. *et al.* Profiling of resveratrol oligomers, important stress metabolites, accumulating in the leaves of hybrid Vitis vinifera (Merzling × Teroldego) genotypes infected with Plasmopara viticola. *J. Agric. Food Chem.* (2011). doi:10.1021/jf200771y

182. Pawlus, A. D. *et al.* Stilbenoid profiles of canes from Vitis and Muscadinia species. *J. Agric. Food Chem.* (2013). doi:10.1021/jf303843z

183. Kulanthaivel, P. *et al.* Naturally occurring protein kinase C inhibitors; II. Isolation of oligomeric stilbenes from Caragana sinica. *Planta Med.* (1995). doi:10.1055/s-2006-957996

184. Syah, Y. M. *et al.* Two oligostilbenes, cis- and trans-diptoindonesin B, from Dryobalanops oblongifolia. *Phytochemistry* (2003). doi:10.1016/S0031-9422(03)00274-7

185. Abdjan, M. I. *et al.* Exploration of stilbenoid trimers as potential inhibitors of sirtuin1 enzyme using a molecular docking and molecular dynamics simulation approach. *RSC Adv.* (2021). doi:10.1039/d1ra02233d

186. Cho, H., Park, J. H., Ahn, E. K. & Oh, J. S. Kobophenol A Isolated from Roots of Caragana sinica (Buc'hoz) Rehder Exhibits Anti-inflammatory Activity by Regulating NF-κB Nuclear Translocation in J774A.1 Cells. *Toxicol. Reports* (2018). doi:10.1016/j.toxrep.2018.05.011

187. Dávid, C. Z., Hohmann, J. & Vasas, A. Chemistry and pharmacology of cyperaceae stilbenoids: A review. *Molecules* (2021). doi:10.3390/molecules26092794

188. Li, L., Henry, G. E. & Seeram, N. P. Identification and bioactivities of resveratrol oligomers and flavonoids from carex folliculata Seeds. *J. Agric. Food Chem.* (2009). doi:10.1021/jf901716j

189. Lee, S. R. *et al.* Kobophenol a inhibits sodium nitroprusside-induced cardiac H9c2 cell death through suppressing activation of JNK and preserving mitochondrial anti-apoptotic Bcl-2 and Mcl-1. *Chem. Pharm. Bull.* (2014). doi:10.1248/cpb.c13-00995

190. Lee, S. R., Kwak, J. H., Park, D. S. & Pyo, S. Protective effect of kobophenol A on nitric oxide-induced cell apoptosis in human osteoblast-like MG-63 cells: Involvement of JNK, NF-κB and AP-1 pathways. *Int. Immunopharmacol.* (2011). doi:10.1016/j.intimp.2011.04.004

191. Kwak, J. H. *et al.* Kobophenol A enhances proliferation of human osteoblast-like cells with activation of the p38 pathway. *Int. Immunopharmacol.* (2013). doi:10.1016/j.intimp.2013.08.015

192. Gangadevi, S. *et al.* Kobophenol A Inhibits Binding of Host ACE2 Receptor with Spike RBD Domain of SARS-CoV-2, a Lead Compound for Blocking COVID-19. *J. Phys. Chem. Lett.* (2021). doi:10.1021/acs.jpclett.0c03119

193. Kawabata, J., Mishima, M., Kurihara, H. & Mizutani, J. Stereochemistry of two tetrastilbenes from Carex species. *Phytochemistry* (1995). doi:10.1016/0031-9422(95)00501-W

194. Ku, K. T., Huang, Y. L., Huang, Y. J. & Chiou, W. F. Miyabenol A inhibits LPS-induced NO production via IKK/IκB inactivation in RAW 264.7 macrophages: Possible involvement of the p38 and PI3K pathways. *J. Agric. Food Chem.* (2008). doi:10.1021/jf8019369

195. Huang, Y. L., Tsai, W. J., Shen, C. C. & Chen, C. C. Resveratrol derivatives from the roots of Vitis thunbergii. *J. Nat. Prod.* (2005). doi:10.1021/np049686p

196. Bakker, J. & Timberlake, C. F. Isolation, Identification, and Characterization of New Color-Stable Anthocyanins Occurring in Some Red Wines. *J. Agric. Food Chem.* (1997). doi:10.1021/jf960252c

197. Fulcrand, H., Benabdeljalil, C., Rigaud, J., Cheynier, V. & Moutounet, M. A new class

of wine pigments generated by reaction between pyruvic acid and grape anthocyanins. *Phytochemistry* (1998). doi:10.1016/S0031-9422(97)00772-3

198. Oliveira, J., de Freitas, V. & Mateus, N. A novel synthetic pathway to vitisin B compounds. *Tetrahedron Lett.* (2009). doi:10.1016/j.tetlet.2009.04.072

199. Azevedo, J. *et al.* Antioxidant features of red wine pyranoanthocyanins: Experimental and theoretical approaches. *J. Agric. Food Chem.* (2014). doi:10.1021/jf404735j

200. Chen, H. H. *et al.* Acarbose Decreases the Rheumatoid Arthritis Risk of Diabetic Patients and Attenuates the Incidence and Severity of Collagen-induced Arthritis in Mice. *Sci. Rep.* **5**, 1–13 (2015).

201. McCarey, D. W. *et al.* Trial of Atorvastatin in Rheumatoid Arthritis (TARA): Double-blind, randomised placebo-controlled trial. *Lancet* **363**, 2015–2021 (2004).

202. Ahmed WMS, H. O. Effect of Atorvastatin and Vitamin D on FreundÂ's Adjuvant-Induced Rheumatoid Arthritis in Rat. *J. Bioequiv. Availab.* **07**, 90–94 (2015).

203. Donate, P. B. *et al.* Bosentan, an endothelin receptor antagonist, ameliorates collagen-induced arthritis: The role of TNF-α in the induction of endothelin system genes. *Inflamm. Res.* **61**, 337–348 (2012).

204. Chang, Y. & Wei, W. Angiotensin II in inflammation, immunity and rheumatoid arthritis. *Clinical and Experimental Immunology* (2015). doi:10.1111/cei.12467

205. Nakatsuka, R., Nozaki, T., Shinohara, M. & Ohura, K. Dilazep decreases lipopolysaccharide-induced nitric oxide and TNF-α synthesis in RAW 264 cells. *J. Pharmacol. Sci.* **113**, 271–275 (2010).

206. Rovenský, J. *et al.* Treatment of rat adjuvant arthritis with flavonoid (Detralex ®), methotrexate, and their combination. *Ann. N. Y. Acad. Sci.* **1173**, 798–804 (2009).

207. Makar, T. K. *et al.* Silencing of Abcc8 or inhibition of newly upregulated Sur1-Trpm4 reduce inflammation and disease progression in experimental autoimmune encephalomyelitis. *J. Neuroinflammation* **12**, 1–13 (2015).

208. Cai, J. *et al.* Glibenclamide attenuates myocardial injury by lipopolysaccharides in streptozotocin-induced diabetic mice. *Cardiovasc. Diabetol.* **13**, 1–11 (2014).

209. Ingham, V., Williams, A. & Bate, C. Glimepiride reduces CD14 expression and cytokine secretion from macrophages. *J. Neuroinflammation* **11**, 1–14 (2014).

210. Models, D. Disease models. *Exp. Anim.* **70**, S69–S76 (2021).

211. Chong, C. R. *et al.* Inhibition of angiogenesis by the antifungal drug itraconazole. *ACS Chem. Biol.* (2007). doi:10.1021/cb600362d

212. Aftab, B. T., Dobromilskaya, I., Liu, J. O. & Rudin, C. M. Itraconazole inhibits angiogenesis and tumor growth in non-small cell lung cancer. *Cancer Res.* (2011). doi:10.1158/0008-5472.CAN-11-0691

213. Sheikh, A., Naqvi, S. H. A., Naqvi, S. H. S. & Sheikh, K. Itraconazole: Its possible role in inhibiting angiogenesis in Rheumatoid Arthritis. *Med. Hypotheses* (2012). doi:10.1016/j.mehy.2012.05.019

214. Kurose, A., Yoshida, W., Yoshida, M. & Sawai, T. Effects of paclitaxel on cultured synovial cells from patients with rheumatoid arthritis. *Cytometry* **44**, 349–354 (2001).

215. Zhao, Y. *et al.* Paclitaxel suppresses collagen-induced arthritis: A reevaluation. *Am. J. Transl. Res.* **8**, 5044–5051 (2016).

216. Takagi, H., Mizuno, Y., Yamamoto, H., Goto, S. N. & Umemoto, T. Effects of telmisartan therapy on interleukin-6 and tumor necrosis factor-alpha levels: A meta-analysis of randomized controlled trials. *Hypertens. Res.* **36**, 368–373 (2013).

217. Sagawa, K., Nagatani, K., Komagata, Y. & Yamamoto, K. Angiotensin receptor blockers suppress antigen-specific T cell responses and ameliorate collagen-induced arthritis in mice. *Arthritis Rheum.* **52**, 1920–1928 (2005).

218. Zucoloto, A. Z. *et al.* Probucol Ameliorates Complete Freund's Adjuvant-Induced Hyperalgesia by Targeting Peripheral and Spinal Cord Inflammation. *Inflammation* **42**, 1474–1490 (2019).

219. Koch, A. E. Chemokines and their receptors in rheumatoid arthritis: Future targets? *Arthritis and Rheumatism* (2005). doi:10.1002/art.20932

220. Alexiou, P. *et al.* Rationally designed less toxic SPD-304 analogs and preliminary evaluation of their TNF inhibitory effects. *Arch. Pharm. (Weinheim).* (2014). doi:10.1002/ardp.201400198

221. Jones, D. S. *et al.* Profiling drugs for rheumatoid arthritis that inhibit synovial fibroblast activation. *Nat. Chem. Biol.* (2017). doi:10.1038/nchembio.2211

222. Ntari, L. *et al.* Combination of subtherapeutic anti-TNF dose with dasatinib restores

clinical and molecular arthritogenic profiles better than standard anti-TNF treatment. *J. Transl. Med.* (2021). doi:10.1186/s12967-021-02764-y

223. Kollias, G. & Kontoyiannis, D. Role of TNF/TNFR in autoimmunity: Specific TNF receptor blockade may be advantageous to anti-TNF treatments. *Cytokine and Growth Factor Reviews* (2002). doi:10.1016/S1359-6101(02)00019-9

224. Cronstein, B. N., Kramer, S. B., Weissmann, G. & Hirschhorn, R. Adenosine: A physiological modulator of superoxide anion generation by human neutrophils. *J. Exp. Med.* (1983). doi:10.1084/jem.158.4.1160

225. Cronstein, B. N. & Sitkovsky, M. Adenosine and adenosine receptors in the pathogenesis and treatment of rheumatic diseases. *Nat. Rev. Rheumatol.* **13**, 41–51 (2017).

226. Cronstein, B. N., Naime, D. & Ostad, E. The antiinflammatory mechanism of methotrexate: Increased adenosine release at inflamed sites diminishes leukocyte accumulation in an in vivo model of inflammation. *J. Clin. Invest.* (1993). doi:10.1172/JCI116884

227. Li, R. W. S. *et al.* Physiological and pharmacological roles of vascular nucleoside transporters. *Journal of Cardiovascular Pharmacology* (2012). doi:10.1097/FJC.0b013e31820eb788

228. Guo, Z. *et al.* Rapamycin-inspired macrocycles with new target specificity. *Nat. Chem.* (2019). doi:10.1038/s41557-018-0187-4

229. Wright, N. J. & Lee, S. Y. Structures of human ENT1 in complex with adenosine reuptake inhibitors. *Nat. Struct. Mol. Biol.* (2019). doi:10.1038/s41594-019-0245-7

230. Curran, M. P. & Perry, C. M. Amisulpride: A review of its use in the management of schizophrenia. *Drugs* (2001). doi:10.2165/00003495-200161140-00014

231. Abbas, A. I. *et al.* Amisulpride is a potent 5-HT7 antagonist: Relevance for antidepressant actions in vivo. *Psychopharmacology (Berl).* (2009). doi:10.1007/s00213-009-1521-8

232. Diarra, D. *et al.* Dickkopf-1 is a master regulator of joint remodeling. *Nat. Med.* (2007). doi:10.1038/nm1538

233. Miao, C., Chang, J., Dou, J., Xiong, Y. & Zhou, G. DNA hypermethylation of SFRP2

influences the pathology of rheumatoid arthritis through the canonical Wnt signaling in model rats. *Autoimmunity* (2018). doi:10.1080/08916934.2018.1516760

234. Teufel, S. *et al.* Loss of the WNT9a ligand aggravates the rheumatoid arthritis-like symptoms in hTNF transgenic mice. *Cell Death Dis.* (2021). doi:10.1038/s41419-021-03786-6

235. Grooten, J., Goossens, V., Vanhaesebroeck, B. & Fiers, W. Cell membrane permeabilization and cellular collapse, followed by loss of dehydrogenase activity: Early events in tumour necrosis factor-induced cytotoxicity. *Cytokine* **5**, 546–555 (1993).

236. Haskó, G. *et al.* Modulation of lipopolysaccharide-induced tumor necrosis factor-α and nitric oxide production by dopamine receptor agonists and antagonists in mice. *Immunol. Lett.* **49**, 143–147 (1996).

237. Brustolim, D., Ribeiro-dos-Santos, R., Kast, R. E., Altschuler, E. L. & Soares, M. B. P. A new chapter opens in anti-inflammatory treatments:The antidepressant bupropion lowers production of tumor necrosis factor-alpha and interferon-gamma in mice. *Int. Immunopharmacol.* (2006). doi:10.1016/j.intimp.2005.12.007

238. Karagianni, N. *et al.* An integrative transcriptome analysis framework for drug efficacy and similarity reveals drug-specific signatures of anti-TNF treatment in a mouse model of inflammatory polyarthritis. *PLoS Comput. Biol.* (2019). doi:10.1371/journal.pcbi.1006933

239. Nair, A. & Jacob, S. A simple practice guide for dose conversion between animals and human. *J. Basic Clin. Pharm.* (2016). doi:10.4103/0976-0105.177703

240. Mateen, S., Moin, S., Khan, A. Q., Zafar, A. & Fatima, N. Increased reactive oxygen species formation and oxidative stress in rheumatoid arthritis. *PLoS One* (2016). doi:10.1371/journal.pone.0152925

241. McKenna, F. *et al.* Dopamine receptor expression on human T- and B-lymphocytes, monocytes, neutrophils, eosinophils and NK cells: A flow cytometric study. *J. Neuroimmunol.* (2002). doi:10.1016/S0165-5728(02)00280-1

242. Nakano, K. *et al.* Dopamine Induces IL-6–Dependent IL-17 Production via D1-Like Receptor on CD4 Naive T Cells and D1-Like Receptor Antagonist SCH-23390 Inhibits Cartilage Destruction in a Human Rheumatoid Arthritis/SCID Mouse Chimera Model.

J. Immunol. (2011). doi:10.4049/jimmunol.1002475

243. Capellino, S. *et al.* Increased expression of dopamine receptors in synovial fibroblasts from patients with rheumatoid arthritis: Inhibitory effects of dopamine on interleukin-8 and interleukin-6. *Arthritis Rheumatol.* (2014). doi:10.1002/art.38746

244. van Nie, L. *et al.* Dopamine induces in vitro migration of synovial fibroblast from patients with rheumatoid arthritis. *Sci. Rep.* (2020). doi:10.1038/s41598-020-68836-z

245. Thirumurugan, P., Matosiuk, D. & Jozwiak, K. Click Chemistry for Drug Development and Diverse Chemical–Biology Applications. *Chem. Rev.* (2013). doi:10.1021/cr200409f

246. Lanning, B. R. *et al.* A road map to evaluate the proteome-wide selectivity of covalent kinase inhibitors. *Nat. Chem. Biol.* (2014). doi:10.1038/nchembio.1582

247. Dango, S. *et al.* DNA unwinding by ASCC3 helicase is coupled to ALKBH3-dependent DNA alkylation repair and cancer cell proliferation. *Mol. Cell* (2011). doi:10.1016/j.molcel.2011.08.039

248. Mary, S. *et al.* Biogenesis of N-cadherin-dependent cell-cell contacts in living fibroblasts is a microtubule-dependent kinesin-driven mechanism. *Mol. Biol. Cell* (2002). doi:10.1091/mbc.01-07-0337

249. Zeng, R., Zhuo, Z., Luo, Y., Sha, W. & Chen, H. Rho GTPase signaling in rheumatic diseases. *iScience* **25**, 103620 (2022).

250. Bijata, M. *et al.* Synaptic Remodeling Depends on Signaling between Serotonin Receptors and the Extracellular Matrix. *Cell Rep.* (2017). doi:10.1016/j.celrep.2017.05.023

251. Kim, J. J., Lee, S. B., Park, J. K. & Yoo, Y. D. TNF-α-induced ROS production triggering apoptosis is directly linked to Romo1 and Bcl-XL. *Cell Death Differ.* (2010). doi:10.1038/cdd.2010.19

252. Linxweiler, M., Schick, B. & Zimmermann, R. Let's talk about secs: Sec61, sec62 and sec63 in signal transduction, oncology and personalized medicine. *Signal Transduct. Target. Ther.* **2**, 1–10 (2017).

253. Olsen, J. V. & Mann, M. Status of large-scale analysis of posttranslational modifications by mass spectrometry. *Molecular and Cellular Proteomics* (2013).

doi:10.1074/mcp.O113.034181

254. Nobes, C. D. & Hall, A. Rho, Rac, and Cdc42 GTPases regulate the assembly of multimolecular focal complexes associated with actin stress fibers, lamellipodia, and filopodia. *Cell* (1995). doi:10.1016/0092-8674(95)90370-4

255. Pongratz, G. & Straub, R. H. The sympathetic nervous response in inflammation. *Arthritis Research and Therapy* (2014). doi:10.1186/s13075-014-0504-2

256. Talbot, S., Foster, S. L. & Woolf, C. J. Neuroimmunity: Physiology and Pathology. *Annu. Rev. Immunol.* (2016). doi:10.1146/annurev-immunol-041015-055340

257. Park, J. H. *et al.* Repositioning of the antipsychotic drug TFP for sepsis treatment. *J. Mol. Med.* (2019). doi:10.1007/s00109-019-01762-4

258. MacDowell, K. S. *et al.* Paliperidone prevents brain toll-like receptor 4 pathway activation and neuroinflammation in rat models of acute and chronic restraint stress. *Int. J. Neuropsychopharmacol.* (2015). doi:10.1093/ijnp/pyu070

259. Yamamoto, S. *et al.* Haloperidol suppresses NF-kappaB to inhibit lipopolysaccharide-induced pro-inflammatory response in RAW 264 cells. *Med. Sci. Monit.* (2016). doi:10.12659/MSM.895739

260. Capellino, S. Dopaminergic Agents in Rheumatoid Arthritis. *Journal of Neuroimmune Pharmacology* (2020). doi:10.1007/s11481-019-09850-5

261. Capellino, S. *et al.* Catecholamine-producing cells in the synovial tissue during arthritis: Modulation of sympathetic neurotransmitters as new therapeutic target. *Ann. Rheum. Dis.* (2010). doi:10.1136/ard.2009.119701

262. Jung, D.-J. *et al.* Novel Transcription Coactivator Complex Containing Activating Signal Cointegrator 1. *Mol. Cell. Biol.* (2002). doi:10.1128/mcb.22.14.5203-5211.2002

263. Shadrick, W. R. *et al.* Discovering new medicines targeting helicases: Challenges and recent progress. *Journal of Biomolecular Screening* (2012). doi:10.1177/1087057113482586

264. Matsuo, Y. *et al.* Ubiquitination of stalled ribosome triggers ribosome-associated quality control. *Nat. Commun.* (2017). doi:10.1038/s41467-017-00188-1

265. Juszkiewicz, S., Speldewinde, S. H., Wan, L., Svejstrup, J. Q. & Hegde, R. S. The ASC-1 Complex Disassembles Collided Ribosomes. *Mol. Cell* (2020).

doi:10.1016/j.molcel.2020.06.006

266. Li, J. *et al.* A short hairpin RNA screen of interferon-stimulated genes identifies a novel negative regulator of the cellular antiviral response. *MBio* (2013). doi:10.1128/mBio.00385-13

267. Kim, H.-J. *et al.* Activating Signal Cointegrator 1, a Novel Transcription Coactivator of Nuclear Receptors, and Its Cytosolic Localization under Conditions of Serum Deprivation. *Mol. Cell. Biol.* (1999). doi:10.1128/mcb.19.9.6323

268. Hayden, M. S. & Ghosh, S. NF-κB, the first quarter-century: Remarkable progress and outstanding questions. *Genes Dev.* (2012). doi:10.1101/gad.183434.111

269. Pfeffer, S. *et al.* Structure of the mammalian oligosaccharyl-transferase complex in the native ER protein translocon. *Nat. Commun.* (2014). doi:10.1038/ncomms4072

270. Fumagalli, F. *et al.* Translocon component Sec62 acts in endoplasmic reticulum turnover during stress recovery. *Nat. Cell Biol.* (2016). doi:10.1038/ncb3423

271. Linxweiler, M. *et al.* Targeting cell migration and the endoplasmic reticulum stress response with calmodulin antagonists: A clinically tested small molecule phenocopy of SEC62 gene silencing in human tumor cells. *BMC Cancer* (2013). doi:10.1186/1471-2407-13-574

272. Körbel, C. *et al.* Treatment of SEC62 over-expressing tumors by Thapsigargin and Trifluoperazine. *Biomol. Concepts* (2018). doi:10.1515/bmc-2018-0006

273. Humby, F. *et al.* Synovial cellular and molecular signatures stratify clinical response to csDMARD therapy and predict radiographic progression in early rheumatoid arthritis patients. *Ann. Rheum. Dis.* (2019). doi:10.1136/annrheumdis-2018-214539

274. Matcham, F., Rayner, L., Steer, S. & Hotopf, M. The prevalence of depression in rheumatoid arthritis: A systematic review and meta-analysis. *Rheumatol. (United Kingdom)* (2013). doi:10.1093/rheumatology/ket169

275. Sturgeon, J. A., Finan, P. H. & Zautra, A. J. Affective disturbance in rheumatoid arthritis: Psychological and disease-related pathways. *Nature Reviews Rheumatology* (2016). doi:10.1038/nrrheum.2016.112

276. Matcham, F. *et al.* The relationship between depression and biologic treatment response in rheumatoid arthritis: An analysis of the British Society for Rheumatology

Biologics Register. *Rheumatol. (United Kingdom)* (2018).
doi:10.1093/rheumatology/kex528

277.   Bora, E., Fornito, A., Pantelis, C. & Yücel, M. Gray matter abnormalities in Major
       Depressive Disorder: A meta-analysis of voxel based morphometry studies. *Journal of
       Affective Disorders* (2012). doi:10.1016/j.jad.2011.03.049

278.   Kappelmann, N., Lewis, G., Dantzer, R., Jones, P. B. & Khandaker, G. M.
       Antidepressant activity of anti-cytokine treatment: A systematic review and meta-
       analysis of clinical trials of chronic inflammatory conditions. *Mol. Psychiatry* (2018).
       doi:10.1038/mp.2016.167

279.   Pan, W. *et al.* Cytokine Signaling Modulates Blood-Brain Barrier Function. *Curr.
       Pharm. Des.* (2011). doi:10.2174/138161211798220918

280.   Leung, L. & Cahill, C. M. TNF-α and neuropathic pain - a review. *Journal of
       Neuroinflammation* (2010). doi:10.1186/1742-2094-7-27

281.   Lorusso, L. *et al.* Immunological aspects of chronic fatigue syndrome. *Autoimmunity
       Reviews* (2009). doi:10.1016/j.autrev.2008.08.003

282.   Matcham, F. *et al.* O05. THE IMPACT OF TARGETED RHEUMATOID ARTHRITIS
       PHARMACOLOGICAL TREATMENT ON MENTAL HEALTH: A SYSTEMATIC REVIEW AND
       NETWORK META-ANALYSIS. *Rheumatology* (2017).
       doi:10.1093/rheumatology/kex061.005

283.   Sellgren, C., Frisell, T., Lichtenstein, P., Landen, M. & Askling, J. The association
       between schizophrenia and rheumatoid arthritis: A nationwide population-based
       swedish study on intraindividual and familial risks. *Schizophr. Bull.* (2014).
       doi:10.1093/schbul/sbu054

284.   Chen, Z. X. & Pervaiz, S. Involvement of cytochrome c oxidase subunits Va and Vb in
       the regulation of cancer cell metabolism by Bcl-2. *Cell Death Differ.* (2010).
       doi:10.1038/cdd.2009.132

285.   Lee, S. Y. *et al.* IL-17-mediated Bcl-2 expression regulates survival of fibroblast-like
       synoviocytes in rheumatoid arthritis through STAT3 activation. *Arthritis Res. Ther.*
       (2013). doi:10.1186/ar4179

286.   de Seny, D. *et al.* Proteins involved in the endoplasmic reticulum stress are
       modulated in synovitis of osteoarthritis, chronic pyrophosphate arthropathy and

rheumatoid arthritis, and correlate with the histological inflammatory score. *Sci. Rep.* (2020). doi:10.1038/s41598-020-70803-7

287.   Stojadinovic, A. *et al.* HYOU1/Orp150 expression in breast cancer. *Med. Sci. Monit.* (2007).

288.   Rao, S. *et al.* Biological function of HYOU1 in tumors and other diseases. *OncoTargets and Therapy* (2021). doi:10.2147/OTT.S297332

9. Publications in peer- reviewed journals during the PhD Thesis

In Silico Discovery of Plant-Origin Natural Product Inhibitors of Tumor Necrosis Factor (TNF) and Receptor Activator of NF-κB Ligand (RANKL)

Georgia Melagraki[1], Evangelos Ntougkos[2], Dimitra Papadopoulou[2,3], Vagelis Rinotas[2,4], Georgios Leonis[5], Eleni Douni[2,4], Antreas Afantitis[2,5*] and George Kollias[2,3*]

Journal of
Translational Medicine

RESEARCH **Open Access**

Combination of subtherapeutic anti-TNF dose with dasatinib restores clinical and molecular arthritogenic profiles better than standard anti-TNF treatment

Lydia Ntari[1], Christoforos Nikolaou[2], Ksanthi Kranidioti[1], Dimitra Papadopoulou[2], Eleni Christodoulou-Vafeiadou[1], Panagiotis Chouvardas[3,4], Florian Meier[5,6], Christina Geka[1], Maria C. Denis[1], Niki Karagianni[1] and George Kollias[2,7*]

International Journal of
Molecular Sciences

MDPI

Article

In Silico Identification and Evaluation of Natural Products as Potential Tumor Necrosis Factor Function Inhibitors Using Advanced Enalos Asclepios KNIME Nodes

Dimitra Papadopoulou[1,2], Antonios Drakopoulos[3], Panagiotis Lagarias[3], Georgia Melagraki[4], George Kollias[1,2,5,6,*] and Antreas Afantitis[3,*]

10. Preprints

New Results   🔔 Follow this preprint

Repurposing of Amisulpride, a known antipsychotic drug, to target synovial fibroblasts activation in arthritis

D. Papadopoulou, F. Roumelioti, C. Tzaferis, P. Chouvardas, A.K. Pedersen, F. Charalampous, E. Christodoulou-Vafeiadou, L. Ntari, N. Karagianni, M. Denis, 🆔 J.V. Olsen, A.N. Matralis, 🆔 G. Kollias

This article is a preprint and has not been certified by peer review [what does this mean?].

New Results   🔔 Follow this preprint

miR-221/222 drive synovial fibroblast expansion and pathogenesis of TNF-mediated arthritis

Fani Roumelioti, Christos Tzaferis, Dimitris Konstantopoulos, Dimitra Papadopoulou, Alejandro Prados, Maria Sakkou, Anastasios Liakos, Panagiotis Chouvardas, Theodore Meletakos, Yiannis Pandis, Niki Karagianni, Maria Denis, 🆔 Maria Fousteri, 🆔 Marietta Armaka, 🆔 George Kollias

This article is a preprint and has not been certified by peer review [what does this mean?].